NUREG/CR-2691
EGG-2186

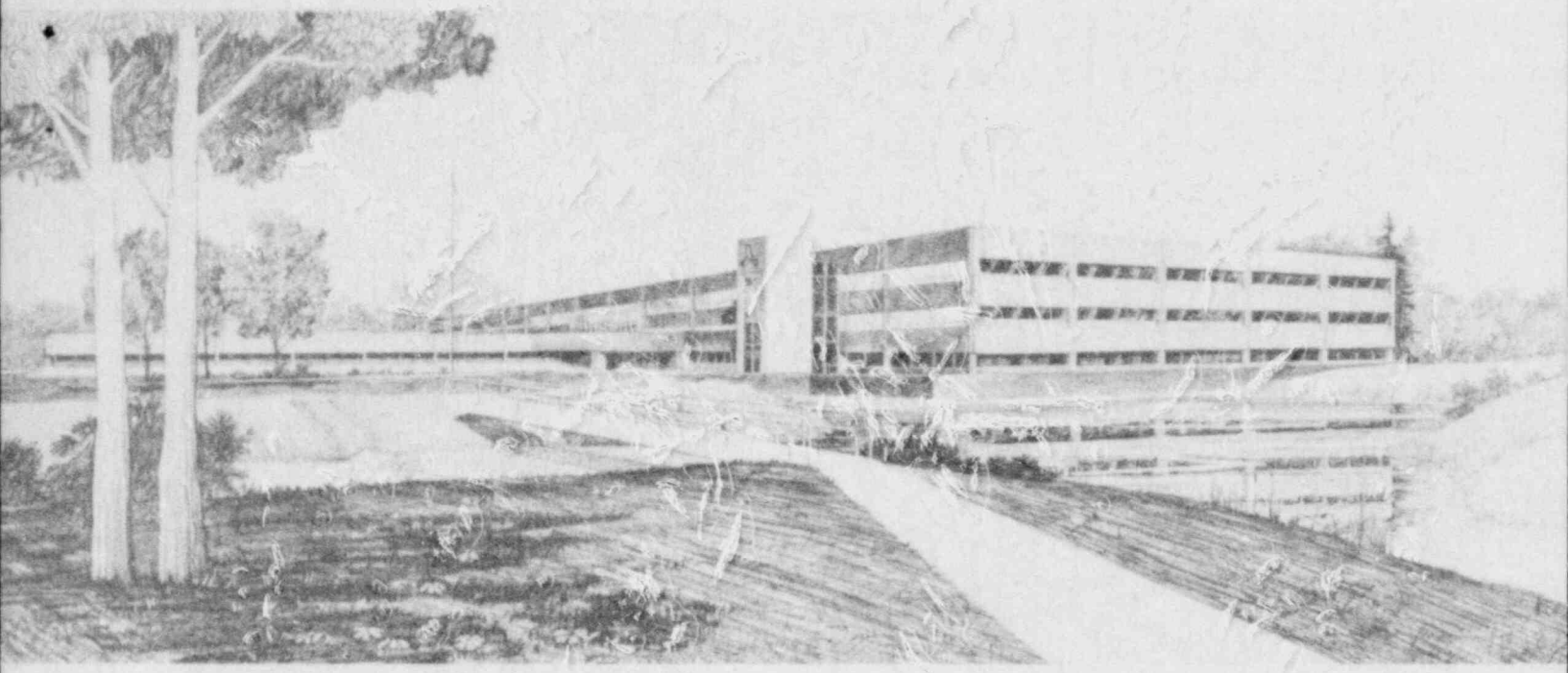

Idaho National Engineering Laboratory
Operated by the U.S. Department of Energy

Effects of Cladding Surface Thermocouples and Electrical Heater Rod Design on Quench Behavior

Richard C. Gottula

February 1984

Prepared for the
U.S. Nuclear Regulatory Commission
Under DOE Contract No. DE-AC07-76IDO1570

EG&G Idaho

Available from

GPO Sales Program
Division of Technical Information and Document Control
U.S. Nuclear Regulatory Commission
Washington, D.C. 20555

and

National Technical Information Service
Springfield, Virginia 22161

NUREG/CR-2691
EGG-2186
Distribution Category: R2

EFFECTS OF CLADDING SURFACE THERMOCOUPLES AND ELECTRICAL HEATER ROD DESIGN ON QUENCH BEHAVIOR

Richard C. Gottula

Published February 1984

EG&G Idaho, Inc.
Idaho Falls, Idaho 83415

Prepared for the
U.S. Nuclear Regulatory Commission
Washington, D.C. 20555
Under DOE Contract No. DE-AC07-76IDO1570
FIN No. A6038

ABSTRACT

A separate effects experiment program was conducted on a bundle of nine electrical heater rods in the Loss-of-Fluid Test (LOFT) Test Support Facility (LTSF) at the Idaho National Engineering Laboratory (INEL). The objectives of the experiment program were to (a) evaluate the effect of cladding external thermocouples on the quench (cooling) behavior of a cartridge-type nuclear fuel rod simulator, (b) determine how accurately cladding external thermocouples measure cladding temperature during a high-pressure quench, (c) provide a functional and reliability test for cladding-embedded thermocouples that are prototypes of a design to be used in the LOFT fuel rods, and (d) compare the quench behavior of a cartridge-type heater rod (which simulates a fuel pellet-cladding gap) with that of a solid-type heater rod (without a pellet-cladding gap) under thermal-hydraulic conditions that could occur during the blowdown phase (0 to 10 s) of a large-break loss-of-coolant accident in a pressurized water reactor.

The prototype cladding-embedded thermocouples did not function correctly during the experiment; however, useful data were obtained such that the objectives of the experiment program could be met. The results of the experiment program indicate that (a) cladding external thermocouples had a negligible effect on the cooldown rate and the quench behavior of a cartridge-type heater rod under rapid (1 to 2 m/s) flooding conditions at high pressure, (b) cladding external thermocouples were selectively cooled during the quenching process and do not accurately measure cladding temperature during that part of the transient, and (c) the time-to-quench was significantly less for the cartridge-type heater rod than for the solid-type heater rod. The cartridge-type heater rod has been shown to satisfactorily simulate the thermal response of a nuclear fuel rod through analytical and experimental data comparisons; therefore, the results from the cartridge-type heater rod are considered applicable to LOFT nuclear fuel rods.

NRC FIN No. A6038—Semiscale Program

SUMMARY

Quenching of the fuel rods in the Loss-of-Fluid Test (LOFT) reactor occurred during the blowdown phase of Loss-of-Coolant Experiments (LOCEs) L2-2 and L2-3, which was earlier than had been predicted. The quenching was measured by 186 thermocouples that were laser welded to the outer surface of the cladding of 76 fuel rods located within the LOFT core. It had been postulated that the cladding external thermocouples may have induced the early LOFT fuel rod quench and that the cladding external thermocouples may have been selectively cooled, and may not have accurately measured the cladding temperature. A separate effects experiment program was conducted in the LOFT Test Support Facility (LTSF) at the Idaho National Engineering Laboratory (INEL) to investigate these effects under high-pressure thermal-hydraulic conditions typical of those in LOFT LOCE L2-3.

The separate effects experiment program was conducted with a nine-rod (three-by-three) bundle of electrical heater rods which were provided by the Karlsruhe Nuclear Reactor Center in Karlsruhe, Germany. The test rod was in the center of the nine-rod configuration. The eight surrounding rods were solid-type (FEBA) heater rods. A REBEKA cartridge-type heater rod and a FEBA solid-type heater rod were each tested in the center position in the nine-rod bundle, which provided a geometry and thermal-hydraulic environment typical of a nuclear fuel rod cluster.

The REBEKA heater rod has Zircaloy cladding and aluminum oxide pellet construction with a pellet-cladding gap to simulate the thermal characteristics of a nuclear fuel rod. The quench behavior of the REBEKA heater rod has been compared with that of a LOFT nuclear fuel rod through calculations using the RELAP4/MOD6 computer code and with that of the Power Burst Facility nuclear fuel rod through experiment data evaluation. Both the analytical and experimental data comparisons showed that the REBEKA heater rod provides a good simulation of nuclear fuel rod thermal response for rapid flooding rates at high pressure in a pressurized water reactor (PWR) loss-of-coolant transient.

The REBEKA heater rod was tested with and without cladding external thermocouples. Prototype LOFT fuel rod cladding-embedded thermocouples were installed in the inner surface of the REBEKA rod cladding to provide an accurate measurement of cladding temperature. The function and reliability of the prototype cladding-embedded thermocouples were investigated in the experiment. In addition, a FEBA solid-type heater rod was tested to provide a direct comparison of the quench behavior of cartridge-type and solid-type electrical heater rods under the same thermal-hydraulic conditions.

The prototype cladding-embedded thermocouples installed in the REBEKA rod did not function correctly. The primary thermocouple junctions that were embedded in the cladding failed prior to the first experiment; however, secondary junctions, formed in the thermocouple wires, provided data of sufficient reliability to meet the objectives of the experiment program. A post-mortem conducted on the REBEKA rod and embedded thermocouples showed that the prototype embedded-thermocouple design tested in this experiment is not adequate for installation in LOFT fuel rods; however, second and third generation thermocouples have been developed which may be more reliable than the prototype thermocouples tested here.

The results of the experiment program indicate that cladding external thermocouples had a negligible effect on the cooldown rate and quench behavior of a REBEKA cartridge-type heater rod. Also, the cladding external thermocouples are selectively cooled during the quenching process and do not accurately measure cladding temperature during this part of the transient. Since the REBEKA rod has been shown to satisfactorily simulate the thermal response of a nuclear fuel rod, these results are considered applicable to LOFT nuclear fuel rods. Consequently, the value of LOFT external thermocouple data in validating computer code models during quenching is somewhat limited.

The results of the experiment program also show that the quench behavior of a FEBA solid-type heater rod is significantly different than that of a cartridge-type (REBEKA) heater rod. The REBEKA rod quenched in less than 2 s from about

900 K, whereas, the FEBA heater rods experienced an extended period (10 s) of precursory cooling before quenching at about 700 K. Since it has been shown that the REBEKA rod provides a good simulation of a nuclear fuel rod, it is inferred that solid-type electrical heater rods do not provide a good simulation of the thermal response of nuclear fuel rods under high-pressure, rapid-flooding thermal-hydraulic conditions that can occur during the blowdown phase of a large-break loss-of-coolant accident in a PWR.

The REBEKA and FEBA heater rod data provide important information from which to assess the capability of best estimate computer codes to predict cladding quench behavior.

ACKNOWLEDGMENTS

The Kernforschungszentrum Karlsruhe (KfK) (Karlsruhe Nuclear Reactor Center) is acknowledged for furnishing the REBEKA and FEBA rods that were used in the nine-rod bundle experiments.

The prototype Loss-of-Fluid Test (LOFT) cladding-embedded thermocouples were developed and fabricated at EG&G Idaho, Inc., under the direction of S. C. Wilkins. Installation procedures and installation of the prototype thermocouples into the cladding of the REBEKA heater rod were developed and conducted by Exxon Nuclear Corporation. Essential liaison between EG&G Idaho and Exxon Nuclear was provided by T. E. Howell of EG&G Idaho.

Attachment of the cladding external thermocouples to the REBEKA heater rod was performed by D. L. Hendrix. In addition to this, the REBEKA heater rod leak check and other machine work on the REBEKA and FEBA heater rods were under the direction of B. R. Dabell.

The mechanical design of the nine-rod bundle was performed by G. H. Weimann.

Bundle assembly and disassembly were performed by the operations personnel at the LOFT Test Support Facility (LTSF). The experiments were set up and conducted in an efficient manner through the dedicated efforts of the operations and measurements personnel at the LTSF. The assistance of N. K. Dyet was invaluable in installing the hardware for the experiments.

Appreciation is expressed to E. L. Tolman and M. L. Carboneau for their valuable technical assistance in establishing the requirements for the experiments and in evaluating the data.

Valuable metallurgical technical advice was provided by C. S. Olsen. The REBEKA rod post-mortem metallurgical samples and photographs were prepared by M. Lindstrom, Jr. Detailed post-mortem analysis and photography of the cladding embedded thermocouples using a scanning electron microscope were conducted by D. V. Miley. The post-mortem pressure test on the REBEKA rod was conducted by G. W. Webb.

Editing of this report was performed by R. Carter and G. Hammer.

Appreciation is expressed to all of the above individuals and many others who assisted in completing this experiment program.

CONTENTS

EFFECTS OF CLADDING SURFACE THERMOCOUPLES AND ELECTRICAL HEATER ROD DESIGN ON QUENCH BEHAVIOR

1. INTRODUCTION

The Loss-of-Fluid Test (LOFT) facility includes an integral nuclear reactor system [50 MW(t)][1] designed to simulate and provide experiment data on the phenomena that are expected occur during a loss-of-coolant accident (LOCA) in a large pressurized water reactor (PWR) system [~1000 MW(e)]. The LOFT facility is located at the Idaho National Engineering Laboratory (INEL) and is operated by EG&G Idaho, Inc., under the direction of the United States Department of Energy.

The LOFT reactor's special experimental instrumentation includes 186 thermocouples that are laser welded to the external surface of 76 fuel rods located within the LOFT core. During LOFT large-break Loss-of-Coolant Experiments (LOCEs) L2-2[2] and L2-3[3], the fuel rod cladding external thermocouples indicated the reactor core was quenched (cooled) early in the blowdown transient, see Figure 1. It had been postulated that the cladding external thermocouples may have induced the fuel rod quench and that the external thermocouples may have been selectively cooled, and may not have accurately measured the cladding temperature during these rapid cooling transients. A previous experiment on a single, solid-type heater rod[4] indicated that cladding external thermocouples significantly

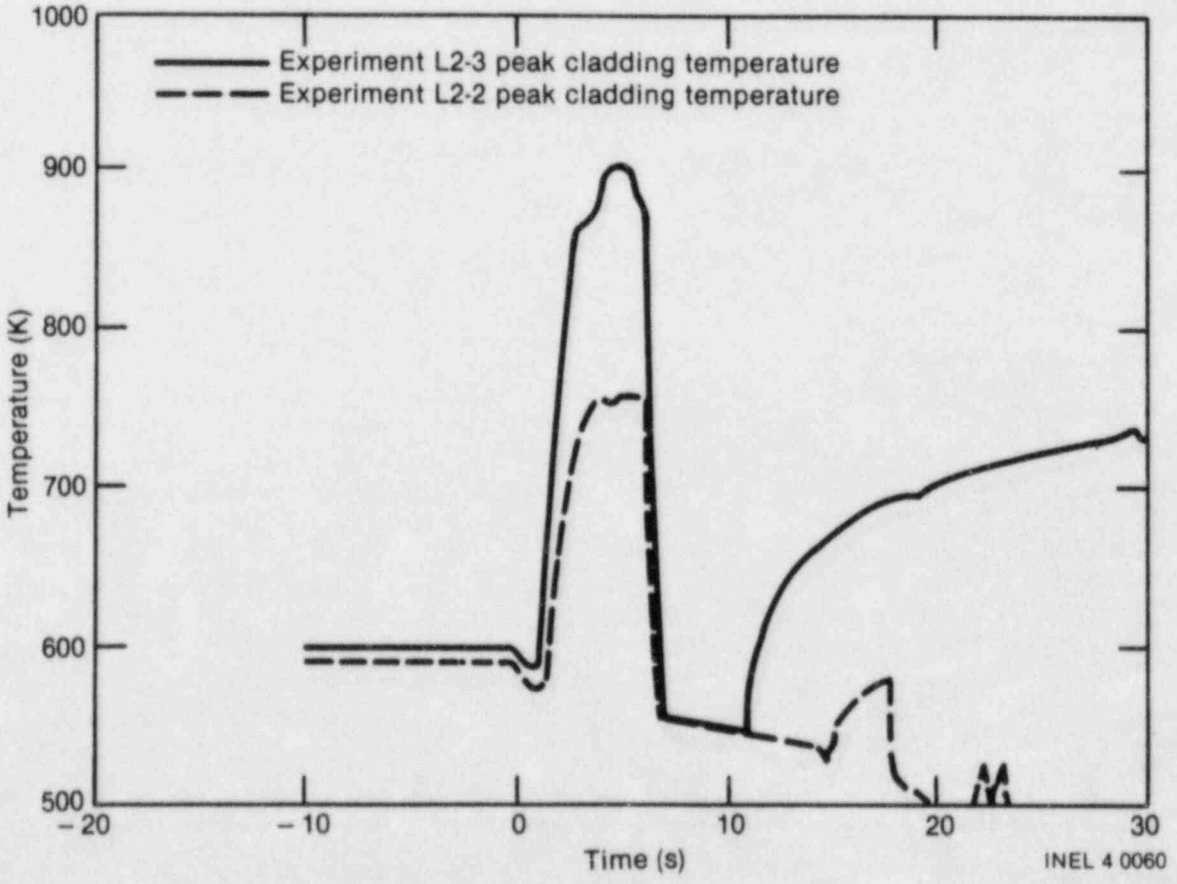

Figure 1. Response of fuel rod cladding external thermocouples during LOFT Experiments L2-2 and L2-3.

reduced the time-to-quench of that type of rod; however, the typicality of the quench behavior of a solid-type electrical heater rod to that of a nuclear fuel rod has been questioned because of the different thermal properties and lack of a simulated fuel pellet-cladding gap of a solid-type heater rod as compared to a nuclear fuel rod.

An additional separate effects experiment program, described herein, was conducted by EG&G Idaho, Inc., in the blowdown loop of the LOFT Test Support Facility (LTSF) at the INEL to address these issues. This experiment program was conducted on a nine-rod (three-by-three) bundle of electrically heated rods in a 6.67-cm inside diameter test vessel. The nine-rod bundle incorporated grid spacers similar to those used in the LOFT core. The heater rods were provided by the Karlsruhe Nuclear Reactor Center in Karlsruhe, Germany. A REBEKA cartridge-type heater rod and a FEBA solid-type heater rod were each tested in the center position in the nine-rod bundle. The eight peripheral rods were FEBA heater rods which provided a geometry and thermal-hydraulic environment typical of a nuclear fuel rod cluster. The REBEKA heater rod was chosen for testing because its Zircaloy cladding and aluminum oxide pellet construction with a pellet-cladding gap provided an improved simulation of the thermal characteristics of a nuclear fuel rod. The test with the FEBA heater rod provided data to compare cartridge-type and solid-type heater rod performance.

The primary objective of the separate effects experiment was to evaluate the effect of cladding external thermocouples on a REBEKA cartridge-type nuclear fuel rod simulator by testing a REBEKA heater rod with and without LOFT-type cladding external thermocouples. These results would then be indicative of the effect of cladding external thermocouples on the quench behavior of LOFT nuclear fuel rods. In addition, two prototype cladding-embedded thermocouples for LOFT fuel rods were installed in the inner surface of the cladding of the REBEKA heater rod for this experiment. These two thermocouples were intended to provide the basic measurements to (a) evaluate the effect of cladding external thermocouples on the quench behavior of the REBEKA rod and (b) provide an accurate measurement of the cladding temperature with which the external thermocouple measurements could be compared to evaluate the ability of external thermocouples to measure the actual cladding temperature during rapid cooling transients. This experiment program also provided an opportunity to evaluate (a) the adequacy of the installation procedure used for the cladding embedded thermocouples and (b) the reliability and lifetime of the embedded thermocouples under operating conditions.

A secondary objective of this experiment relates to the ability of a cartridge-type heater rod (with a simulated fuel pellet-cladding gap) and a solid-type heater rod (without a pellet-cladding gap) to simulate the thermal response of nuclear fuel rods in a large-break LOCE.[5] The heater rod material thermal properties and type of construction (such as pellet-cladding gap versus no gap) affect the cooling rate and time-to-quench of a heater rod. The inherent differences in thermal characteristics between nuclear rods and electrical fuel rod simulators causes difficulties in relating heater rod quench data from nonnuclear experiments to nuclear rod thermal response. This separate effects experiment using FEBA solid-type and REBEKA cartridge-type heater rods provided important data regarding the relative quench behavior of solid- and cartridge-type heater rods under rapid flooding conditions at high pressure. These data will be useful in gaining a better understanding of the limitations of electric heater rods to simulate the thermal response of nuclear fuel rods under large-break LOCA conditions. In addition, the REBEKA and FEBA rod data provide important information from which to assess the ability of best estimate computer codes to predict cladding quench behavior. These computer codes are then ultimately used to predict the nuclear fuel rod thermal response during a LOCA.

The conditions for this separate effects experiment were designed to simulate the thermal-hydraulic conditions existing in the LOFT core during LOCE L2-3. However, there is a reasonable amount of uncertainty in the LOFT experiment conditions due to inadequate flow and density measurements in the LOFT core. Therefore, a range of mass fluxes and fluid qualities were used in the separate effects experiment to bracket the thermal-hydraulic conditions thought to exist in the LOFT core, so that meaningful inferences could be made regarding the perturbation effect and accuracy of the LOFT cladding external thermocouples during LOFT LOCE L2-3.

The test facility, test section, and instrumentation are described in Section 2. The experiment conditions and operating procedure are described in

Section 3. Section 4 describes the performances of the REBEKA heater rod and of the cladding embedded thermocouples in the REBEKA rod. Section 5 describes the analysis and presents results of the separate effects experiment. Conclusions based on the results of the experiment are stated in Section 6.

Supplemental information to support the analysis is provided in Appendixes A through F. Appendix A contains a description of the development and design of the cladding-embedded thermocouples. Results of a post-mortem conducted on the REBEKA rod and the embedded thermocouples as well as potential failure mechanisms of the embedded thermocouples are discussed in Appendix B. Appendix C includes a description of the INVERT computer model used in the evaluation of the data. Appendixes D, E, and F contain a measurements list, REBEKA rod diameter measurements taken during the test program, and measurement uncertainties, respectively.

2. TEST FACILITY DESCRIPTION

The separate effects experiment program was conducted in the blowdown loop of the LTSF at the INEL. The blowdown loop, which is normally used to conduct blowdown-type experiments, was modified for the quench experiments. The modified loop configuration is shown in Figure 2. The main loop consists of a pressure vessel, a coolant pump, a warmup heater vessel, and associated valves and piping, and has a volume of 0.322 m^3. A high-pressure nitrogen source connected to the top end of the pressure vessel provides regulated pressure in the main loop to drive the primary coolant into the test section, which contained the heater rod bundle. A surge tank equipped with a steam relief valve was used to maintain constant regulated pressure in the test section during an experiment run. The surge tank and test section were initially pressurized with nitrogen to a nominal 7 MPa.

The flow rate to the test section was controlled by the nitrogen pressure in the main loop pressure vessel and by an orifice, see Table 1, located immediately upstream from the test section. The pressure in the primary loop was maintained high enough to keep the fluid upstream from the test initiation valve (FCV-1T) constantly subcooled so that the flow rate to the test section could be accurately measured with a turbine meter (FE-FCV-1T).

The following sections briefly describe the blowdown loop control system, data acquisition system, test section, and instrumentation and measurements used for the separate effects experiment program.

Control System

Test loop process measurements and controls were accomplished using a microprocessor controller. All loop operations from startup through experiment sequencing were programmed into the controller, and a complete experiment series was run with minimum operator intervention. The process measurements and loop parameters were displayed on a cathode ray tube (CRT) terminal with a keyboard which allows operator monitoring and on-line setpoint modifications at any time prior to the actual period of experiment sequencing and data acquisition.

Data Acquisition System

Experimental measurements on the blowdown loop and associated test hardware were monitored by a central data acquisition system. This system is comprised of a 256-channel digital recording system and a medium-to-wide bandwidth analog recording system.

The digital system is equipped with a NEFF 620 acquisition system that converts analog input signals to digital format for processing by a MODCOMP II/45 computer. The analog-to-digital conversion provides 16-bit resolution at a throughput rate of 50,000 samples per second. The signal conditioning system provides the input conditioning required for Type K thermocouples, bridge transducers, and resistance temperature detectors (RTDs). Filter bandwidths of 1 Hz to 1 kHz are available.

Data reduction can be accomplished immediately following an experiment. Standard 6- by 8-in. plots are produced in engineering units.

Test Section

The test section consisted of a bundle of nine electrical heater rods installed in a 3-in. Schedule 160 stainless steel pipe with an inside diameter of 6.67 cm. The primary data were obtained on the center rod in the bundle with the outer eight rods providing boundary conditions typical of surrounding rods in a nuclear fuel rod bundle. The heated length of the bundle was 3.9 m. The bundle contained 10 grid spacers to simulate the effects of grid spacers in the LOFT core.

A bundle of nine FEBA heater rods was tested first. Then the center rod was replaced with a REBEKA heater rod, see Figure 3, which was tested both with and without LOFT-type cladding external thermocouples. The heater rods and grid spacers are described in the following sections.

Heater Rods. In order to provide data typical of a nuclear fuel rod, an electrical heater rod with thermal characteristics typical of a nuclear fuel rod was required. The REBEKA heater rod, which is a

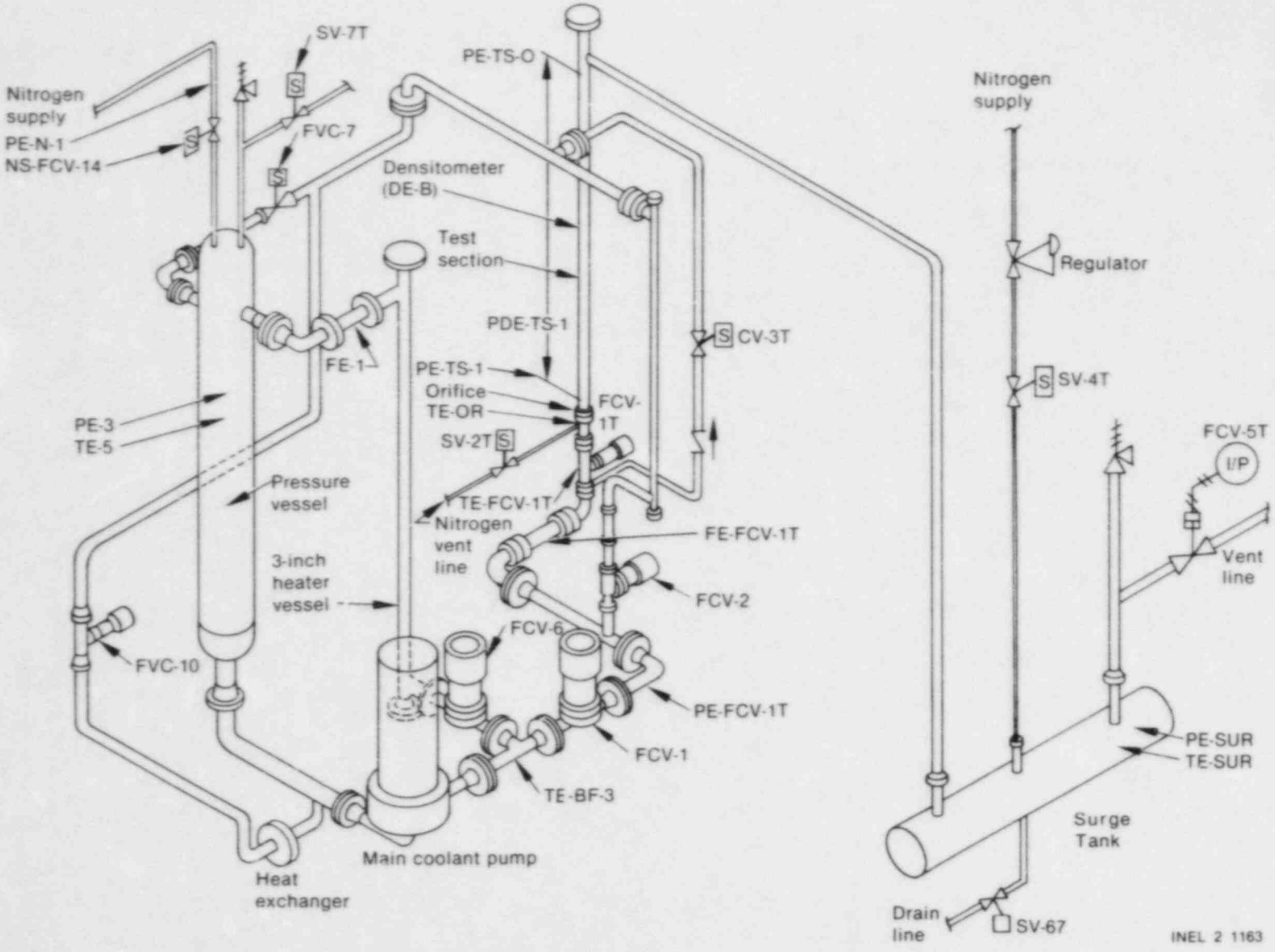

Figure 2. Test loop configuration.

Table 1. Flow-control orifice sizes

Experiment	Orifice Size (mm)
1	6.954
2	9.957
3	4.153
4	6.954
5	1.955
6	3.556
7	2.515
8	1.778

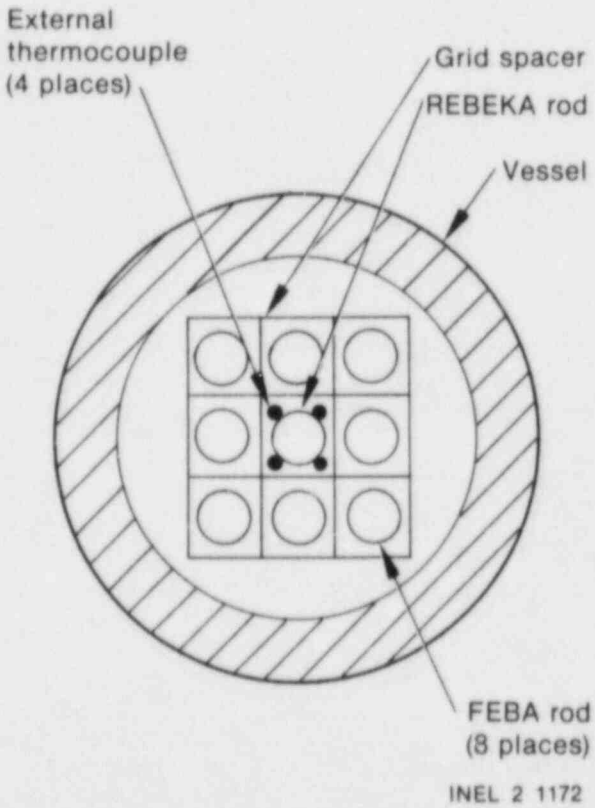

Figure 3. Nine-rod bundle configuration.

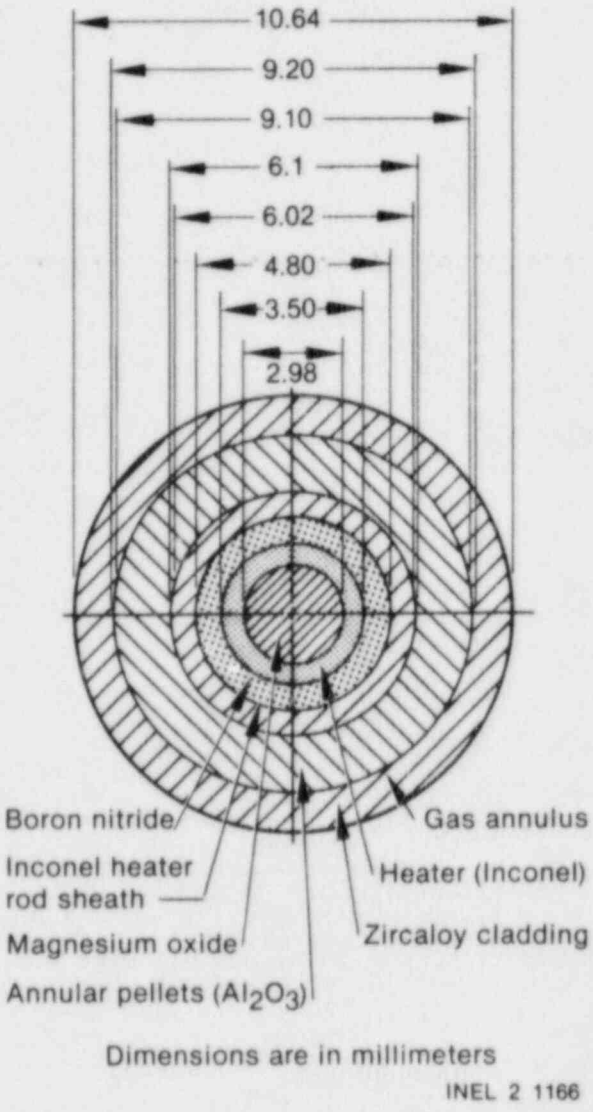

Figure 4. REBEKA heater rod cross section at 1950-mm elevation.

cartridge-type heater rod provided by the Karlsruhe Nuclear Reactor Center (KfK) in Germany, was selected for this purpose. The REBEKA rod has Zircaloy cladding, aluminum oxide (Al_2O_3) pellets, a nominal 0.1-mm gap between the pellets and cladding, and an internal heater assembly. A cross section of the REBEKA rod is shown in Figure 4. The quench behavior of the REBEKA rod has been compared with that of a LOFT nuclear fuel rod analytically through calculations using the RELAP4/MOD6 computer code.[6] Figure 5 shows the calculated relative cooldown rates of the REBEKA rod and a nuclear fuel rod for hydraulic conditions simulating those in the LOFT core during LOCE L2-3. The calculations show that the REBEKA heater rod is expected to simulate the nuclear rod behavior very well. Therefore, experiments using the REBEKA heater rod are expected to provide data applicable to a nuclear fuel rod.

The external pressure on the REBEKA rod during testing was 7 MPa. Analysis has shown that there is a potential for Zircaloy cladding collapse

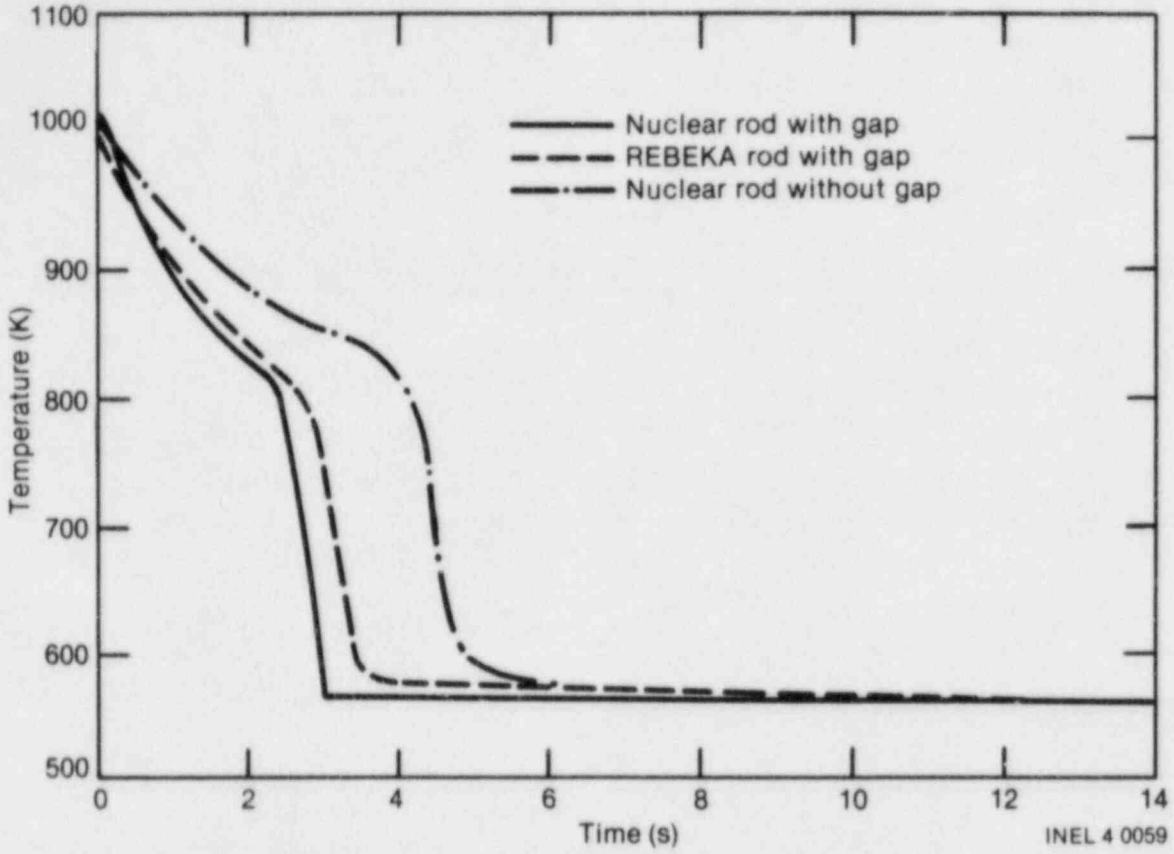

Figure 5. RELAP4/MOD6 calculated cooldown rates for a REBEKA heater rod and a nuclear fuel rod.

onto the Al_2O_3 pellets under conditions of 900 K temperature and a 7-MPa pressure differential across the cladding.[7] Therefore, the rod was pressurized internally with helium to 2.4 MPa prior to the experiments to reduce the pressure difference across the cladding to about 2.1 MPa at 900 K during the experiments and prevent the cladding from collapsing. The REBEKA rod was leak checked after prepressurization to 2.4 MPa by placing the rod inside a pipe which was then sealed and evacuated. The amount of helium leaked from the rod inside the pipe was then measured. The leak rate was measured to be 1×10^{-6} std cm^3/s, which was negligible. However, an important factor in the leak check, that was brought to light after the quench tests had been conducted, was that the ends of the embedded thermocouple leads were not contained inside of the pipe. This provided a possible leak path outside the pipe through the embedded thermocouples which would not be detected. This is discussed further in Section 4.

The REBEKA rod had a nonuniform axial power profile, as shown in Figure 6, with a peak-to-average power ratio of 1.183.

The FEBA heater rods, also furnished by KfK, are a solid-type heater rod with Inconel cladding, magnesia insulator, an internal heater element, and no simulated pellet-cladding gap. A cross section of the FEBA rod is shown in Figure 7. The FEBA rod had an axial power distribution identical to the REBEKA rod.

Grid Spacers. The rod bundle incorporated 10 Inconel grid spacers designed for a three-by-three array of rods. The design of the grid spacers is identical to the grid spacers used in the LOFT core. The grids are spaced axially at intervals of 42.2 cm, the same as in the LOFT core, to simulate any effects the grid spacers may have on the quench behavior of the rods. The grids are 4.45 cm in length. The locations of the upstream edge of the grid spacers

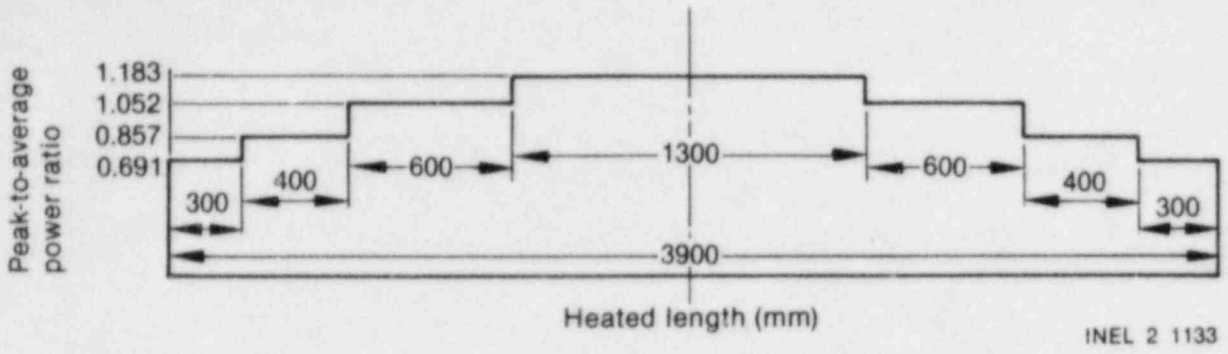

Figure 6. REBEKA heater rod axial power distribution.

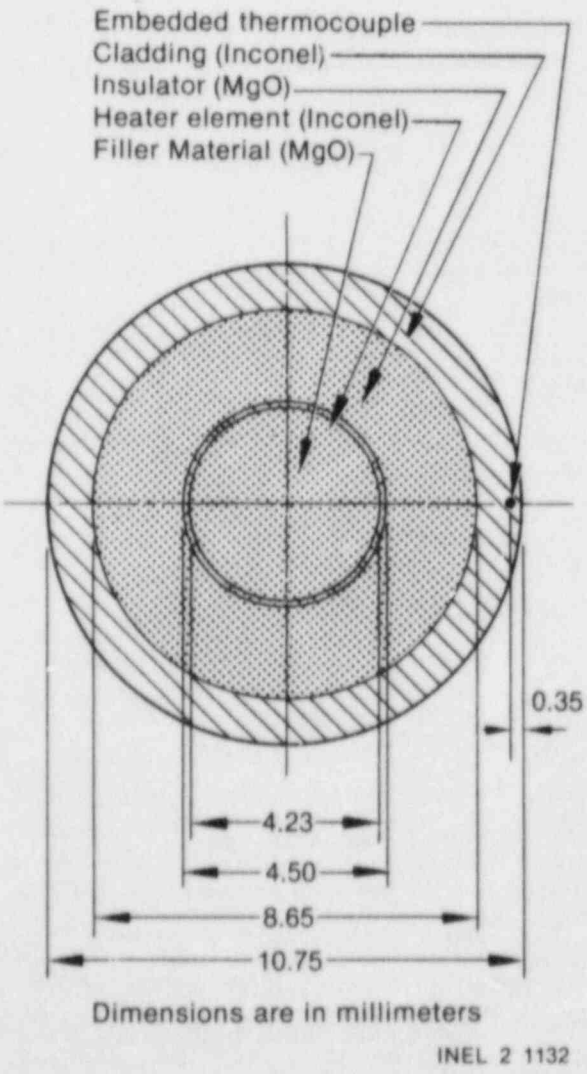

Figure 7. FEBA heater rod cross section.

are shown in Figure 8 relative to the axial power distribution of the rods and the axial locations of the FEBA and REBEKA rod thermocouples.

Instrumentation and Measurements

Numerous measurements were taken for process control and experimental data. A complete measurements list is given in Appendix D, including the measurement identification number, the range, and a description of each measurement. All measurements were sampled and recorded at a rate of 50 samples per second.

Process Control Measurements. Process control measurements were monitored to control the main loop and to set up the initial experiment conditions. These included fluid temperature (TE-5) and pressure (PE-3) measurements in the main loop, pipe temperatures at the test section inlet (TE-P-1, TE-P-2, TE-P-3, and TE-P-4) to control heater tapes on the inlet piping and valves, surge tank pressure (PE-SUR), and nitrogen supply tank pressure (PE-N-1). Several rod thermocouple measurements at the hot spot of the heater rods (1950-mm elevation) were used to control the power to the heater rods and monitor their temperature prior to an experiment.

Experimental Measurements. The experimental measurements included heater rod temperatures, test section pressure and pressure drop, heater rod power level, test section flow rate, fluid density at the hot spot of the test section (1950-mm elevation), and test section wall temperatures. Also, the voltage signal to open test section inlet Valve FCV-1T was recorded. This parameter was used to define the start time of each experiment run.

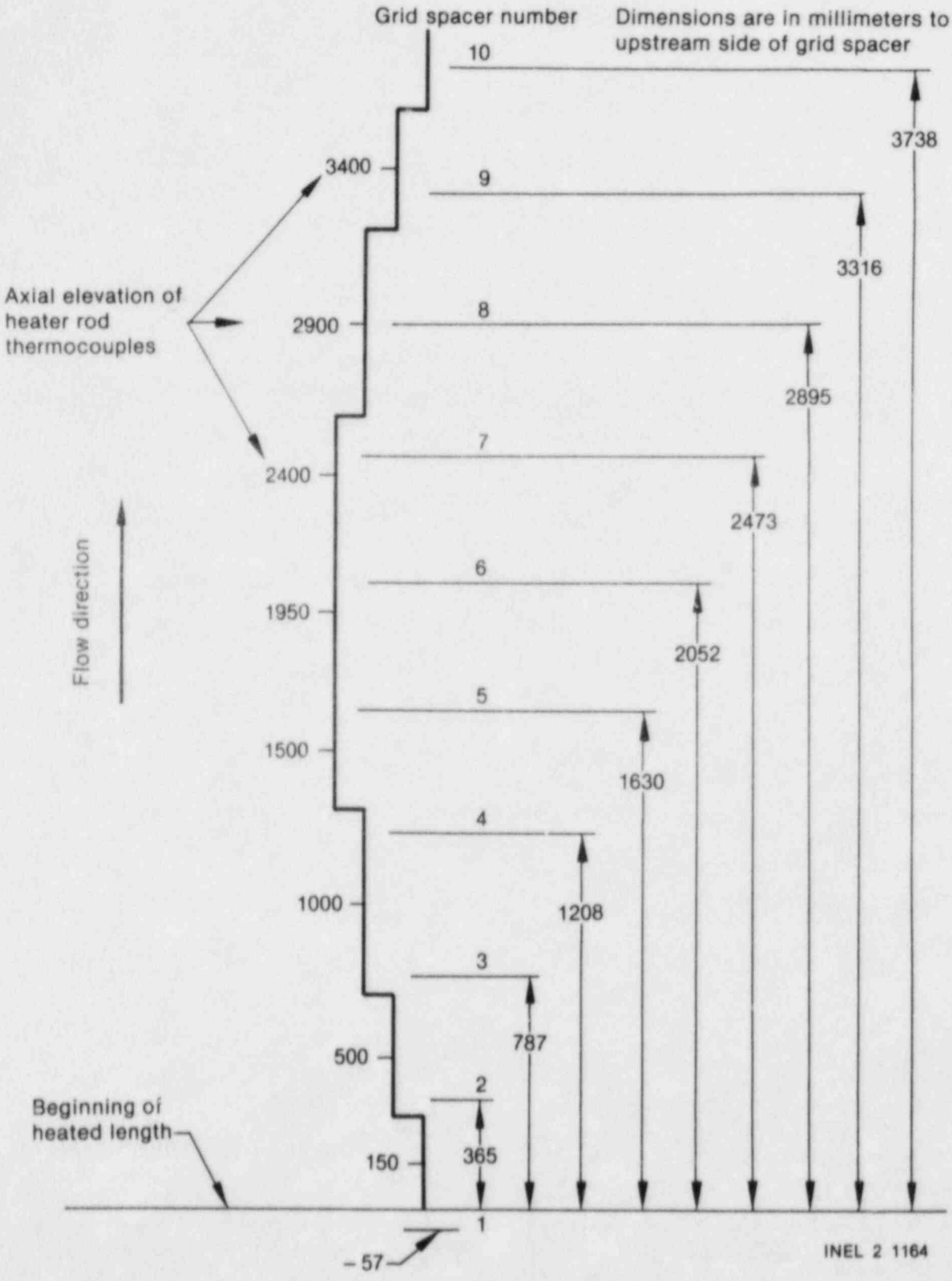

Figure 8. Axial location of grid spacers from beginning of rod heated length.

Cladding External Thermocouples. Four thermocouples were laser welded to the outer surface of the REBEKA heater rod cladding with junctions and attachments similar to the thermocouples on LOFT fuel rods. The thermocouples were Type K with a titanium sheath and an outer diameter of 1.02 mm. Dummy thermocouple extensions were attached to the rod from the three thermocouple junctions highest on the rod to the level of the lowest thermocouple junction (that is, closest to the beginning or bottom of the heated length of the rod) to duplicate the LOFT configuration. Figure 9 shows the attachment configuration of the cladding external thermocouples on a LOFT fuel rod. The axial location and azimuthal placement of the external thermocouples are given in Table 2.

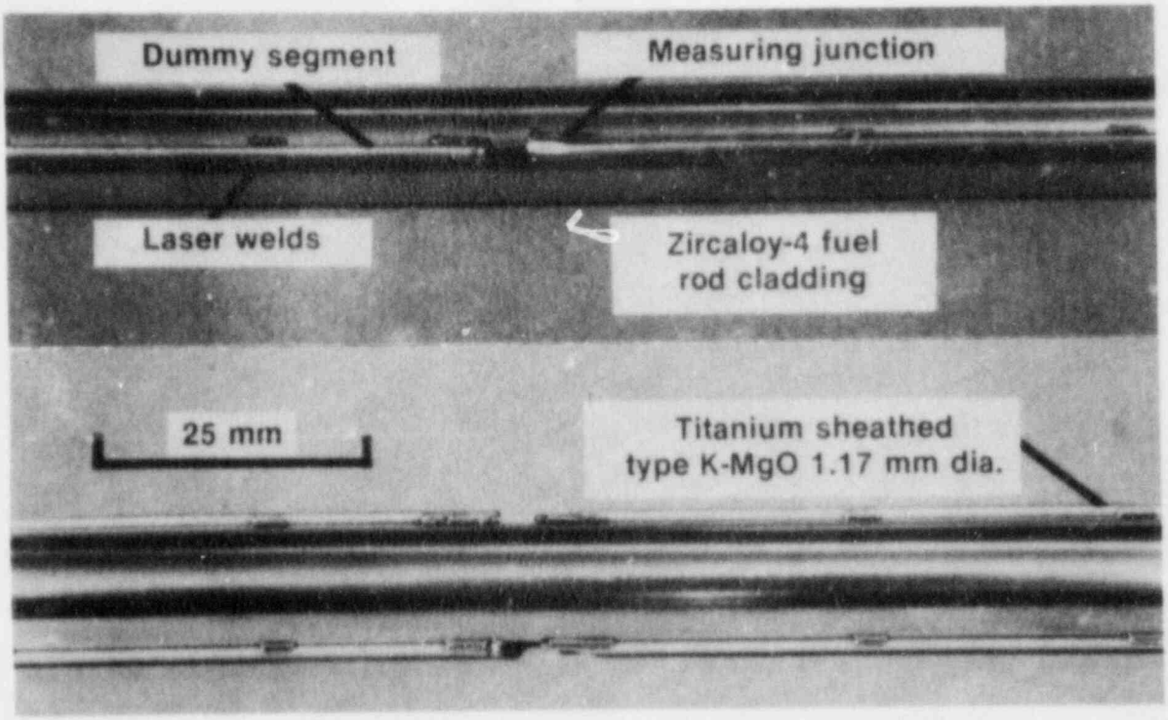

Figure 9. LOFT fuel rod cladding external thermocouple attachment.

Table 2. External thermocouple locations on REBEKA heater rod

Thermocouple	Location of Thermocouple Junction from Bottom of Heated Length (mm)	Azimuthal Location in a Clockwise Direction Looking Down from the Top End of the Rod (degrees)
TE-REB-X1	150	45
TE-REB-X2	1950	135
TE-REB-X3	1000	225
TE-REB-X4	[illegible]90	315

After completing the experiments with the cladding external thermocouples in place, the REBEKA rod was removed from the bundle and the external thermocouples were carefully removed from the cladding. The laser weld material was then removed from the cladding surface, and the surface was redressed.

Cladding Embedded Thermocouples. Thermocouples to be embedded in the internal side of the cladding of LOFT nuclear fuel rods were recently developed. A description of the prototype design of this instrument is contained in Appendix A. The final design and fabrication of the thermocouples used in the LOFT fuel rods are slightly different than the prototype instruments used in the REBEKA rod, as explained in Appendix A. Two prototype instruments were installed in the REBEKA rod to obtain data on the adequacy of the design and installation procedures and to perform a functional test on the thermocouples. These two embedded thermocouples were also to function as the primary cladding temperature measurement to determine the quench behavior of the REBEKA rod both with and without the external thermocouples.

The embedded thermocouples were Type K, with alumina insulation and a Zircaloy sheath. The basic thermocouple had a sheath diameter of 0.762 mm. The junction end of the thermocouple was swaged to a diameter of 0.457 mm and flattened to a thickness of 0.254 mm over a length of about 40 mm. The flattened end was laser welded into a groove in a patch of cladding. The patch (or insert) was then laser welded into a corresponding slot in the main piece of cladding. The thermocouple lead extended toward the top of the rod through a 1.016-mm groove running axially in the alumina pellets, see Figure 10, penetrated the cladding near the top of the rod through a specially designed fixture, see Figure 11, and passed through a Conax fitting in the top head of the test section. A cross section of an embedded thermocouple installed in a piece of cladding is shown in Figure 12. The axial location and azimuthal placement of the embedded thermocouples are given in Table 3. The junctions of both embedded thermocouples were located at the middle of the heated length (or hot spot) of the REBEKA rod (1950 mm from the bottom of the heated length of the rod), and azimuthally relative to the external thermocouples as shown in Figure 13.

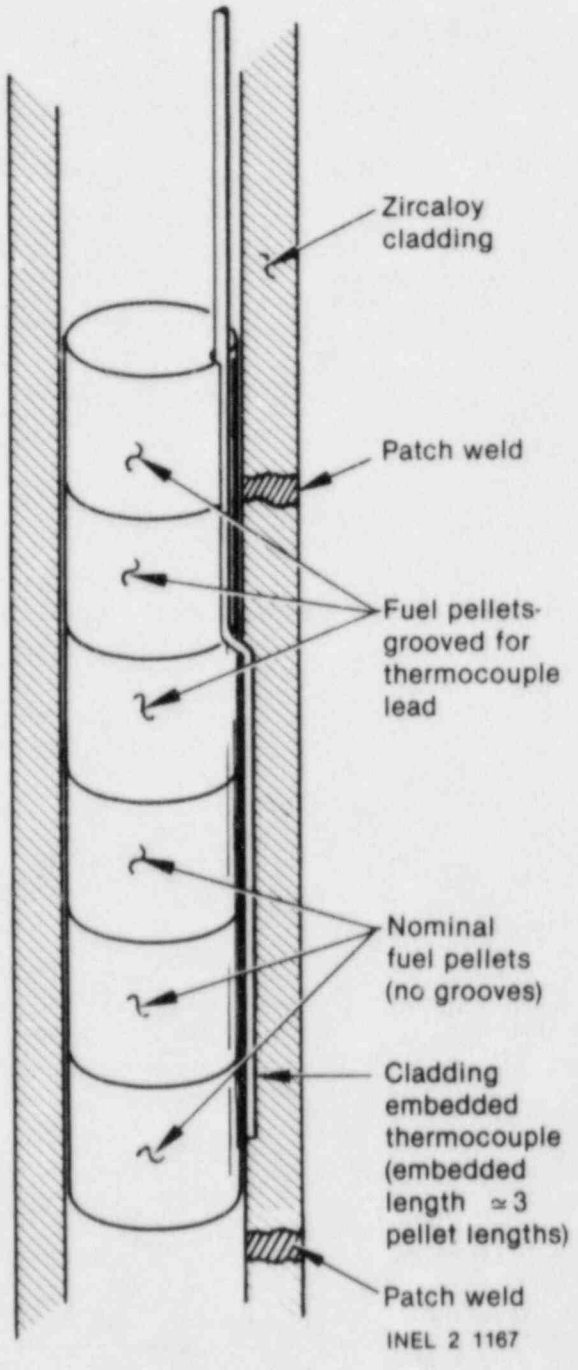

Figure 10. Illustration of cladding embedded thermocouple installation.

REBEKA Rod Internal Thermocouples. The REBEKA rod was originally fabricated at KfK with three internal thermocouples. These thermocouples were Type K and were 0.25 mm in diameter. The thermocouples were embedded in the surface of the Inconel sheath surrounding the heater element. These thermocouples were not intended to be the

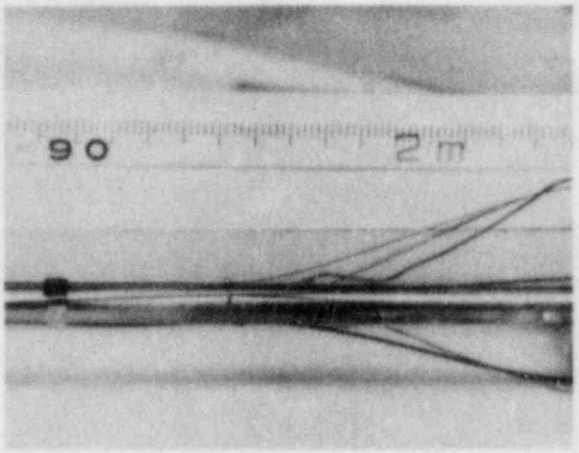

Figure 11. Embedded thermocouple lead penetration through cladding.

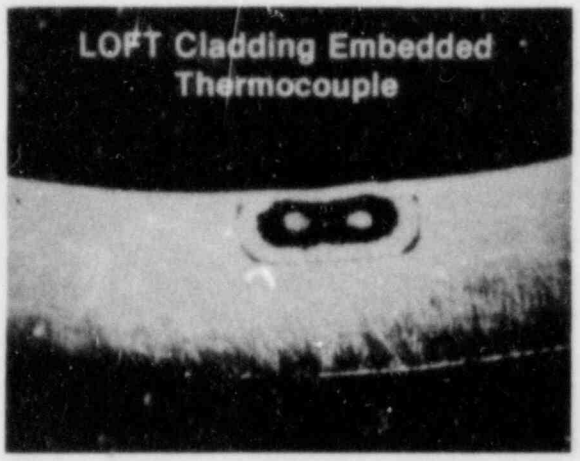

Figure 12. Cladding cross section showing embedded thermocouple installation.

Table 3. Embedded thermocouple locations in REBEKA heater rod

Thermocouple	Location of Thermocouple Junction from Bottom of Heated Length (mm)	Azimuthal Location in a Clockwise Direction Looking Down from the Top End of the Rod (degrees)
TE-REB-E1	1950	0
TE-REB-E2	1950	135

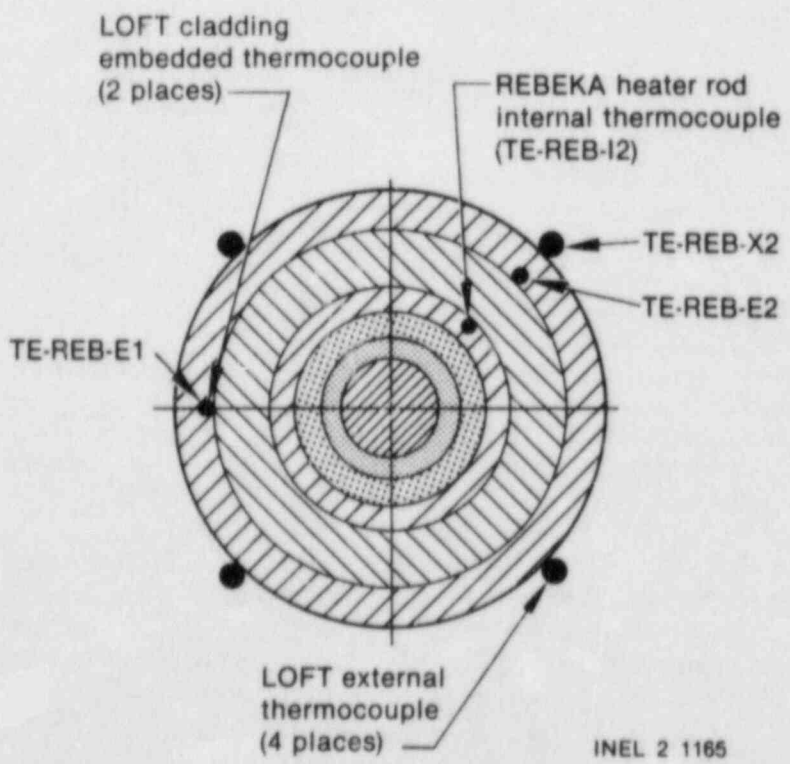

Figure 13. REBEKA heater rod thermocouple locations.

primary indicator of the quench behavior of the rod due to their radial distance from the cladding; however, these measurements were valuable after the experiments were conducted for comparison with inverse heat conduction calculations that were performed on the rod. The locations of the internal thermocouples in the REBEKA rod are given in Table 4.

Thermocouple TE-REB-I2 was located at the hot spot of the rod adjacent to an embedded thermocouple (TE-REB-E2) and an external thermocouple (TE-REB-X2) for comparison purposes (see Figure 13).

FEBA Rod Thermocouples. Each FEBA rod had four Type K thermocouples embedded and brazed in the outer surface of the cladding at 90-degree intervals azimuthally. Two different sets of axial locations of the junctions were used. The thermocouple junction locations are shown in Figures 14 and 15. The thermocouple locations on each rod are related to the thermocouple identification numbers in Appendix D.

Test Section Wall Thermocouples. Six thermocouples were installed in the heater vessel wall to measure the heatup rate of the vessel. Locations of the thermocouple junctions were 150, 500, 1000, 1950, 2900, and 3400 mm from the bottom of the heated length of the rods. The thermocouples were installed in a small hole in the pipe wall such that the junction was only 1.59 mm radially from the inside surface of the test section wall.

Test Section Flow Rate. The flow rate to the test section (FE-FCV-1T) was measured with a turbine meter located upstream of Valve FCV-1T. The pressure in the main loop was maintained at least 1.8 MPa above the saturation pressure of the fluid in the main loop such that the turbine meter measured single-phase liquid flow at all times.

Fluid Density Measurement. A one-beam gamma densitometer (DE-B) was located on the test section at the hot spot of the rods (1950-mm elevation). The purpose of this measurement was primarily to determine when the slug of high-density fluid reached the midpoint of the rods where the two embedded thermocouple junctions and one external thermocouple junction were located.

Table 4. Internal thermocouple locations in REBEKA heater rod

Thermocouple	Location of Thermocouple Junction from Bottom of Heated Length (mm)	Azimuthal Location in a Clockwise Direction Looking Down from the Top End of the Rod (degrees)
TE-REB-I1	1000	240
TE-REB-I2	1950	120
TE-REB-I3	2900	0

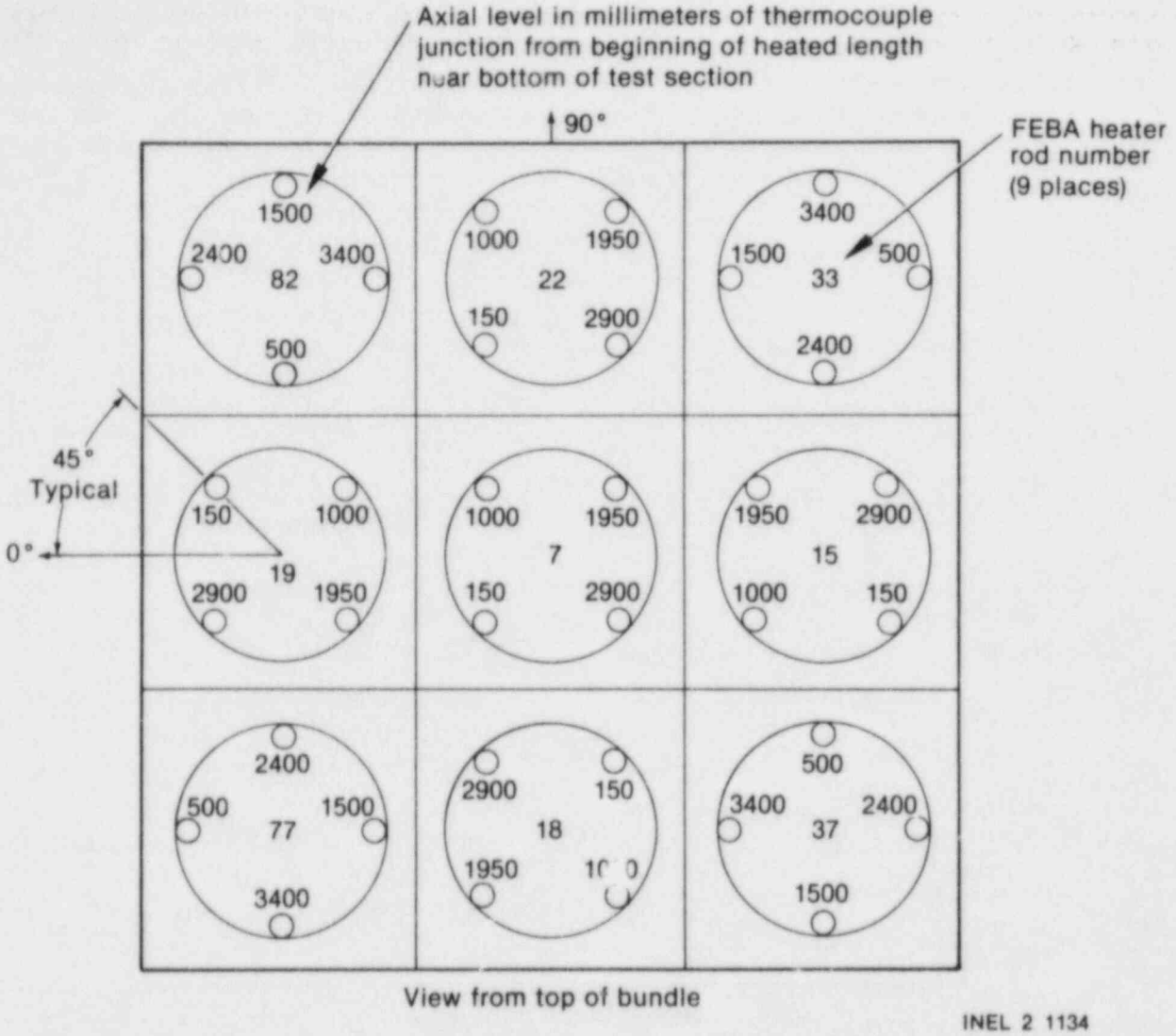

Figure 14. Nine-rod bundle of FEBA heater rods.

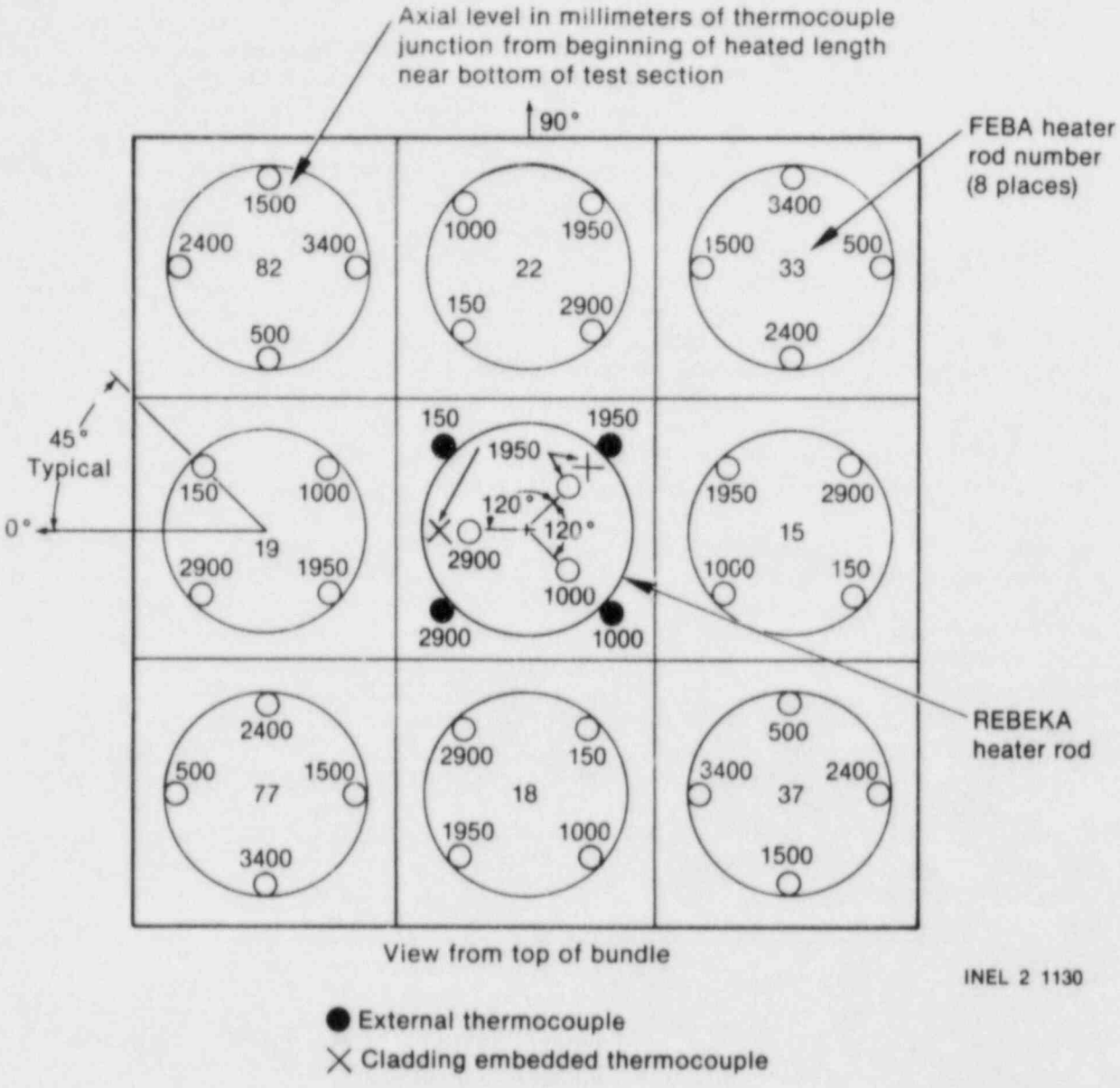

Figure 15. Nine-rod bundle with a REBEKA center heater rod.

3. EXPERIMENT CONDITIONS AND OPERATING PROCEDURE

The experiment conditions and operating procedure for the separate effects experiment of the FEBA and REBEKA heater rods in the LTSF are described in the following sections. Also, repeatability of the experiment conditions is discussed.

Experiment Matrix

The thermal-hydraulic conditions for this experiment were chosen to reproduce the thermal-hydraulic conditions believed to have existed in the LOFT core at the time of the fuel rod quenching that occurred during the blowdown phase of LOFT LOCE L2-3. The pressure in the LOFT core was measured to be about 7 MPa at the time of quench. No direct measurements were made of the fluid density and velocity; however, calculations have been made for these parameters from other measurements in the LOFT core in order to bound the thermal-hydraulic conditions.

The upper bound estimate on LOFT core mass flux during LOCE L2-3 was calculated using the cladding thermocouple measurements on the fuel rods, and the self-powered neutron detectors (SPNDs). The relative quench times of the thermocouples axially indicated a slug of fluid moved through the core from bottom to top at a velocity of 1 to 2 m/s. The SPND measurements indicated the fluid density to be 613 ± 80 kg/m^3 and 738 ± 118 kg/m^3 in the central and peripheral fuel bundles, respectively, at about 6 s into the blowdown, when the quench occurred.[8] Therefore, the upper bound on mass flux ranged from 1107 to 1328 kg/s-m^2, depending on which density was used.

The lower bound on LOFT core mass flux during LOCE L2-3 was estimated from postexperiment calculations using RELAP4/MOD1.[9] These calculations showed the core inlet velocity and density to be 1.4 m/s and 317 kg/m^3, respectively, at the time the fuel rods quenched. This resulted in a lower bound estimate on mass flux of 444 kg/s-m^2.

Since there was a fairly large uncertainty in the thermal-hydraulic conditions in the LOFT core during LOCE L2-3, the test section inlet hydraulic conditions for this separate effects experiment were intended to approximately cover the range in uncertainty in mass flux and fluid quality in the LOFT core. However, it was also desired to limit the number of experiment runs with and without cladding external thermocouples because it was not known how long the prototype cladding-embedded thermocouples would function and provide data relative to the cladding external thermocouple effects on quench behavior. Therefore, a compromise was made in the number of experiment runs performed. A total of 10 experiment runs was originally planned, five with cladding external thermocouples and five without. Test section inlet fluid velocities of 1 and 2 m/s with saturated liquid at the inlet were established to cover a range of mass fluxes from 746 to 1492 kg/s. Fluid quality effects were investigated by using a test section inlet fluid quality of 10% at a velocity of 2 m/s, representing a mass flux of 502 kg/s-m^2. The experiment matrix included a repeat of the first experiment run and a low-pressure experiment run to investigate cladding external thermocouple effects under low-pressure, low-flow reflood conditions. LOFT fuel rod cladding temperatures of about 900 K prior to quench were simulated in these experiment runs.

Table 5 lists the conditions for each experiment run. Experiment Runs 1 through 5 and 1A through 5A were to be conducted to investigate cladding external thermocouple effects on quench behavior. Run 3AR was a repeat of Run 3A. Prior to the experiment runs using the REBEKA rod, Runs 1F through 5F were conducted on a bundle of nine FEBA heater rods to provide data for comparison of the quench behavior of solid- and cartridge-type heater rods.

Three test runs at lower mass fluxes (Runs 6A, 7A, and 8A) were conducted on the bare REBEKA rod at 7 MPa at the end of the experiment program to investigate the quench behavior of the REBEKA rod as a function of mass flux.

Experiment Operating Procedure

The rod bundle with nine FEBA rods was assembled and installed for the first series of experiment runs (Runs 1F through 5F). These runs provided data on the quench behavior of a solid-type heater rod in a nine-rod bundle geometry and also provided system checkout tests prior to installing the REBEKA heater rod. The FEBA bundle configuration along with rod identification numbers is

Table 5. Experiment matrix

Experiment Run	Test Section Pressure (MPa)	Test Section Inlet Fluid Quality (%)	Test Section Inlet Fluid Velocity (m/s)	Test Section Mass Flux (kg/s-m^2)	Rod Hot Spot Initial Temperature (REBEKA and FEBA Rods) (K)
1F[a], 1[b], 1A[c]	7.0	0	1	746	900
2F, 2, 2A	7.0	0	2	1492	900
3F, 3, 3A 3AR[d]	7.0	10	2	502	900
4F, 4, 4A	7.0	0	1	746	900
5F, 5, 5A	0.35	0	0.04	39.3	900
6A	7.0	0	0.27	200	900
7A	7.0	0	0.135	100	900
8A	7.0	0	0.067	50	900

a. Runs 1F through 5F were conducted on the bundle of nine FEBA rods.

b. Runs 1 through 3 were conducted on the bundle with the REBEKA rod with cladding external thermocouples. Runs 4 and 5 were not performed.

c. Runs 1A through 8A were conducted on the bundle with the REBEKA rod without cladding external thermocouples.

d. Run 3AR was a repeat of Run 3A.

shown in Figure 14. After Experiment Runs 1F through 5F were completed, the bundle was removed from the test section and the center FEBA rod (No. 7) was replaced with the REBEKA rod with cladding external thermocouples attached. The bundle was then reinstalled in the test section. Upon completing the experiment runs using the REBEKA rod with cladding external thermocouples attached, the bundle was removed from the test section and the REBEKA rod was removed from the bundle. The cladding external thermocouples were then removed from the REBEKA rod, and the bundle was reassembled and placed back in the test section. Nine experiment runs (Runs 1A through 8A) were then conducted on the bundle with the REBEKA rod without cladding external thermocouples.

It was desired to conduct Experiment Runs 1F through 4F, 1 through 4, and 1A through 4A in a manner that would simulate the thermal-hydraulic conditions in the LOFT core at the time of the high-pressure quench during the blowdown phase of LOCE L2-3. In LOCE L2-3, the fuel rods experienced critical heat flux (CHF) about 1 s after the initiation of the blowdown. After the reactor was scrammed, the fuel rod cladding continued to heat up to about 900 K due to stored heat and decay heat, as shown in Figure 1. At about 6 s into the

transient, the cladding temperature stabilized near 900 K in a film boiling condition, low heat flux mode, with predominately steam in the core. Then a higher-density slug of coolant moved through the core from bottom to top at a rapid rate, apparently quenching the fuel rods, as indicated by the fuel rod cladding external thermocouples.

To simulate the LOCE L2-3 thermal-hydraulic conditions, the following procedure was used. First, the fluid in the main loop was heated to the required temperature needed to provide fluid at the test section inlet at the specified quality. Then nitrogen was injected into the empty test section through the surge tank, with Valve FCV-1T closed, until the pressure in the test vessel and surge tank reached 7 MPa. Power to the REBEKA and FEBA heater rods was then turned on until the rods heated up to 900 K at the hot spot. The heatup rate of the rods was approximately 4 K/s. Power to the rods was programmed to maintain the rod hot spot (1950-mm elevation) temperatures, as measured by Thermocouples TE-REB-E2 and TE-15-3, at a constant 900 K until the experiment was initiated. The test section wall was allowed to heat up by radiation from the heater rods and convection until the wall temperature at the 1950-mm elevation (measured by TE-VWTC4) reached about 700 K. At this point, the heater rods had a fairly uniform temperature radially, were at a very low power level, and were judged to produce a reasonable simulation of the LOFT fuel rods in film boiling at about 6 s into the LOCE L2-3 transient. Just prior to experiment initiation, the main loop pump was turned off, the small circulation line from FCV-1T to the pump inlet was closed, and the nitrogen vent line at the test section inlet was closed. Also, the nitrogen supply line from the nitrogen supply tanks to the main loop pressure vessel was opened, pressurizing the main loop to 12 MPa. This provided the driving pressure to force the fluid in the main loop into the test section and to assure a subcooled fluid condition at the turbine meter (FE-FCV-1T) so that an accurate measurement of the flow rate into the test section could be obtained. The experiment run was then initiated by opening Valve FCV-1T. This simulated a rapid flooding rate into the LOFT core at the time of the quench during LOCE L2-3. The flow rate to the test section was controlled by the nitrogen overpressure in the main loop and an orifice plate located immediately downstream of Valve FCV-1T at the test section inlet.

Once the experiment was initiated by opening Valve FCV-1T, the power to the REBEKA and FEBA heater rods was controlled at a constant value equivalent to the power level on the rods immediately prior to experiment initiation. However, this power level was very low (approximately 0.2 kW/m at the hot spot of the REBEKA and FEBA rods) and had no influence on the cooldown rate or quench time of the rods.

Several thermocouples along the length of the REBEKA and FEBA rods were monitored to determine when the rods were quenched. When the rods were completely quenched, Valve FCV-1T was closed to end the experiment.

Repeatability of Experiment Conditions

The experiment conditions in the test section were duplicated very well for experiment runs requiring the same experiment conditions. Comparisons of the test section flow rate and pressure for Experiment Runs 1, 1A, and 4A are shown in Figures 16 and 17, respectively. Similarly, comparisons of the test section flow rate and pressure for Experiment Runs 3A and 3AR are shown in Figures 18 and 19, respectively. The test section inlet fluid quality was repeatable within a fraction of 1% for the various experiment runs with the same experiment conditions. The good repeatability of experiment conditions allows for meaningful comparisons of the thermal response of the REBEKA rod with and without external thermocouples and comparisons of the quench behavior of the REBEKA and FEBA heater rods.

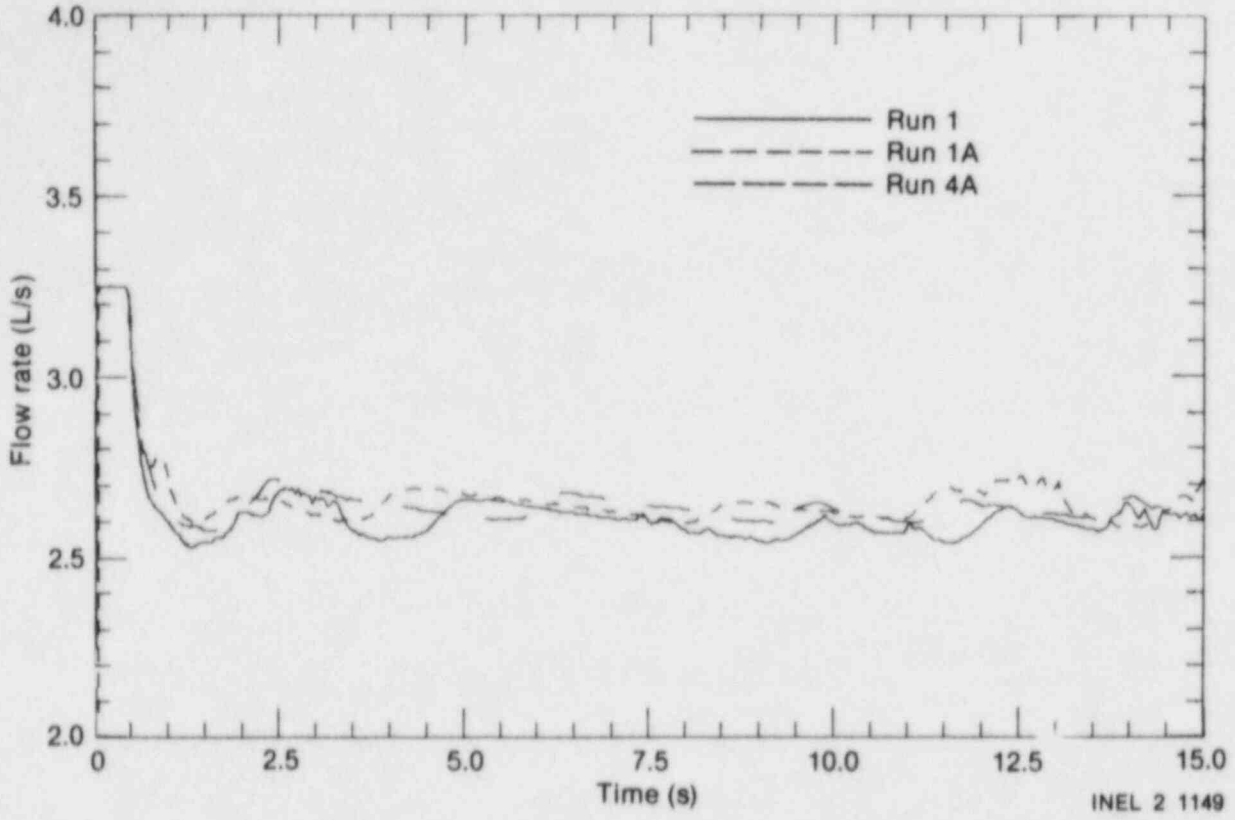

Figure 16. Repeatability of test section flow rate for Runs 1, 1A, and 4A.

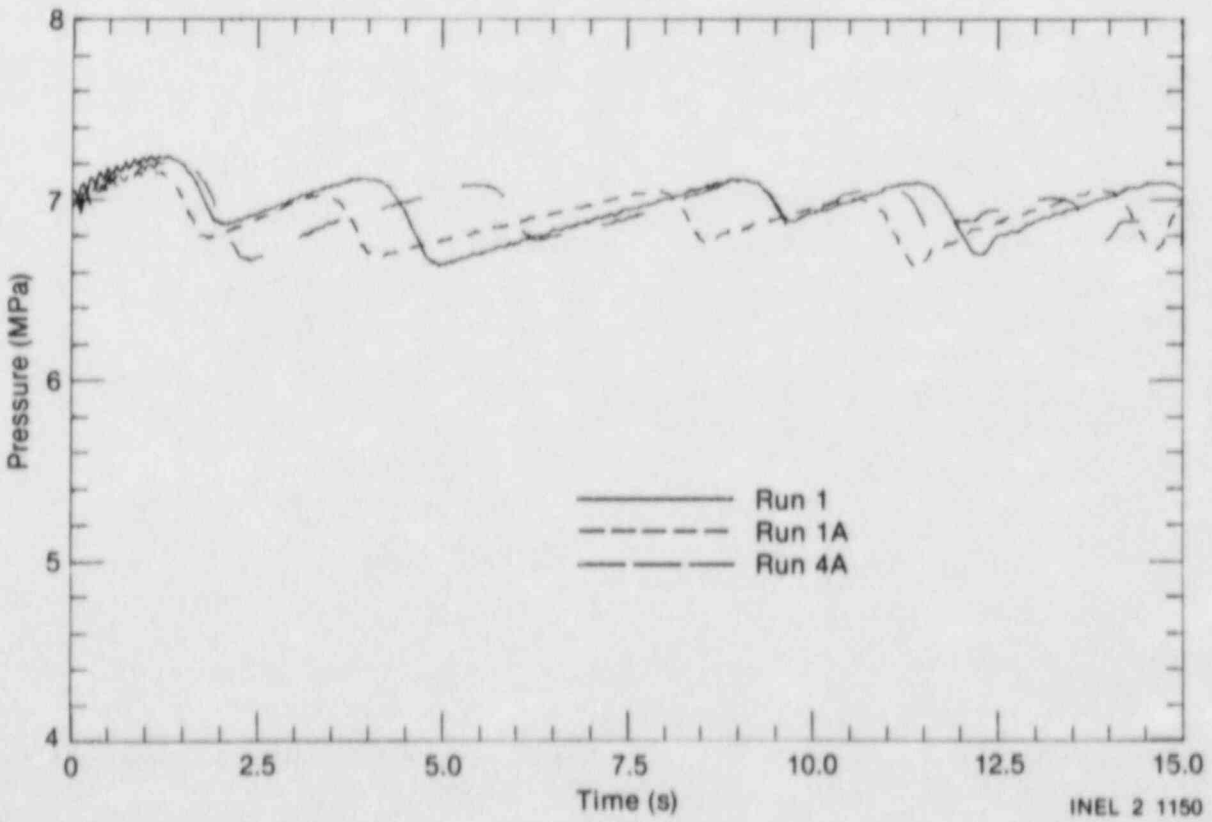

Figure 17. Repeatability of test section pressure for Runs 1, 1A, and 4A.

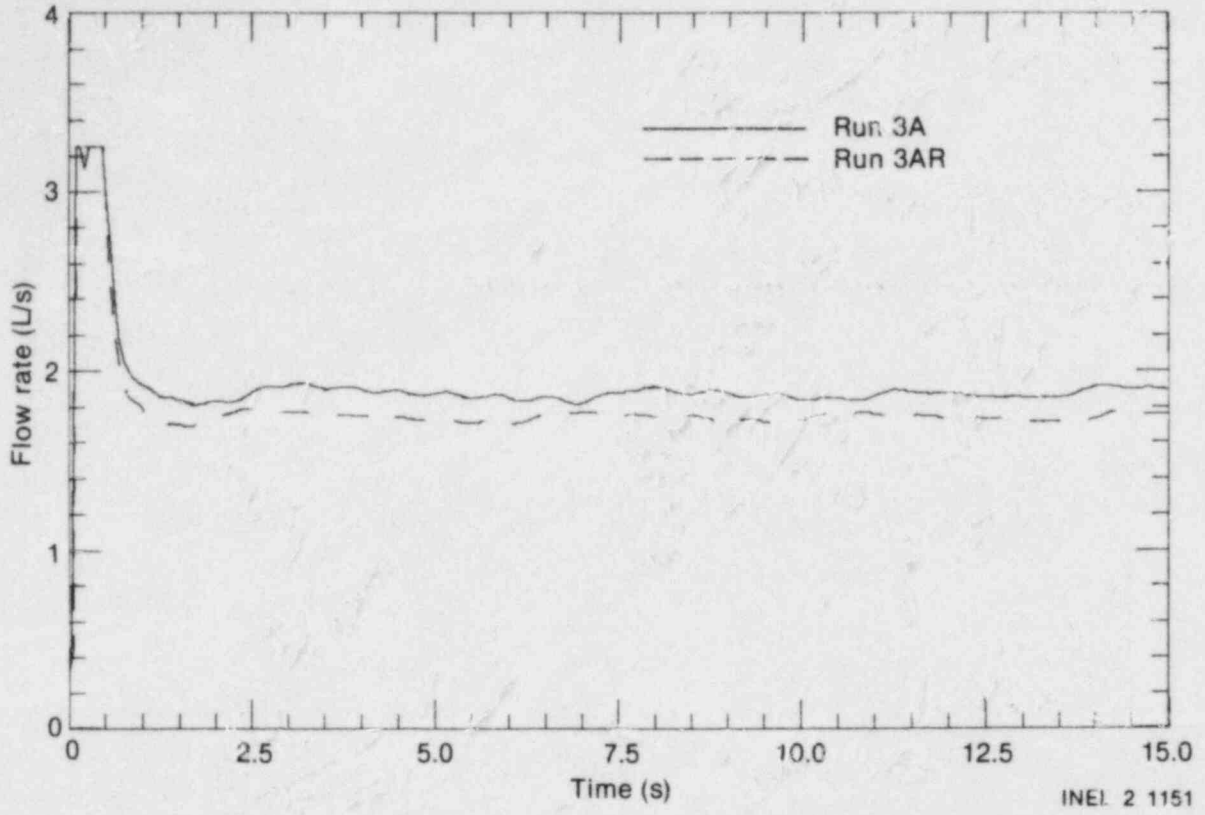

Figure 18. Repeatability of test section flow rate for Runs 3A and 3AR.

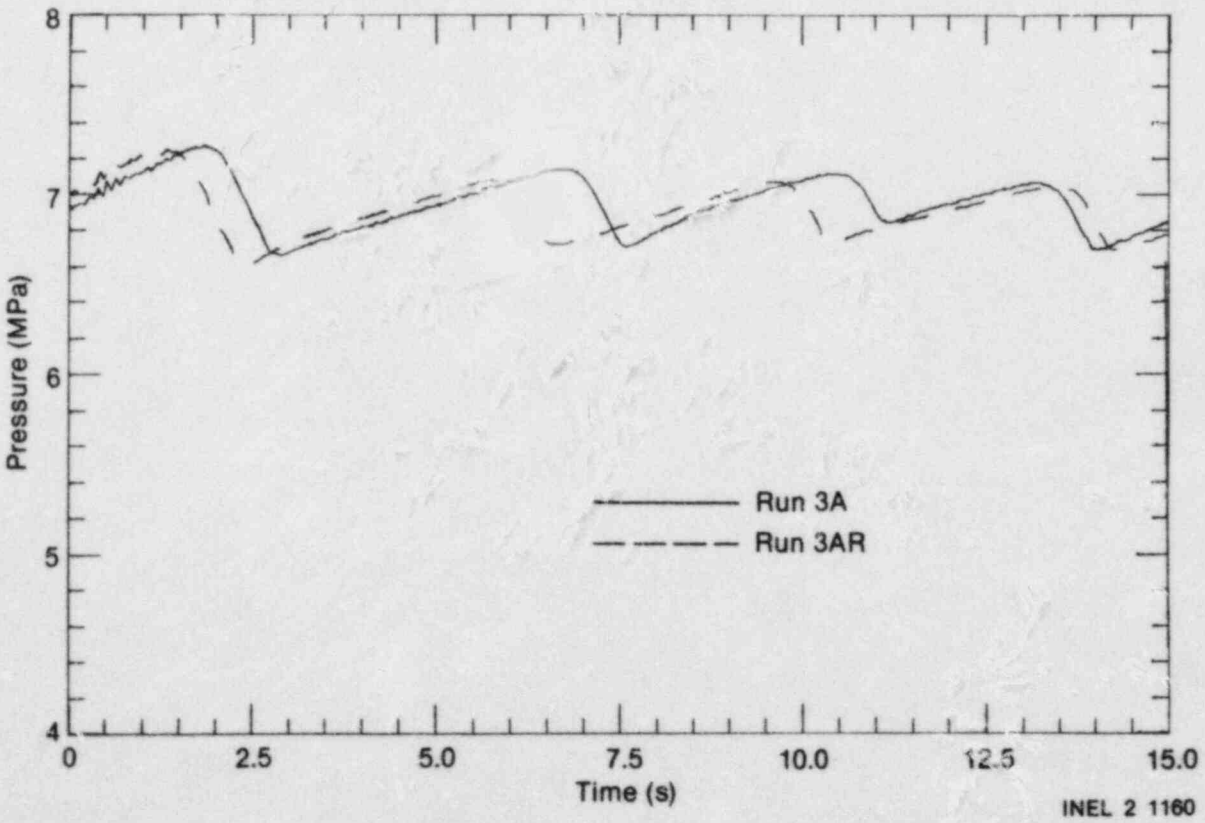

Figure 19. Repeatability of test section pressure for Runs 3A and 3AR.

4. EXPERIMENT PERFORMANCE OF CLADDING EMBEDDED THERMOCOUPLES AND OF REBEKA ROD

This section of the report describes the scenario of the performance of the cladding embedded thermocouples in the REBEKA rod and the performance of the REBEKA rod itself during the experiment runs with and without external thermocouples on the REBEKA rod. The primary junctions of the cladding embedded thermocouples failed early in the experiment, however, secondary junctions were formed. Also, REBEKA rod cladding creepdown occurred throughout the experiment. A description of these events is important in order to understand how the data from the secondary junctions of the cladding embedded thermocouples (TE-REB-E1 and TE-REB-E2) were used to compare the quench behavior of the REBEKA rod with and without external thermocouples (see Section 5).

Cladding Embedded Thermocouple History Prior to Experimentation

The prototype LOFT cladding embedded thermocouples were intended to be the primary instruments to measure the quench behavior of the REBEKA rod and to provide an accurate measurement of the cladding temperature to compare with the external thermocouple measurements. The prototype cladding embedded thermocouples were fabricated at the INEL, as described in Appendix A. The technique for laser welding the thermocouples into the cladding was developed at the INEL and at Exxon Nuclear Corporation. The REBEKA rod was disassembled at Exxon Nuclear Corporation, and the embedded thermocouples were laser welded into a cladding insert, which was then laser welded into the cladding as shown in Figure 20. The REBEKA rod was then reassembled at Exxon and shipped to the INEL.

The LOFT-type cladding external thermocouples were laser welded to the REBEKA rod at the INEL, as shown in Figure 9. Also, a pin hole leak in one of the welds on the REBEKA rod was fixed, and a helium leak test on the rod was conducted. The rod was then pressurized internally to 2.4 MPa with helium and shipped to the LTSF for bundle assembly and experimentation.

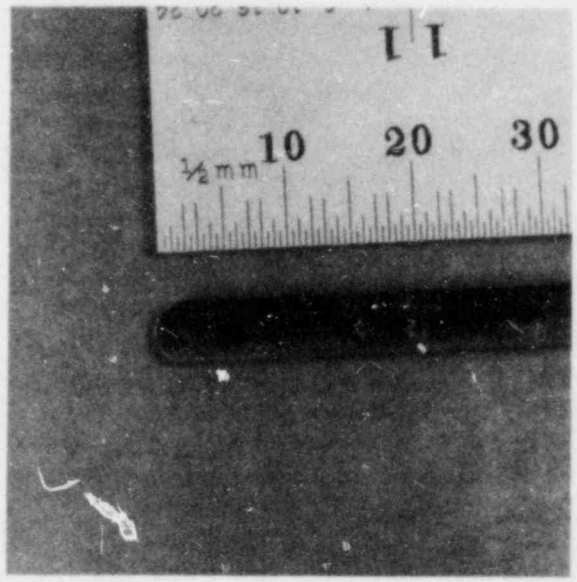

Figure 20. Installation of embedded thermocouple in cladding insert.

During the period of embedded and external thermocouple installation on the REBEKA rod, loop resistance measurements on all of the rod thermocouples were taken continuously and found to be normal. A hot gun test indicated all thermocouples to be functioning properly prior to bundle assembly. However, after final bundle assembly and just prior to installing the nine-rod bundle into the test loop, erratic loop resistance measurements on the embedded thermocouples were obtained as well as normal measurements. No particular reason for this behavior was apparent. The decision was made to run the experiments, with optimism that the embedded thermocouples would function long enough to obtain quench data on the REBEKA rod.

Experiments with External Thermocouples on REBEKA Rod

During the heatup for Experiment Run 1 (see Table 5), the cladding-embedded Thermocouple TE-REB-E2 appeared to be functioning properly; however, TE-REB-E1 appeared to have an open junction until the rods started to heat up, at which time TE-REB-E1 began working and both

embedded thermocouples functioned throughout the experiment. Cladding temperatures of 900 K prior to Experiment Run 1 were measured by both embedded thermocouples, which agreed very closely with cladding external Thermocouple TE-REB-X2 and REBEKA rod internal Thermocouple TE-REB-I2 at the same axial elevation.

A comparison of the cooldown rates measured by the internal thermocouple (TE-REB-I2), the cladding embedded thermocouples (TE-REB-E1 and TE-REB-E2), and the cladding external thermocouple (TE-REB-X2) for Experiment Run 1 are shown in Figure 21. The internal and external thermocouple responses were as expected; however, the temperatures recorded by the embedded thermocouples did not indicate a distinct quench from a high temperature, as was expected based on the observed quench behavior of other heater and nuclear rods. It appeared that the embedded thermocouples were not measuring the cladding temperature of the REBEKA rod at the embedded junction, but rather a gap temperature.

Experiment Run 3 was conducted next. Both of the cladding embedded thermocouples functioned during this run, showing basically the same type of cooldown rate as for Run 1.

Experiment Run 2 followed Run 3. Embedded Thermocouple TE-REB-E1 was functioning prior to bundle heatup; however, TE-REB-E2 indicated an open junction. During heatup, TE-REB-E2 began functioning and functioned throughout Experiment Run 2. However, TE-REB-E1 did not give a consistent reading during Run 2.

At this point in the experiment program, it was not known how long the embedded thermocouples would continue to function, and it was desired to obtain some comparison data on the REBEKA rod without cladding external thermocouples in order to meet the experiment objectives. A decision was made not to do Experiment Runs 4 and 5, and instead, to remove the bundle from the test loop. The REBEKA rod was removed from the bundle

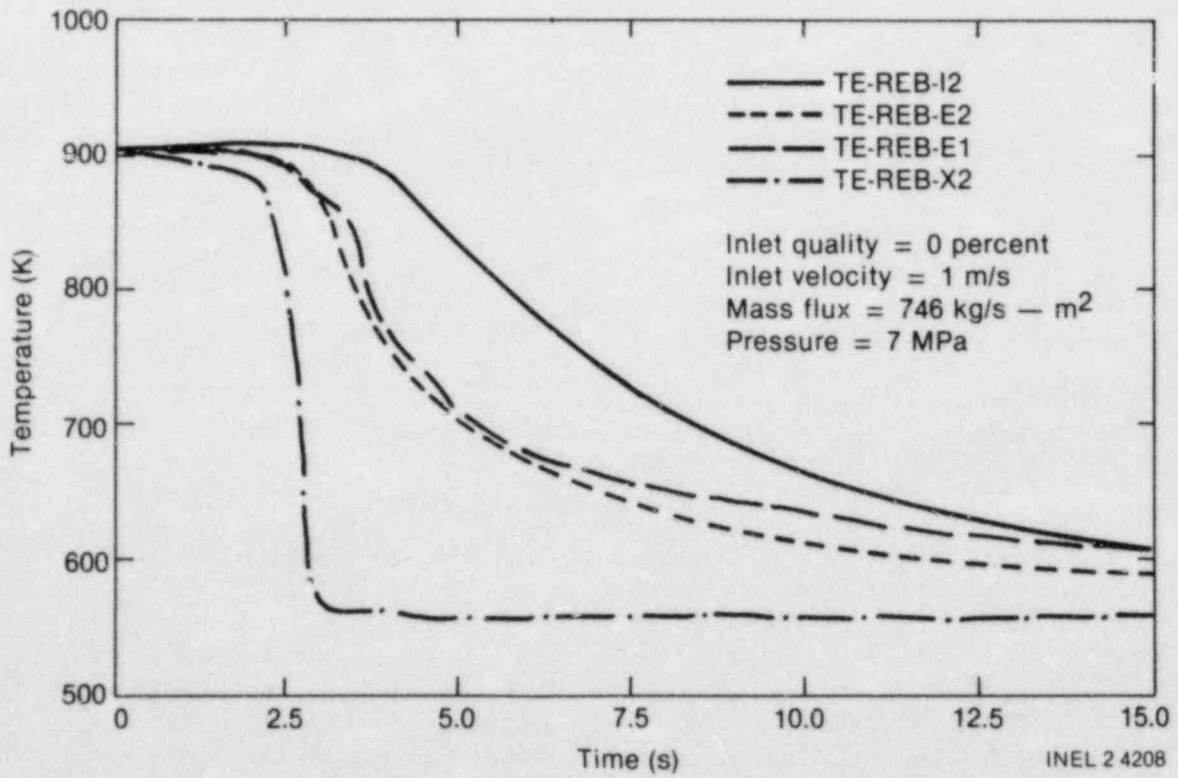

Figure 21. REBEKA heater rod measured temperature response for Run 1.

and the four cladding external thermocouples were removed from the REBEKA rod as described in Section 2.

While the REBEKA rod was out of the bundle, a hot gun test was conducted on both cladding embedded thermocouples. It was verified that the embedded junctions were not functioning at all. However, a secondary junction had formed in each of the embedded thermocouple wires, but the new junctions were just above the region where the thermocouples were embedded in the cladding insert. The secondary junction on embedded Thermocouple TE-REB-E2 was located 5 cm downstream of the embedded junction and about 1.8 cm downstream of where the thermocouple wire comes out of the groove in the cladding insert and into the groove in the Al_2O_3 pellets. This is also the location where the embedded thermocouple necked down from 0.762 to 0.457 mm diameter. The secondary junction on embedded Thermocouple TE-REB-E1 was located 58.5 cm downstream of the embedded junction. The locations of the secondary junctions explained the peculiar cooldown rates measured by the embedded thermocouples. That is, they were actually measuring a temperature inside of the cladding and across the gap in the heater rod. The secondary junctions that were formed were still close to the middle of the rod and well within the highest heating zone of the rod, which explained why the initial measured temperatures of 900 K were consistent with the internal and external thermocouple measurements at the middle of the rod axially.

The cause of the failure of the primary embedded thermocouple junctions or why secondary junctions were formed was not known at the time the experiments were performed.

REBEKA rod cladding deformation, which could affect the results of the experiments was evaluated by taking diameter measurements at various axial and azimuthal positions on the rod throughout the experiment. All values are tabulated in Appendix E for comparison with preexperiment measurements. It was found that the cladding did collapse somewhat during the first three experiment runs, but not enough to close the gap between the cladding and Al_2O_3 pellets. For example, preexperiment measurements indicated the cladding outer diameter was 10.74 mm at the 1950-mm axial elevation of the rods. The Al_2O_3 pellets had an outer diameter of 9.093 mm and a cladding thickness of 0.72 mm. This resulted in an average initial radial gap of 0.1035 mm.

The rod diameters measured after the first three experiment runs are plotted as a function of length in Appendix E. At the 1950-mm elevation, the average rod diameter was 10.6 mm and the average radial gap was 0.0335 mm. This indicated the possibility of a leak in the rod and a decreased internal rod pressure during the experiment, since the rod cladding was not expected to collapse with the initial 2.4 MPa pressurization.

Due to the abnormal behavior of the embedded thermocouples and the collapse of the cladding, a post-mortem was conducted on the rod at the completion of the experiment program (a) to investigate the failure mechanism of the primary embedded thermocouple junctions, (b) to investigate the reason for the formation of the secondary junctions in the embedded thermocouple wires, and (c) to measure the internal pressure in the REBEKA rod to determine why the cladding collapsed. The results are reported in Appendix B. It was determined that the primary thermocouple junctions failed prior to the first experiment run and that the REBEKA rod depressurized during the experiment. The formation of the secondary thermocouple junctions is not fully understood at this time.

Experiments Without External Thermocouples on REBEKA Rod

Although problems were encountered during the first series of experiments with the collapse of the REBEKA rod cladding and the cladding embedded thermocouples as discussed in the preceding section, it was determined that reasonable comparisons of the quench behavior of the REBEKA rod with and without external thermocouples could be obtained provided the secondary junctions in the embedded thermocouple wires would continue to function. The REBEKA rod without cladding external thermocouples was reinstalled into the nine-rod bundle, and Experiment Runs 1A through 8A, listed in Table 5, were performed.

For Experiment Run 1A, embedded Thermocouple TE-REB-E1 was working and TE-REB-E2 was not working prior to bundle heatup. During heatup, TE-REB-E2 began working and functioned

throughout the experiment; however, TE-REB-E1 did not function during the experiment. Thermocouple TE-REB-E2 provided reasonable data for comparison with Experiment Run 1.

Experiment Run 3A was conducted next. Both embedded thermocouples functioned throughout the run, as shown in Figure 22. However, Thermocouple TE-REB-E2 indicated an extended precursory cooldown time with a lower and more distinct quench temperature, similar to solid heater rods. This indicated that the gap may have closed near TE-REB-E2. Thermocouple TE-REB-E1 showed a cooldown rate very similar to earlier experiment runs and could be used for comparisons. Thermocouple TE-REB-E2 was not used for comparison purposes from this point on.

Experiment Run 2A followed Run 3A. Both Thermocouples TE-REB-E1 and TE-REB-E2 functioned during this run. Thermocouple TE-REB-E2 indicated an extended precursory cooling time again, so only data from TE-REB-E1 was used for comparison with Experiment Run 2.

Experiment Run 4A was a repeat of Run 1A, and both Thermocouples TE-REB-E1 and TE-REB-E2 functioned during the run. Thermocouple TE-REB-E1 provided data for comparison with TE-REB-E2 for Run 1A and with TE-REB-E1 and TE-REB-E2 for Run 1.

Experiment Runs 6A, 7A, 8A, and 5A, respectively, were conducted at successively lower flooding rates. Both embedded thermocouples functioned during these runs.

After these experiment runs were conducted, the bundle was removed from the test loop, and the REBEKA rod was removed from the bundle. Diameter measurements were again taken at various axial and azimuthal locations on the rod. The results are tabulated and plotted in Appendix E. These measurements indicated the cladding had continued to collapse during this series of experiment runs. This is consistent with the measurements from Thermocouple TE-REB-E2, which indicated the gap between the Al_2O_3 pellets and the cladding had closed during and after Experiment Run 3A. Diameter measurements at the 1950-mm elevation

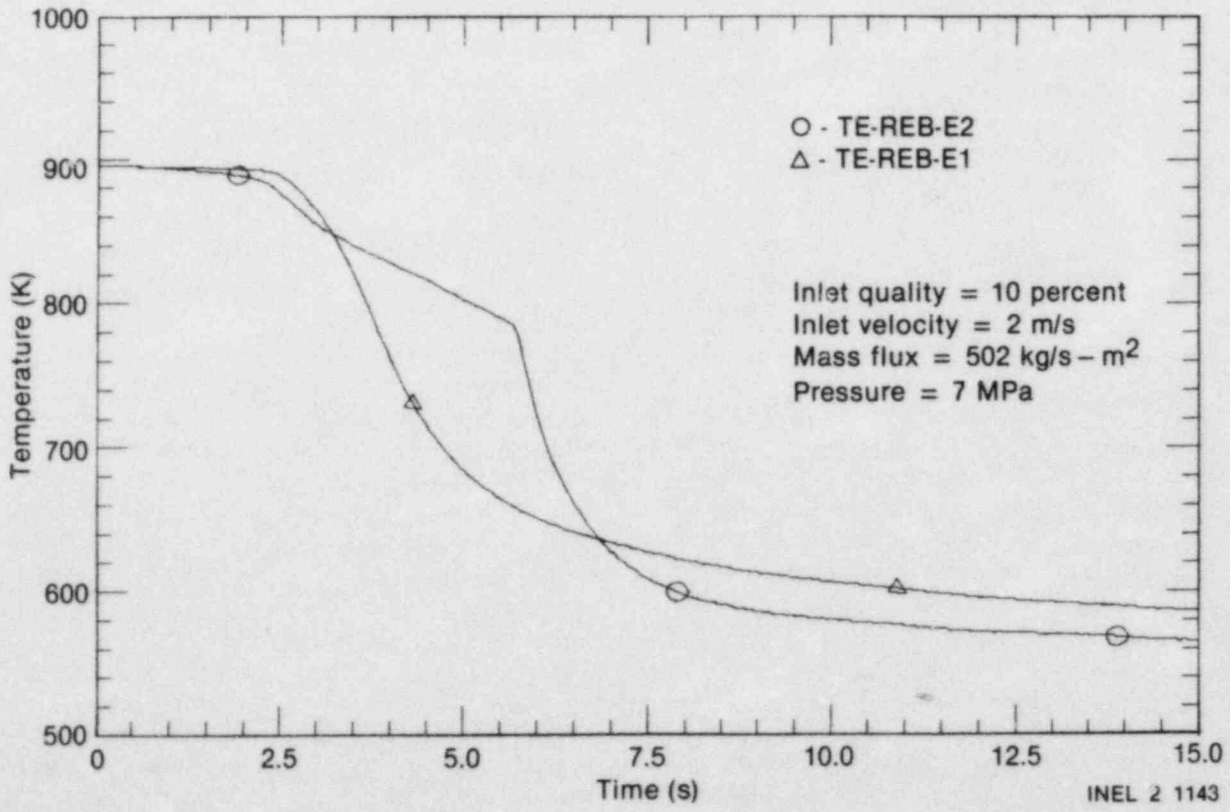

Figure 22. REBEKA heater rod measured temperature response for Run 3A.

on the heater rod indicated the average diameter to be 10.59 mm. The measurements indicated some nonuniform cladding collapse had occurred, since the diameter measurements were not uniform around the rod at this axial level and varied from 10.56 to 10.66 mm. On an average, the heater rod still had a radial gap of 0.0535 mm at the 1950-mm elevation.

At the axial level of the secondary junction of Thermocouple TE-REB-E1 (2535-mm elevation) the heater rod diameter was also nonuniform around the rod, with an average diameter of 10.63 mm. This resulted in an average radial gap of 0.0485 mm at the 2535-mm elevation, compared with an average radial gap of 0.074 mm after Experiment Runs 1, 2, and 3, and 0.104 mm initially.

5. ANALYSIS AND RESULTS

This section presents results from the experiment run with the FEBA nine-rod bundle and from experiment runs with the REBEKA rod. The REBEKA rod quench behavior is compared with that of a nuclear fuel rod, and the applicability of REBEKA rod experimental results to LOFT fuel rod performance is discussed. The REBEKA and FEBA rod responses are compared to determine whether the FEBA rod (solid-type heater rod) can simulate a nuclear fuel rod under LOFT LOCE blowdown conditions. Also, low-flow experimental results are presented which compare the quench behavior of the FEBA rods with that of the REBEKA rod at low-pressure and low-flow reflood conditions.

FEBA Nine-Rod Bundle Results

The primary data for analysis from the FEBA nine-rod bundle experiment were from FEBA Rod 7 in the center of the bundle (see Figure 14) with the surrounding eight FEBA rods providing boundary conditions typical of a nuclear reactor rod bundle. Experiment Runs 1F through 5F in Table 5 were conducted on the FEBA rod bundle at the same experiment conditions used for the REBEKA rod experiments. This allowed a comparison of quench behavior between solid- and cartridge-type heater rods.

At high flooding rates, the FEBA rods demonstrated a consistent thermal response at the hot spot, across the bundle. Figure 23 shows the temperature responses of FEBA Rods 7, 15, 18, 19, and 22 from thermocouples located axially at the hot spot of the rods (1950 mm from the bottom of the heated length of the rod) for a flooding rate of 1 m/s. The rods all had essentially the same precursory cooldown rate and quenched at about the same time (12 s) and at the same temperature of 700 ± 10 K. In Figure 23, the three solid line curves represent thermocouples which face interior channels in the bundle, while the two dashed lines curves repre ent thermocouples which face the test section wall. No significant differences in quench behavior were apparent among these rods.

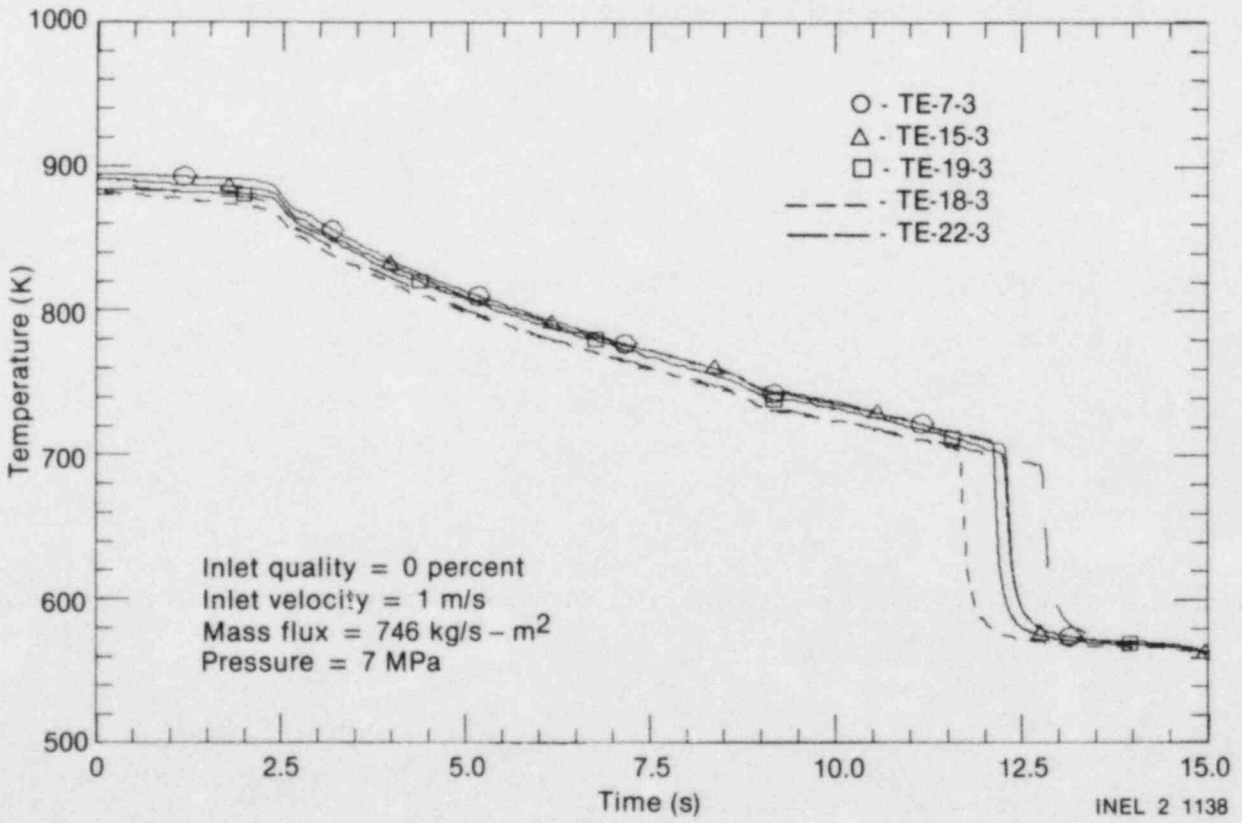

Figure 23. FEBA heater rod temperature response for F 1F.

Similarly, for a flooding rate of 2 m/s, Figure 24 shows the temperature responses of FEBA Rods 7, 15, 18, 19, and 22 for Experiment Run 2F. The same general behavior was exhibited as for Run 1F; however, the precursory cooling rate was a little higher, causing a slightly earlier quench time of 10.5 s. The quench temperature of the rods was still 700 K. Similar results were observed for Experiment Runs 3F and 4F. The uniform temperature response indicates that the thermal characteristics (material thermal properties and no pellet-cladding gap) of the solid-type heater rod control the quench behavior of the rod, rather than its position in the bundle.

The quench behavior of the FEBA rods was nearly identical to the quench behavior observed on other solid-type heater rods, such as the Semiscale rod,[4] at high-pressure and rapid flooding conditions. The rods spent a significant length of time in a precursory cooling mode in film boiling before being quenched about 10 to 12 s into the transient.

Experiment Run 5F was conducted at a low pressure (0.35 MPa) and a low flooding rate (0.04 m/s) to provide a comparison with the REBEKA rod at these conditions. Figure 25 shows the temperature response of Rods 7, 15, 19, 18, and 22 at the 1950-mm elevation for Run 5F. The rods underwent precursory cooling for about 115 s prior to quenching. The quench temperature varied from 600 to 655 K for these rods.

Accuracy of External Thermocouple Measurement and Effect of External Thermocouples on REBEKA Rod Quench Behavior

Due to the failure of the primary junctions of the cladding embedded thermocouples, no direct comparisons of the REBEKA rod cladding temperature response with and without external thermocouples could be made with these instruments. Also, no direct comparison could be made between the cladding temperature measured by the cladding embedded thermocouples and the temperature measured by the adjacent external thermocouple (TE-REB-X2). However, the experimental data obtained did allow comparisons to be made through inverse heat conduction calculations as discussed in the following paragraphs.

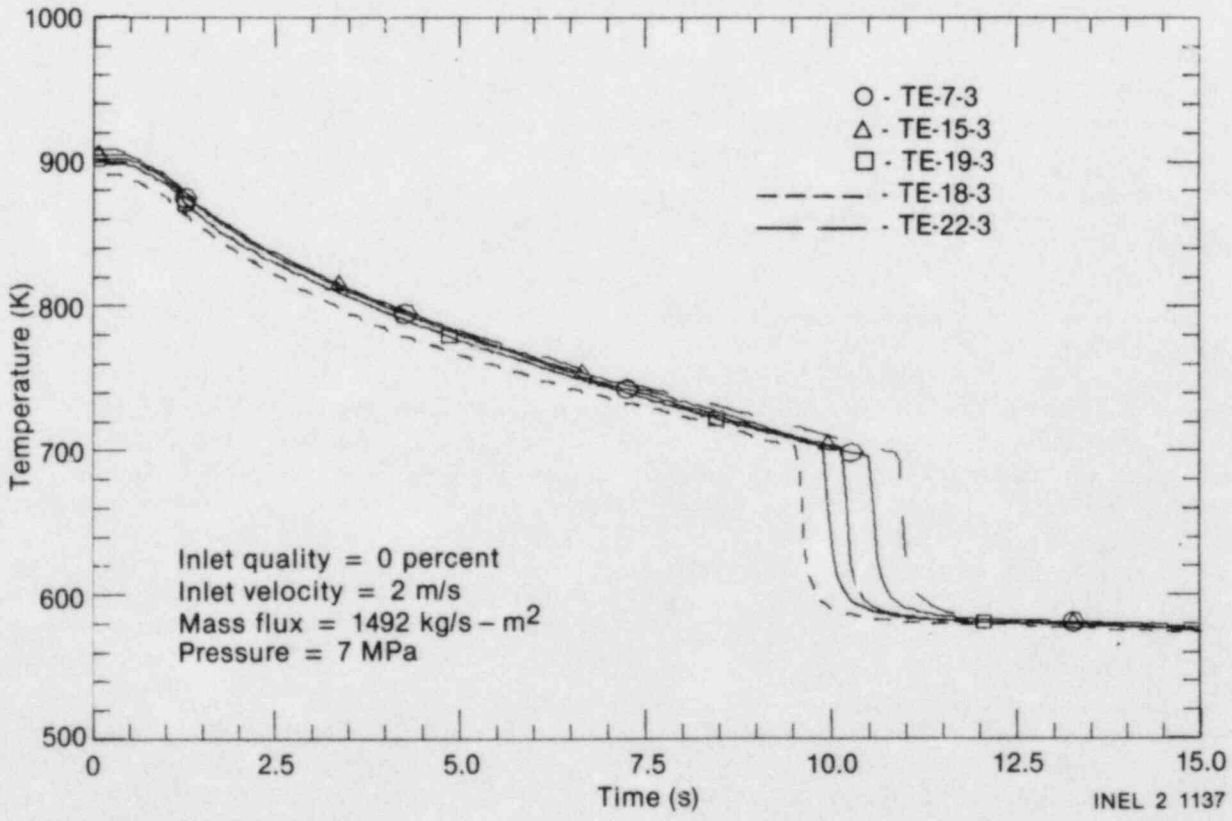

Figure 24. FEBA heater rod temperature response for Run 2F.

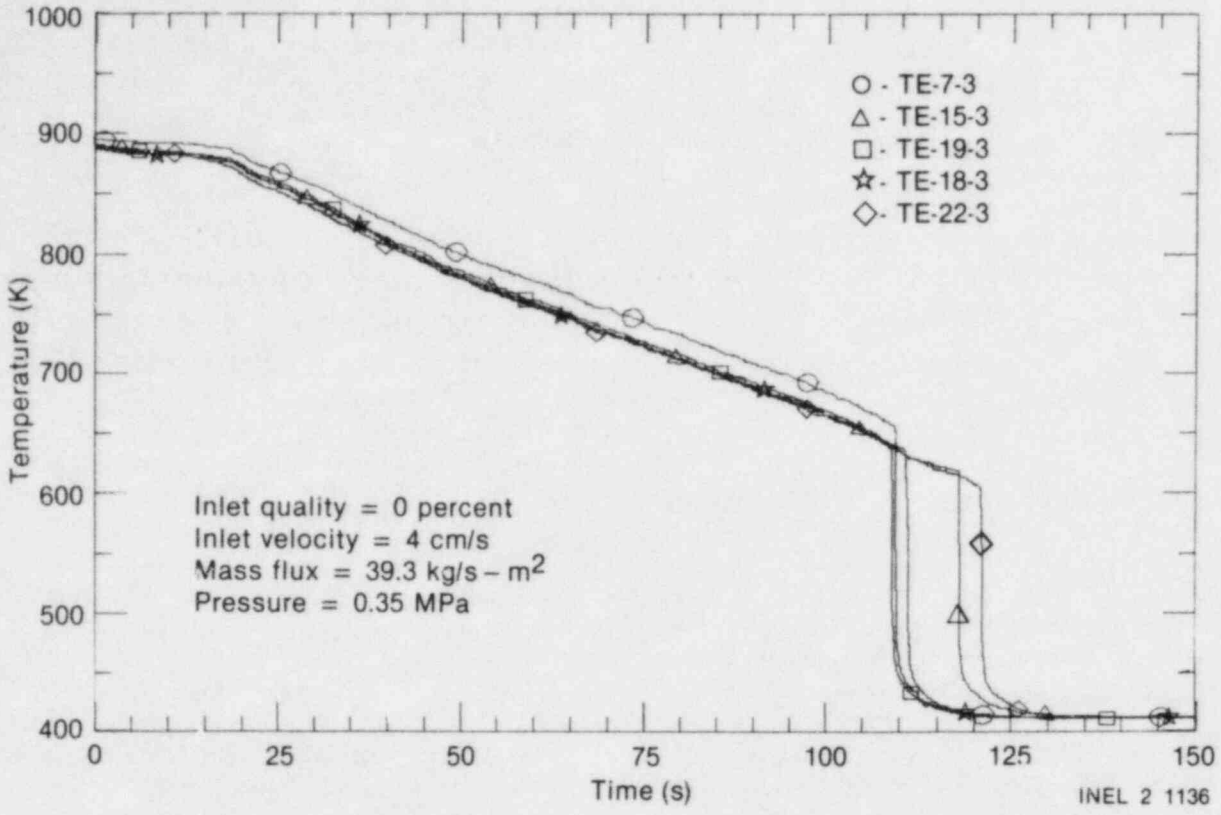

Figure 25. FEBA heater rod temperature response for Run 5F.

The secondary junctions of the cladding-embedded thermocouples provided data to compare the relative response of the REBEKA rod with and without external thermocouples even though they did not measure the actual cladding temperature. Direct comparisons of these measurements were made.

In addition, inverse heat conduction calculations were made with the INVERT code[10] using the secondary junctions of the embedded thermocouples and internal Thermocouple TE-REB-I2 to predict the actual cladding temperature. Comparisons were then made of the cladding surface temperature response of the REBEKA rod with and without external thermocouples based on these calculations. Also, a comparison was made between the predicted cladding surface temperature and the external thermocouple measurement to quantify the ability of the external thermocouple to measure cladding temperature. The details of the model and assumptions used in the INVERT calculations are given in Appendix C. Estimated gaps between the cladding and Al_2O_3 pellets were included in the model based on the rod diameter measurements that were made throughout the experiment program.

The data indicate that the external thermocouple was selectively cooled and quenched sooner than the cladding as shown in Figure 26 where the embedded thermocouple measurement (TE-REB-E2) and the calculated cladding surface temperature are compared with the external thermocouple measurement (TE-REB-X2) for Experiment Run 1. The initiation of the quench was indicated correctly by the external thermocouple and the final time to quench was indicated within 1 to 2 s of the actual cladding quench. However, the actual cladding temperature was not measured accurately during the quenching process. Similar results were observed for Experiment Runs 2 and 3, as shown in Figures 27 and 28, respectively. The external thermocouple quenched faster as the flow rate increased, as shown in Figure 29. Run 2 had the highest mass flow rate, and therefore the external thermocouple in that run had the fastest cooldown rate as compared to Runs 1 and 3.

The quench behavior of the REBEKA rod was essentially the same with and without external thermocouples over the range of flow rates and fluid qualities established for the experiments. Comparisons of the relative quench behavior of the

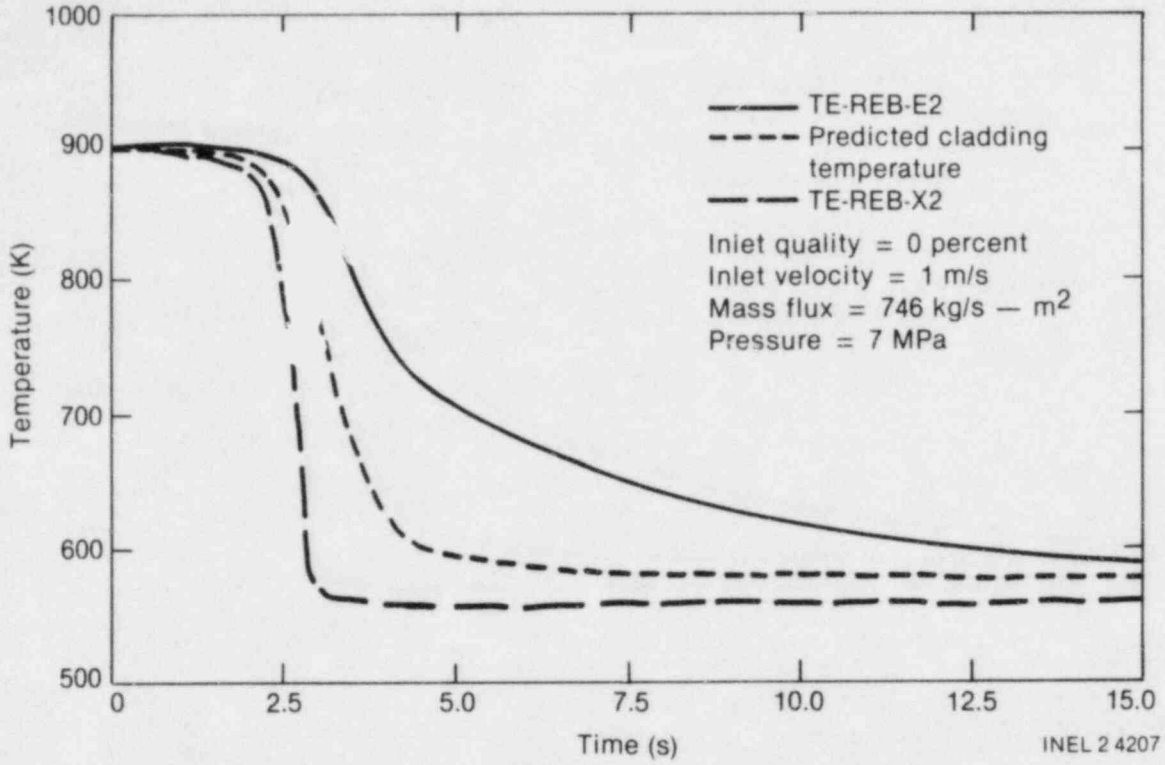

Figure 26. REBEKA heater rod measured and calculated temperature responses for Run 1.

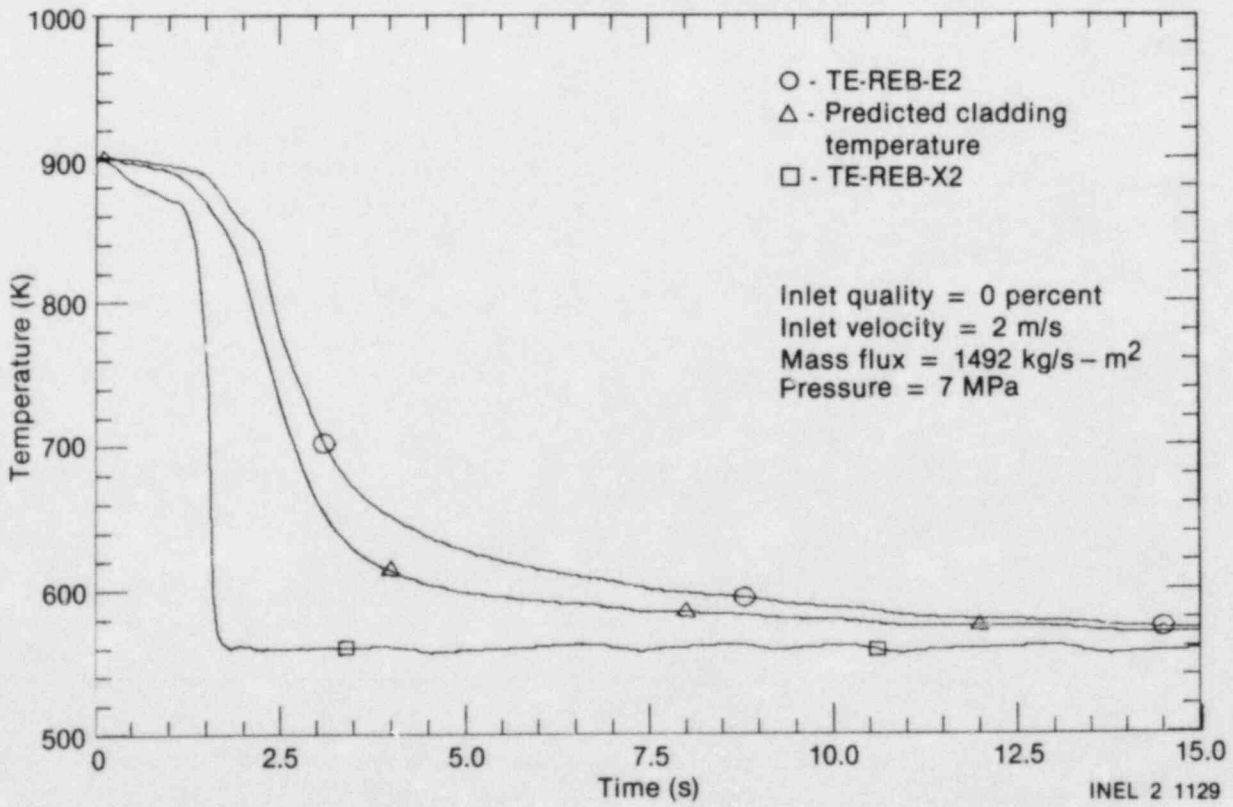

Figure 27. REBEKA heater rod measured and calculated temperature responses for Run 2.

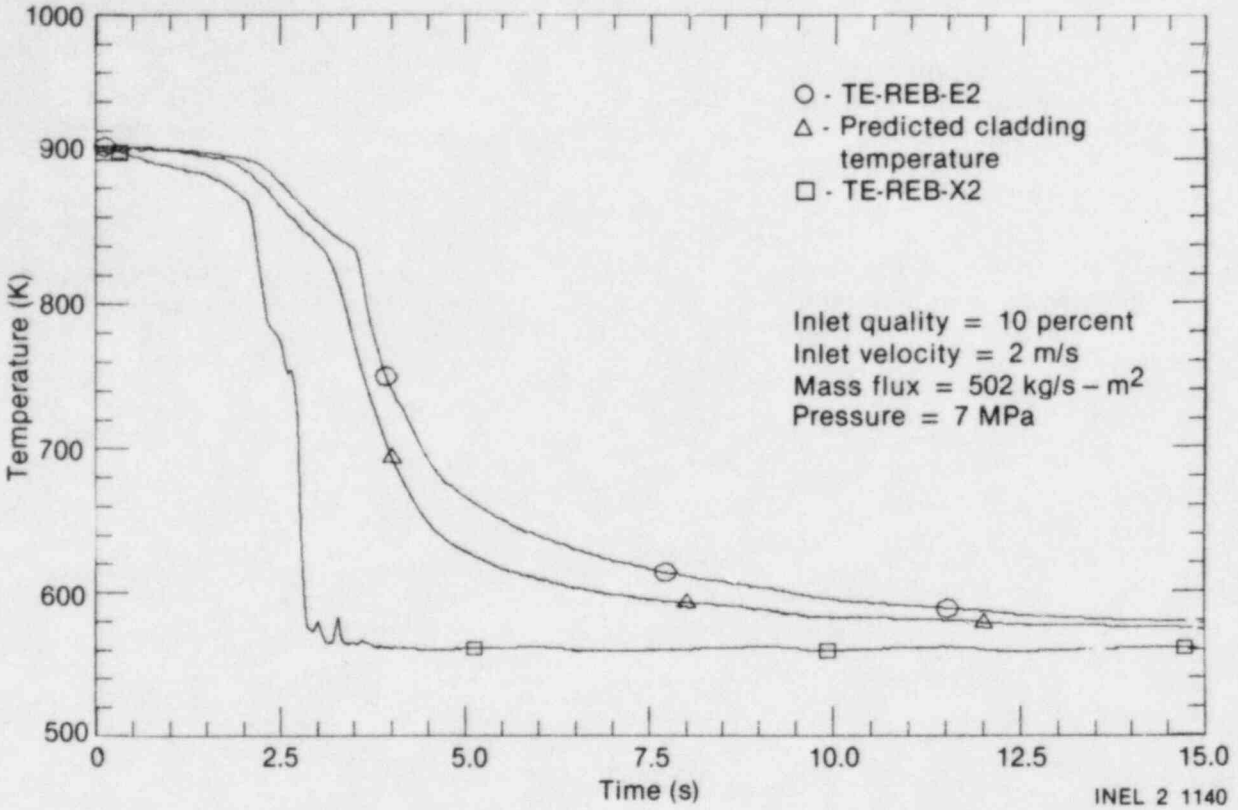

Figure 28. REBEKA heater rod measured and calculated temperature responses for Run 3.

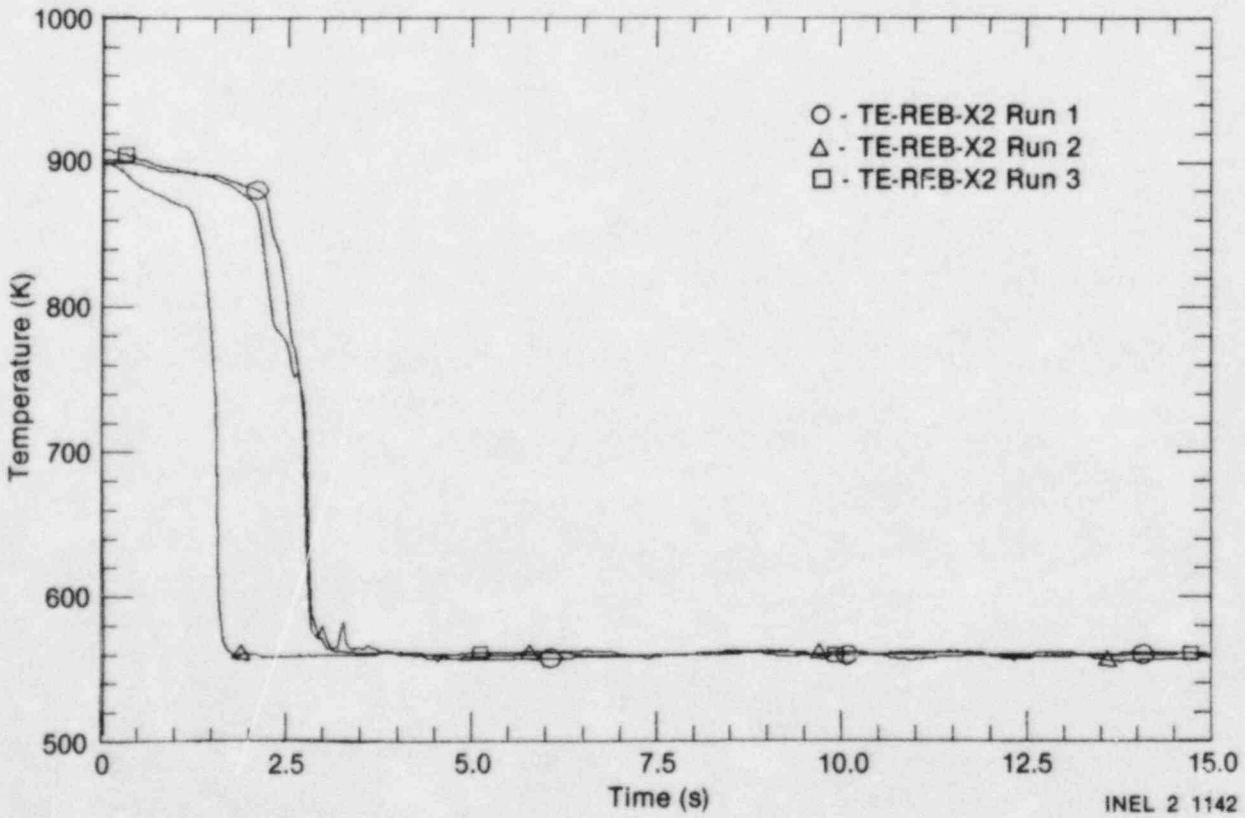

Figure 29. External thermocouple cooldown rates for Runs 1, 2, and 3.

REBEKA rod with and without external thermocouples are shown in Figures 30, 31, and 32 using the measurements of the secondary junctions of the embedded thermocouples. Similar comparisons are made in Figures 33, 34, and 35 using the calculated cladding surface temperatures from the INVERT code. The results were essentially the same in that the external thermocouples did not significantly influence the quench behavior of the REBEKA rod.

Comparison of REBEKA Rod Quench Behavior with That of a Nuclear Rod in a Similar Experiment

Similar experiments to evaluate the effects of external thermocouples on the quench behavior of a nuclear fuel rod and to proof test the LOFT cladding embedded thermocouples have been conducted in the Power Burst Facility (PBF) at the INEL.[11] Additional credibility can be given to the results of the REBEKA rod experiments by comparing the cooldown rates of the REBEKA rod and a PBF nuclear fuel rod under similar flooding conditions. A comparison of the cladding temperature response of the REBEKA rod with external thermocouples and a nuclear fuel rod with external thermocouples, where the initial temperatures of the rods prior to quenching were about the same (900 K), is shown in Figure 36. The cooldown rates were nearly the same. Similar results exist for rods without cladding external thermocouples. Also, the external thermocouple responses were nearly the same. The external thermocouples were selectively cooled and quenched prior to cladding quench on both rods. The similarity of the external thermocouple cooldown rates indicates that the flooding conditions were comparable between the LTSF and the PBF experiments. The quench behavior of the REBEKA rod is similar to that of a nuclear fuel rod.

Applicability of Experiment Results to LOFT Fuel Rods

The comparison of the LTSF REBEKA rod and PBF nuclear rod quench behavior verifies the RELAP4/MOD6 computer code calculations (discussed in Section 2), showing that the REBEKA rod provides a good simulation of nuclear fuel rod

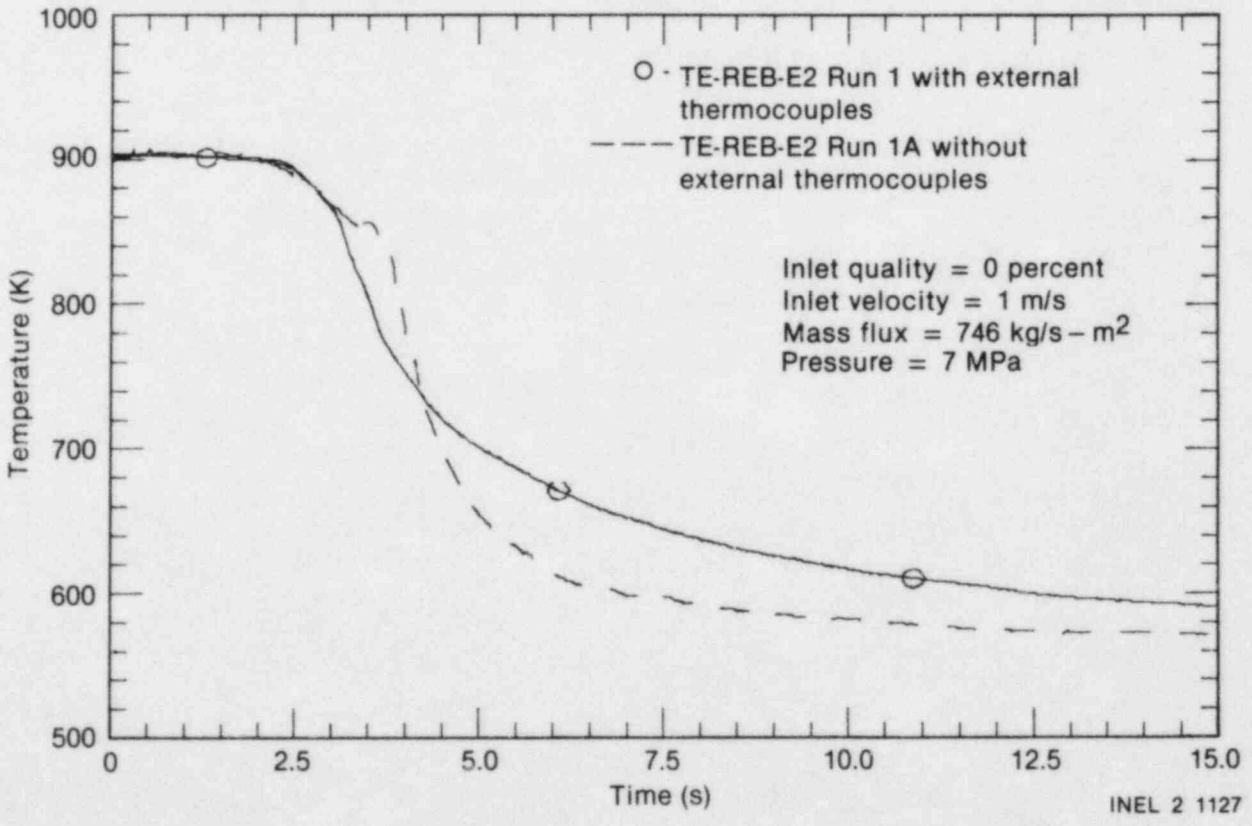

Figure 30. Measured REBEKA heater rod temperature responses with and without cladding external thermocouples for Runs 1 and 1A.

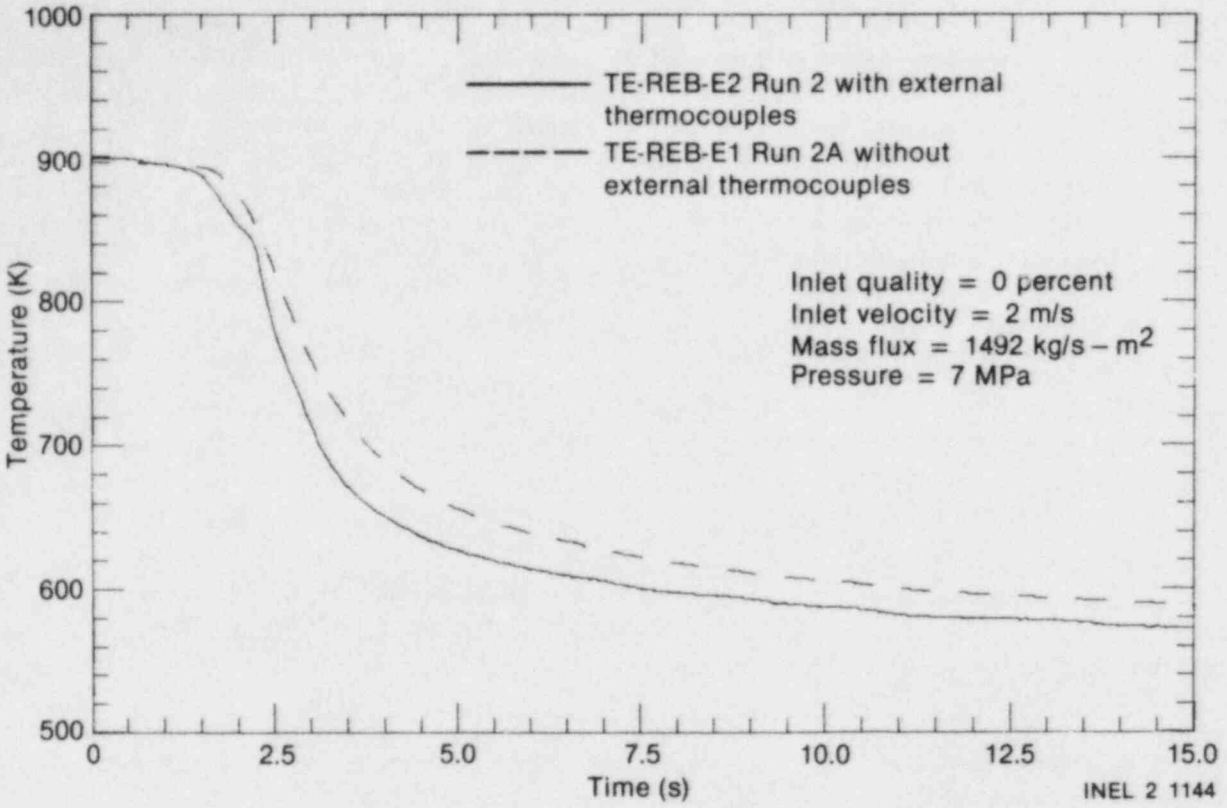

Figure 31. Measured REBEKA heater rod temperature responses with and without cladding external thermocouples for Runs 2 and 2A.

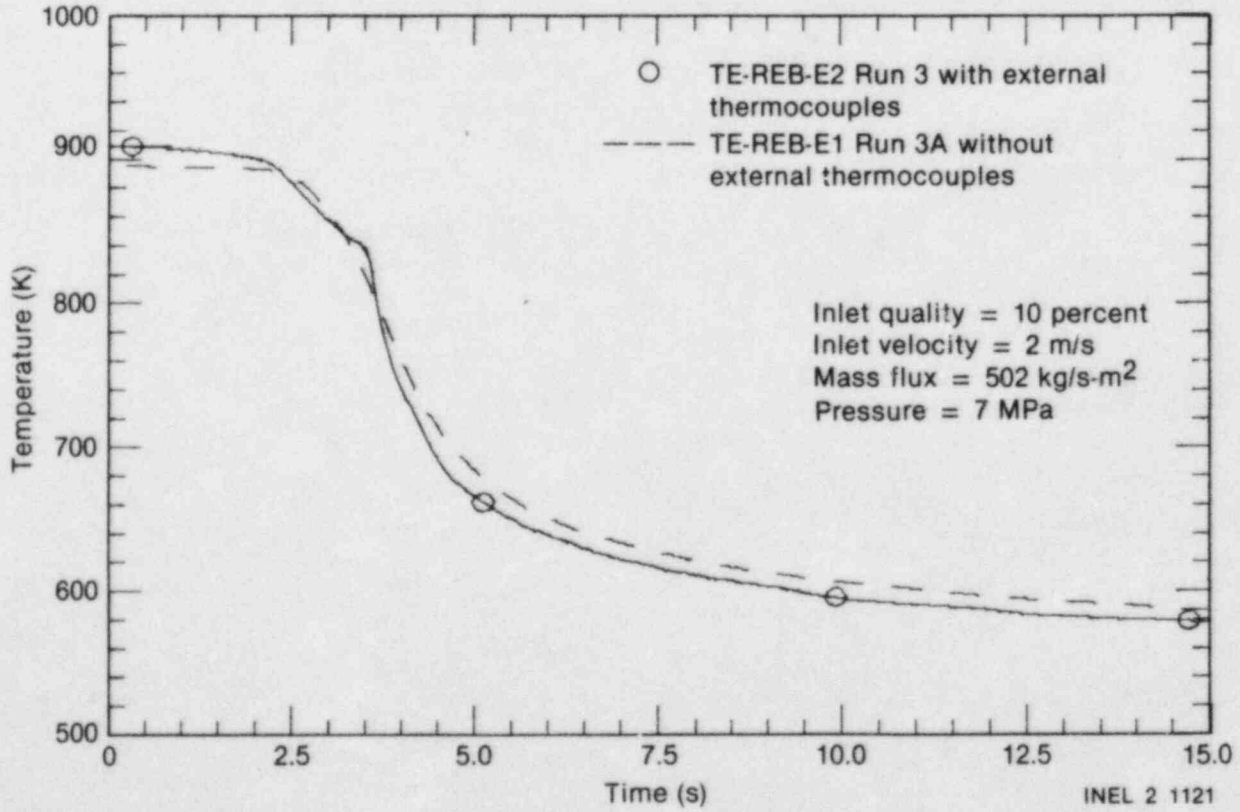

Figure 32. Measured REBEKA heater rod temperature responses with and without cladding external thermocouples for Runs 3 and 3A.

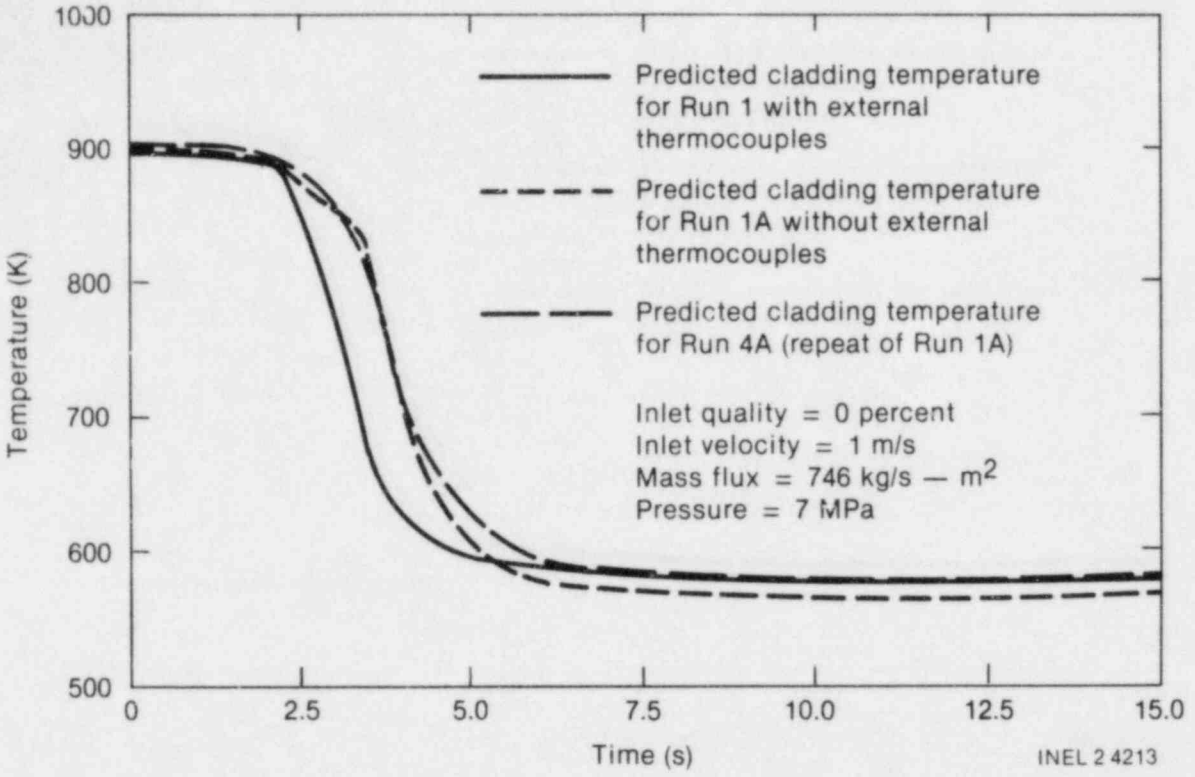

Figure 33. INVERT calculated REBEKA heater rod temperature responses with and without cladding external thermocouples for Runs 1, 1A, and 4A.

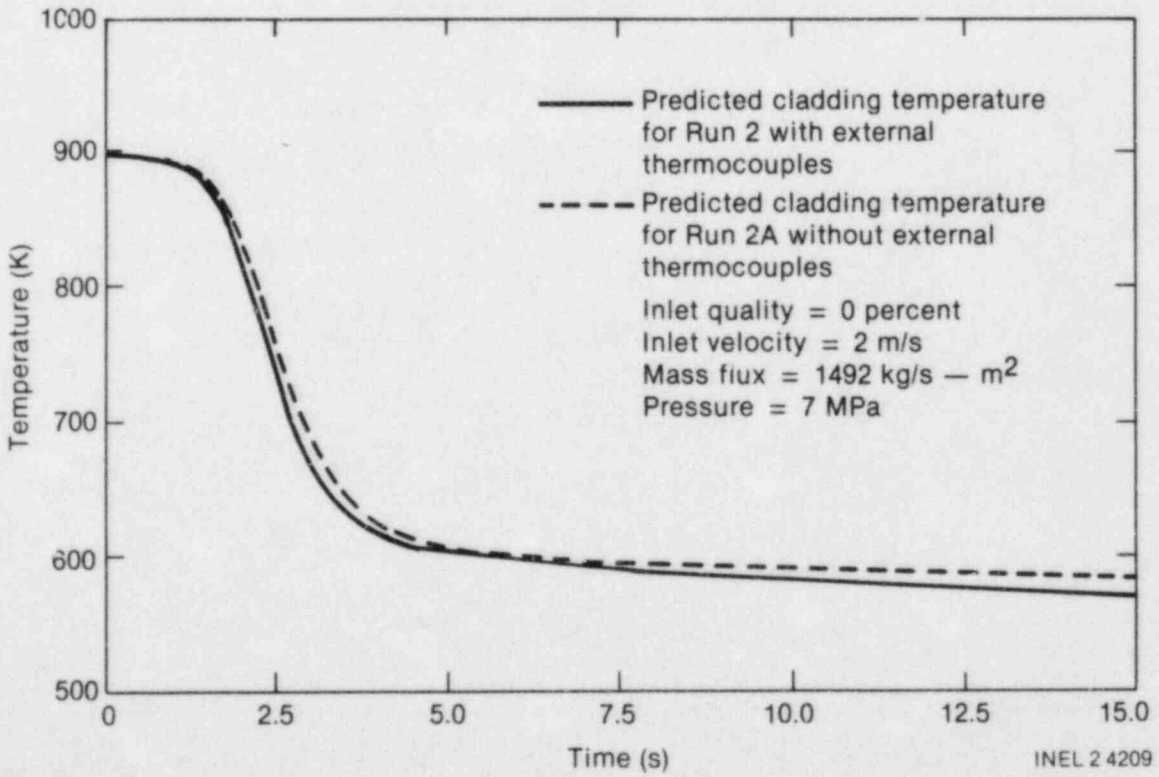

Figure 34. INVERT calculated REBEKA heater rod temperature responses with and without cladding external thermocouples for Runs 2 and 2A.

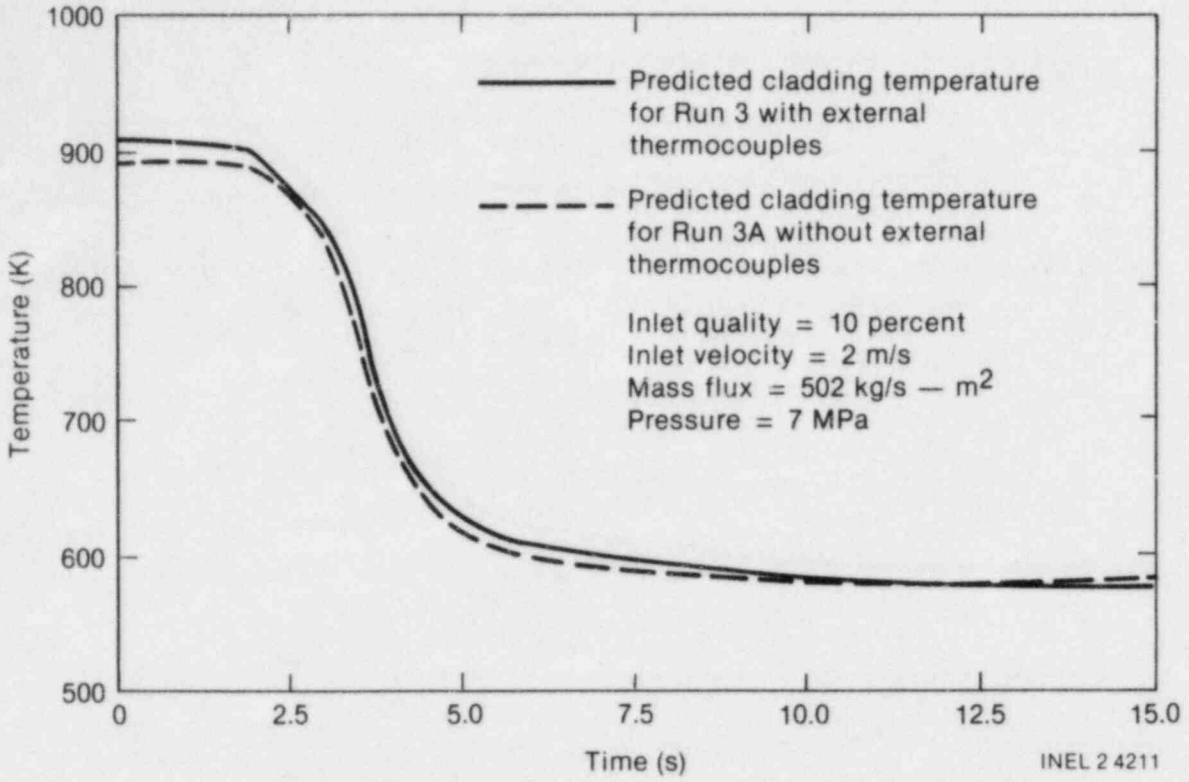

Figure 35. INVERT calculated REBEKA heater rod temperature responses with and without cladding external thermocouples for Runs 3 and 3A.

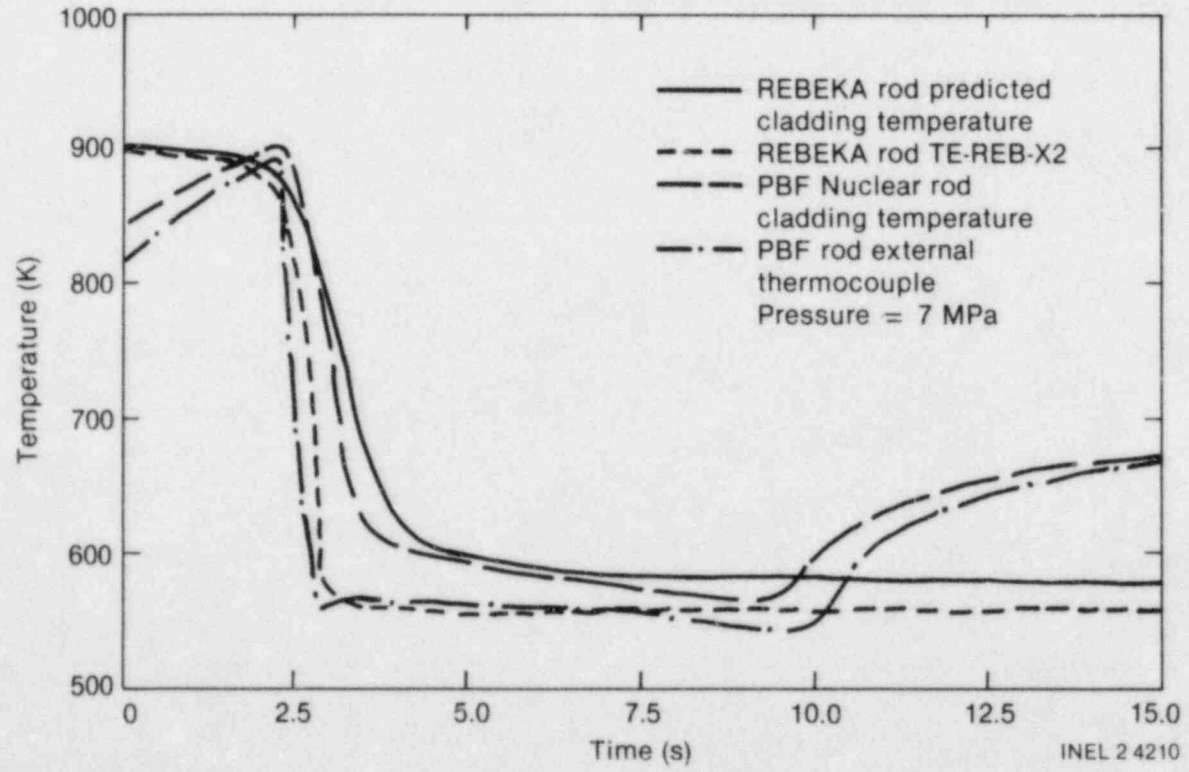

Figure 36. Quench behaviors for a REBEKA heater rod and a nuclear fuel rod with cladding external thermocouples.

thermal response for rapid flooding rates at high pressure in a PWR loss-of-coolant transient. Therefore, the results of these experiments are considered applicable to LOFT nuclear fuel rods. This implies that cladding external thermocouples on LOFT fuel rods had a negligible influence on the quench behavior of the LOFT rods during LOCEs L2-2 and L2-3. However, the LOFT external thermocouples were most probably selectively cooled and did not accurately measure the cladding temperature during the blowdown quench in LOCEs L2-2 and L2-3. Consequently, the value of LOFT external thermocouple data in validating computer code models during quenching is somewhat limited.

Comparison of REBEKA and FEBA Rod Thermal Responses

It was shown earlier in Section 5 that the REBEKA rod provides a very good simulation of the thermal response of a nuclear fuel rod under LOFT LOCE hydraulic conditions. A comparison of the thermal response of a REBEKA and a FEBA rod was considered analogous to a comparison of the thermal response of a FEBA rod (or other solid-type heater rods such as in the Semiscale facility at the INEL or in the Westinghouse FLECHT facility) and a nuclear fuel rod. Implications were then made concerning the ability of solid-type heater rods to simulate the thermal response of nuclear fuel rods.

It has been postulated that solid-type electrical heater rods do not adequately simulate the thermal response of nuclear fuel rods under large-break LOCA conditions in an integral test facility. Comparison of the relative thermal responses of the REBEKA and FEBA rods in this experiment program provides valuable evidence to support this contention. The experimental objective, comparing the quench behavior of solid-type (FEBA) and cartridge-type (REBEKA) electrical heater rods, was accomplished by testing both types of rods under similar thermal-hydraulic conditions. The FEBA and REBEKA rod responses were compared in several ways.

Comparisons were made between the responses of the center REBEKA rod and the eight peripheral FEBA rods in the same bundle, and then between the REBEKA rod and the center FEBA rod (Rod 7) in the bundle of nine FEBA rods under the same experiment conditions. Finally, a comparison was made between the responses of the eight peripheral FEBA rods in both bundles to show what effect on these peripheral rods was caused by putting the REBEKA rod in the center of the bundle. These comparisons were made under both high-pressure, high-flow and low-pressure, low-flow reflood conditions, and are discussed in the following sections.

High-Pressure Experiment Results. The responses of the REBEKA rod and of the surrounding FEBA rods in the same bundle were compared under high-pressure, high-flow reflood conditions in Experiment Run 1A, as shown in Figure 37. The REBEKA rod is shown to have quenched about 6 s earlier and from a higher temperature than the FEBA rods. FEBA Rod 19 quenched from a higher temperature (775 K) and, therefore, 4 s earlier than FEBA Rods 15, 18, and 22. A similar comparison is shown in Figure 38 for Experiment Run 2A.

A comparison of the response of the REBEKA rod for Experiment Run 1A with the response of FEBA Rod 7 located in the center of the nine-rod FEBA bundle for Experiment Run 1F under the same experiment conditions is shown in Figure 39. Again it is apparent that the REBEKA rod quenched much earlier and from a higher temperature than did FEBA Rod 7. The differences in cooling rates and time-to-quench are due to differences in material thermal properties and rod construction. For example, the thermal conductivity of the FEBA solid-type heater rod filler material is approximately three times greater than that of nuclear fuel. This combined with the lack of a gap between the filler material and the cladding allows heat to flow readily from the interior of the rod to the cladding. These factors delay the cladding quench. The REBEKA cartridge-type heater rod, however, has alumina pellets whose thermal conductivity is about twice that of nuclear fuel. It also has a gap between the pellets and the cladding. The pellet-cladding gap thermally decouples the cladding from the filler material, reduces heat flow to the cladding, and allows the cladding to quench readily.

A comparison of the responses of FEBA Rods 15 and 22 for Experiment Runs 1F and 1A, with FEBA Rod 7 in the center of the bundle followed by the REBEKA rod in the center of the bundle, respectively, is shown in Figure 40. The earlier quench of the REBEKA rod is shown to have influenced the cooldown rate and quench time of the surrounding FEBA rods. With the REBEKA rod in the center of the bundle, the precursory cooldown rate

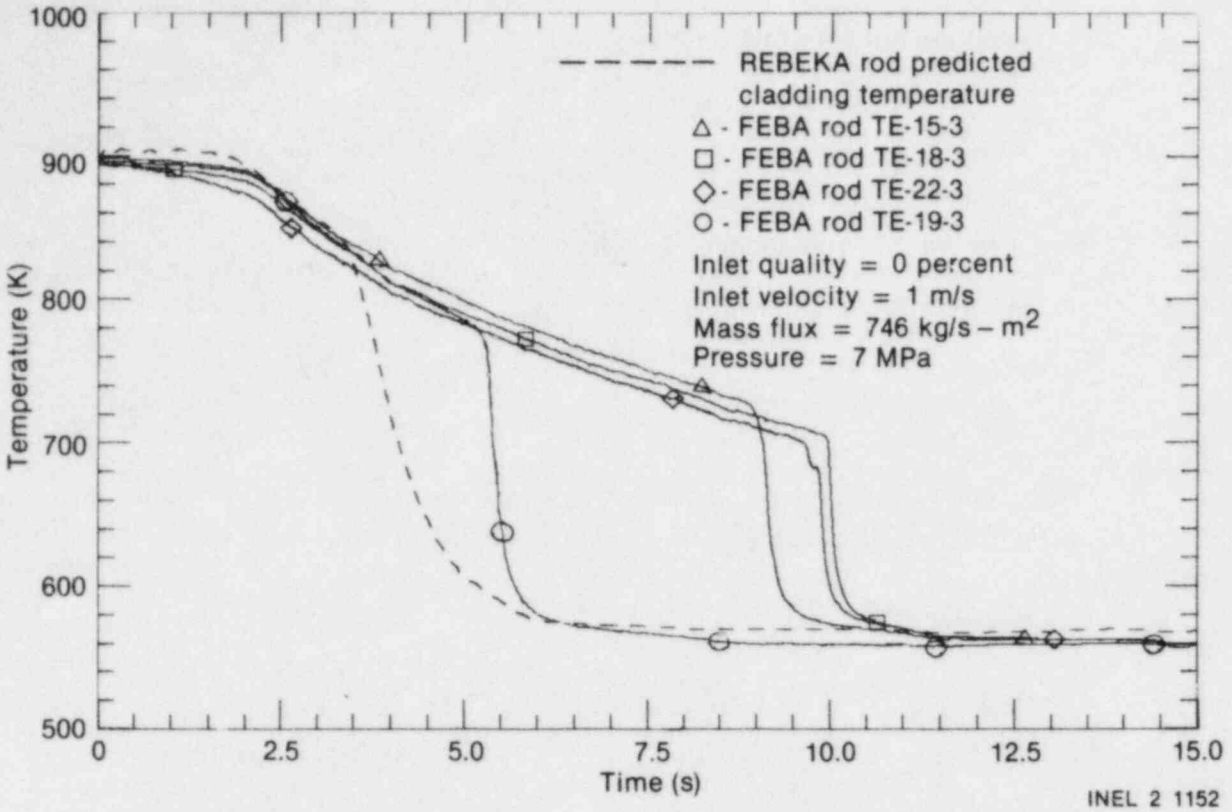

Figure 37. REBEKA and FEBA heater rod temperature responses in the same bundle for Run 1A.

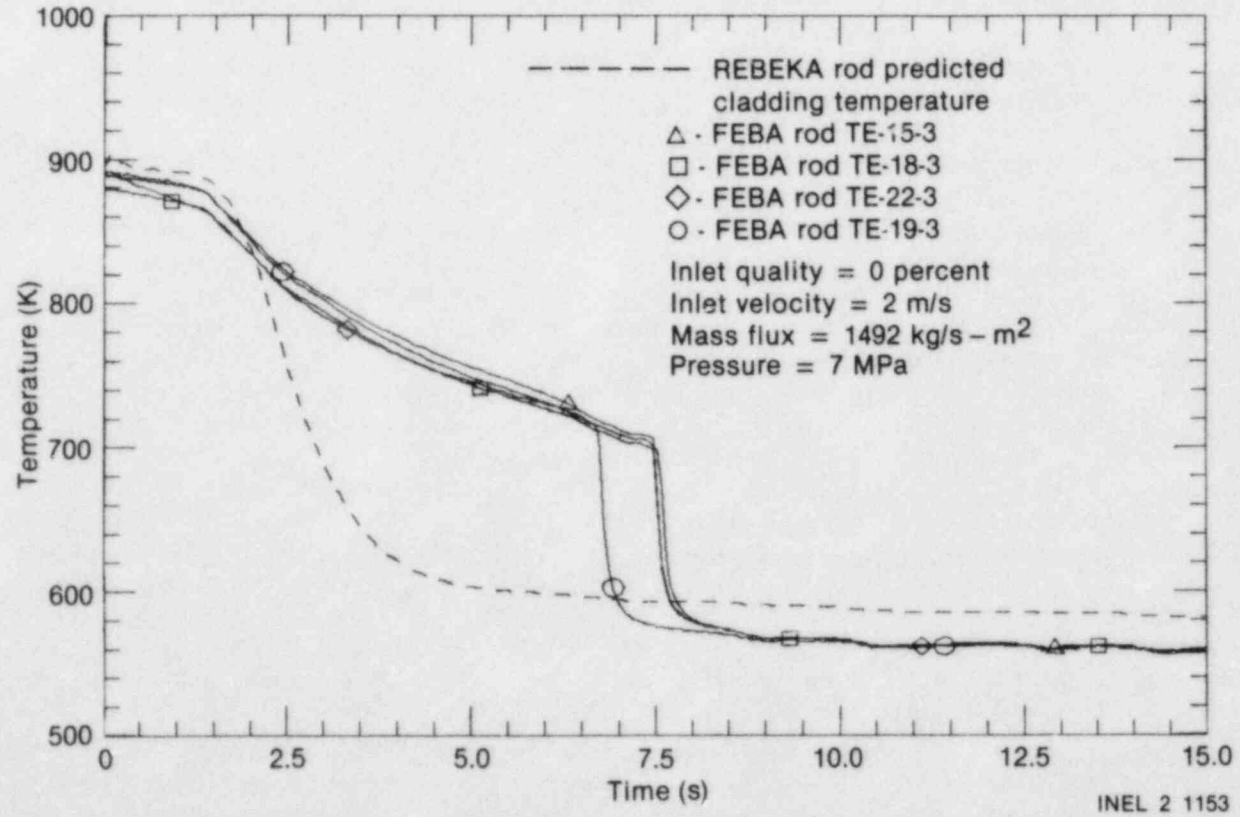

Figure 38. REBEKA and FEBA heater rod temperature responses in the same bundle for Run 2A.

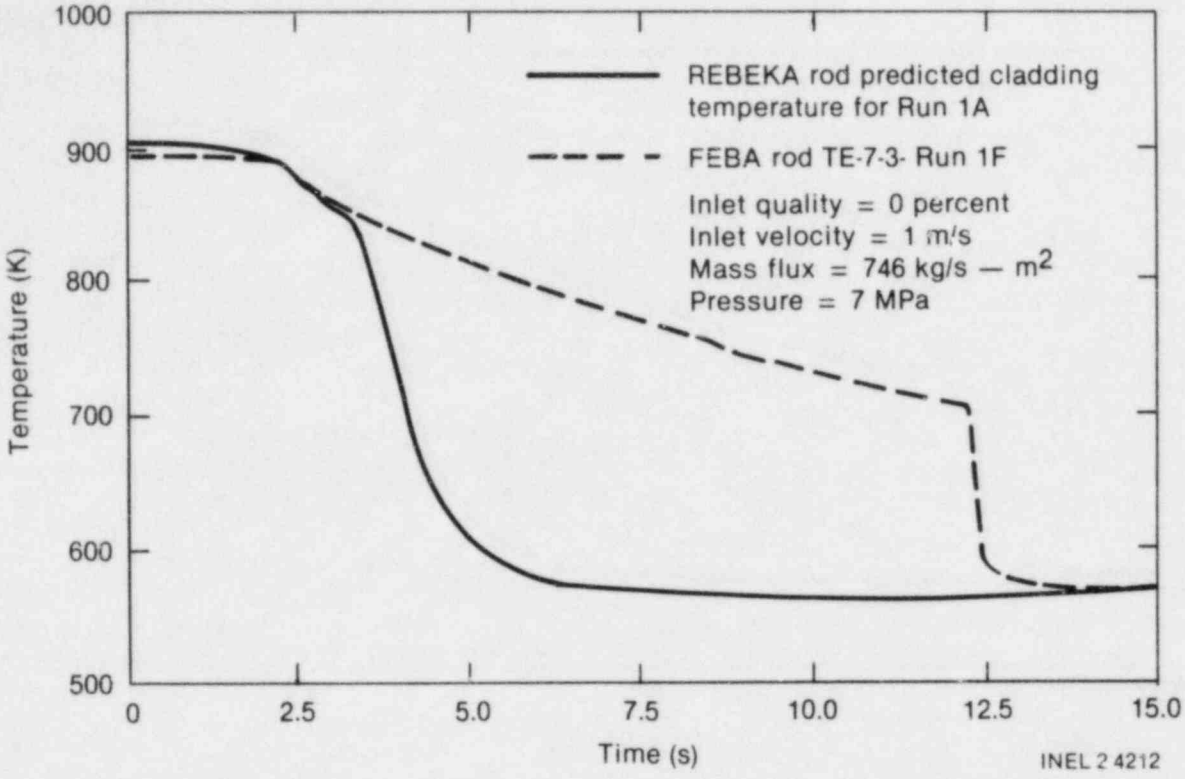

Figure 39. REBEKA and FEBA heater Rod 7 temperature responses for Runs 1A and 1F.

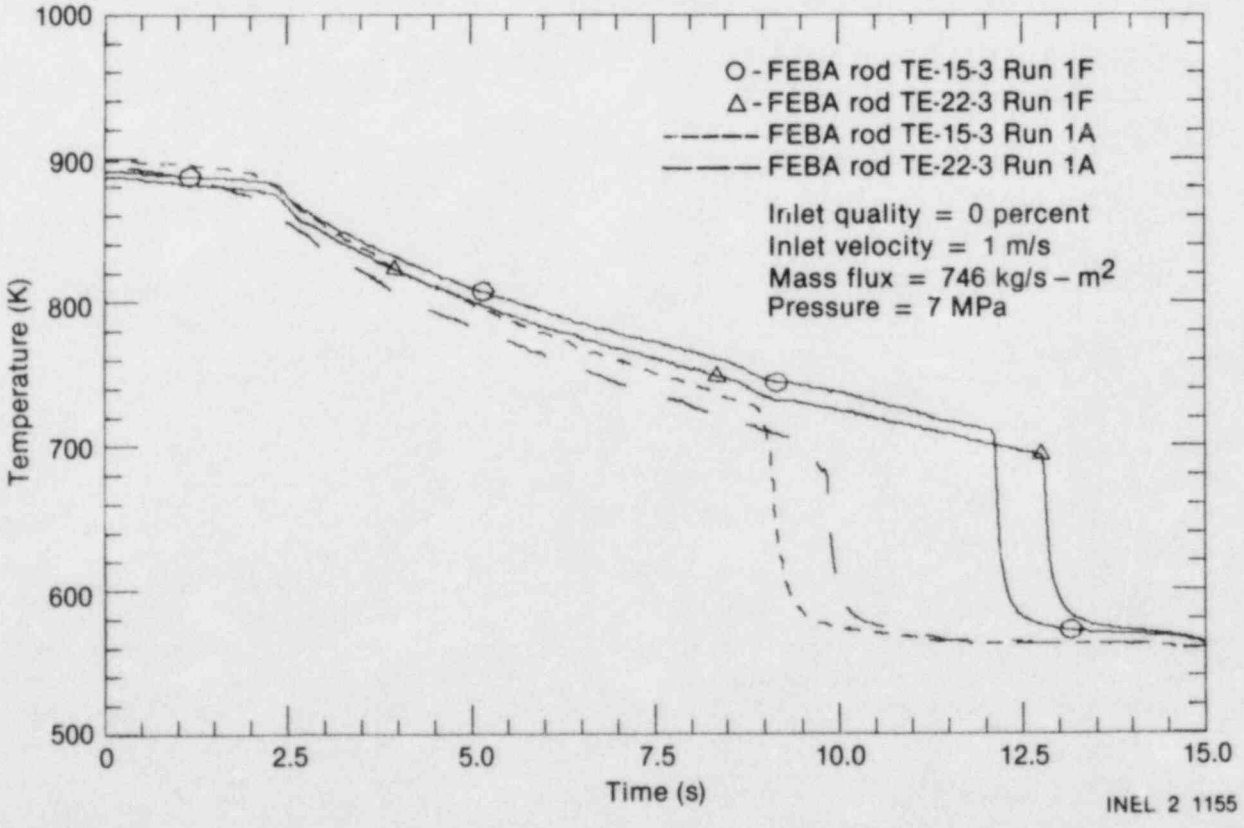

Figure 40. FEBA heater rod temperature responses with a FEBA or a REBEKA heater rod in center of bundle for Runs 1F and 1A.

of the surrounding FEBA rods was higher, and the FEBA rods quenched from a higher temperature and, therefore, sooner than when FEBA Rod 7 was in the center of the bundle. The presence of the REBEKA rod and its earlier quench tended to increase the heat transfer coefficient and cooling rate of the surrounding FEBA rods during precursory cooling. The significance of this effect is that rods in a bundle that quench sooner than others have a propagating effect on surrounding rods.

The FEBA rod's precursory cooldown time prior to cladding quench has been shown to be much longer than that of the REBEKA cartridge-type heater rod. The FEBA rod's long precursory cooldown time is typical of that observed for other solid-type heater rods under similar experiment conditions.[4]

As shown earlier in Section 5, the combined effects of pellet-cladding gap, material thermal properties, and initial stored heat allow the REBEKA cartridge-type heater rod to cool and quench in a manner similar to that of a nuclear fuel rod. This indicates that the thermal response of solid-type electrical heater rods is different than that of nuclear fuel rods under rapid flooding conditions as were experienced during blowdown in the LOFT LOCE L2-3.

Low-Pressure Experiment Results. Experiment Runs 5 and 5A were to provide a comparison of the quench behavior of the REBEKA rod with and without cladding external thermocouples to quantify the effect of the external thermocouples at low-pressure and low-flow reflood conditions. Due to the early failure of the cladding-embedded thermocouples, Experiment Run 5 was not conducted, so a comparison was not possible. However, Experiment Runs 5F and 5A were conducted which allowed a comparison of the quench behavior of the FEBA rods with that of the REBEKA rod at low-pressure and low-flow reflood conditions. A comparison of the quench behavior of the REBEKA rod and FEBA Rod 7 for Experiment Runs 5A and 5F, where the REBEKA rod and FEBA Rod 7 were in the center of the bundle for the respective experiment runs, is shown in Figure 41. The precursory cooldown rate was similar for the two rods; however, the REBEKA rod quenched from 740 K,[a] whereas the FEBA rod quenched from 650 K. The REBEKA rod quenched about 17 s earlier than the FEBA rod.

A comparison of the quench behavior of the REBEKA rod and FEBA Rod 15 in the same bundle for Experiment Run 5A is shown in Figure 42. The precursory cooldown rates for the two rods were nearly identical; however, the REBEKA rod quenched from 740 K, as compared to 680 K for FEBA Rod 15, and therefore, 33 s earlier. FEBA Rods 15, 18, 19, and 22 consistently quenched from a temperature 50 K higher with the REBEKA rod in the center of the bundle, indicating that the earlier quench of the REBEKA rod has some influence on the quench behavior of the surrounding FEBA rods.

The results of the low-pressure low-flow experiments were consistent with the results of the high-pressure high-flow experiments in that the REBEKA rod quenched from a higher temperature and sooner than did the solid-type FEBA heater rods. The differences in thermal properties and construction of the two different types of heater rods again are the contributing factors as explained in the preceding subsection.

Mass Flux Effect on Quench Behavior of REBEKA Rod at High Pressure

Experiment Runs 6A, 7A, and 8A were conducted to observe any differences in REBEKA rod quench behavior resulting from differences in mass flux. Experiment Runs 6A, 7A, and 8A had mass fluxes of 200, 100, and 50 kg/s-m^2, respectively. Figures 43 and 44 show the relative cooldown rate of the REBEKA rod for Experiment Runs 1A, 6A, 7A, and 8A using data from Thermocouples TE-REB-E2 and TE-REB-I2, respectively. The quench behavior of the REBEKA rod was basically the same for the various mass fluxes, other than having longer precursory cooling times at the lower mass fluxes. The REBEKA rod quenched from a temperature of over 800 K for all experiment runs.

The temperature responses of the REBEKA rod and FEBA Rod 15 in the same bundle at various flow rates are compared in Figure 45. The REBEKA rod quenched from a higher temperature and, therefore, sooner than the FEBA rod in each case, consistent with other experimental results.

a. For low flooding rates, the REBEKA rod embedded thermocouple gave a reasonable indication of the cladding temperature since the radial temperature distribution in the rod is fairly uniform during precursory cooling.

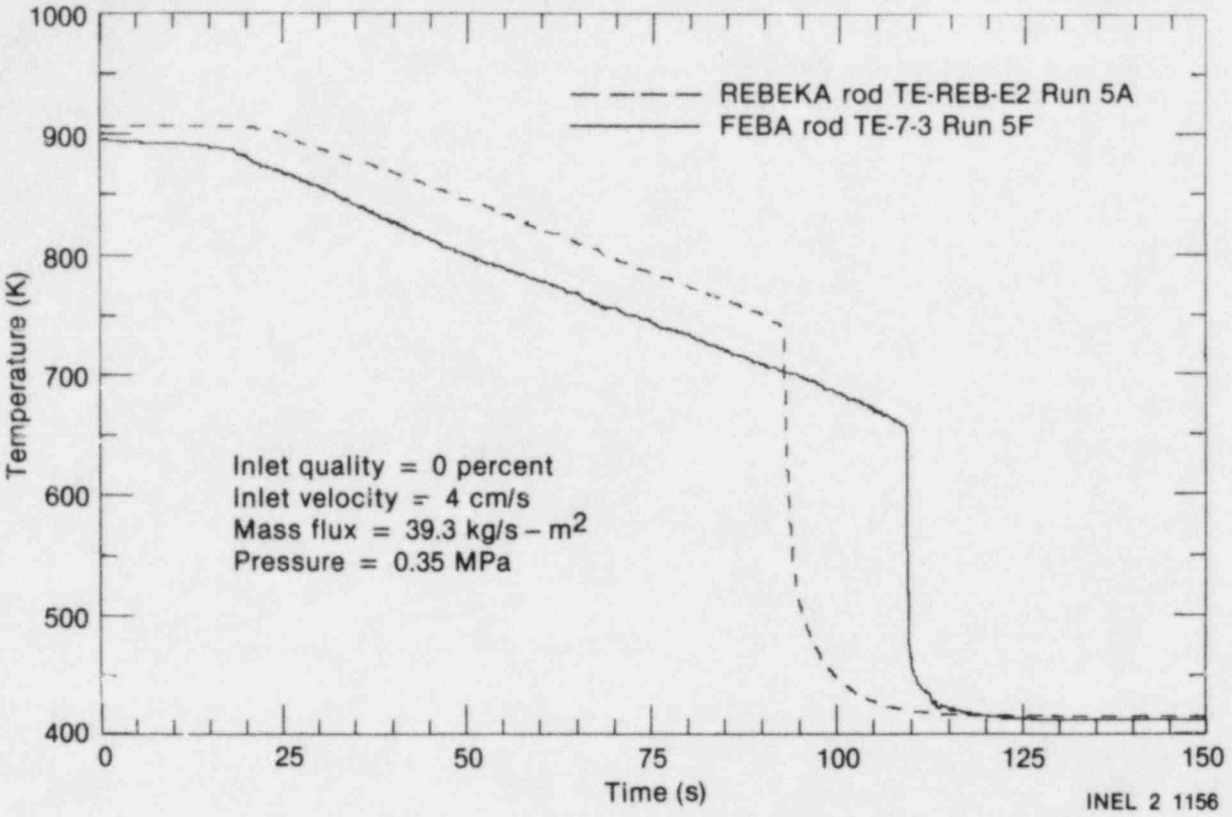

Figure 41. REBEKA heater rod and FEBA heater Rod 7 temperature responses at low flow and low pressure for Runs 5A and 5F.

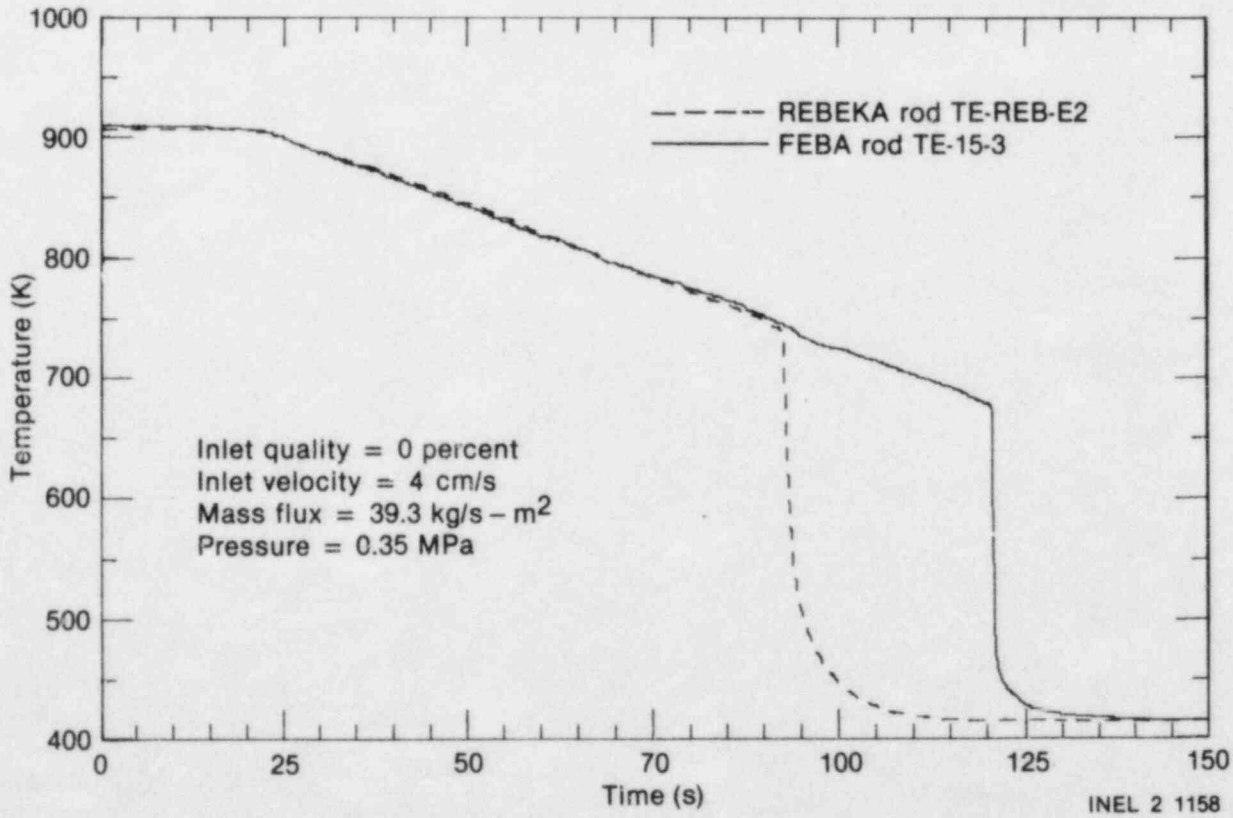

Figure 42. REBEKA and FEBA heater rod temperature responses in the same bundle at low flow and low pressure for Run 5A.

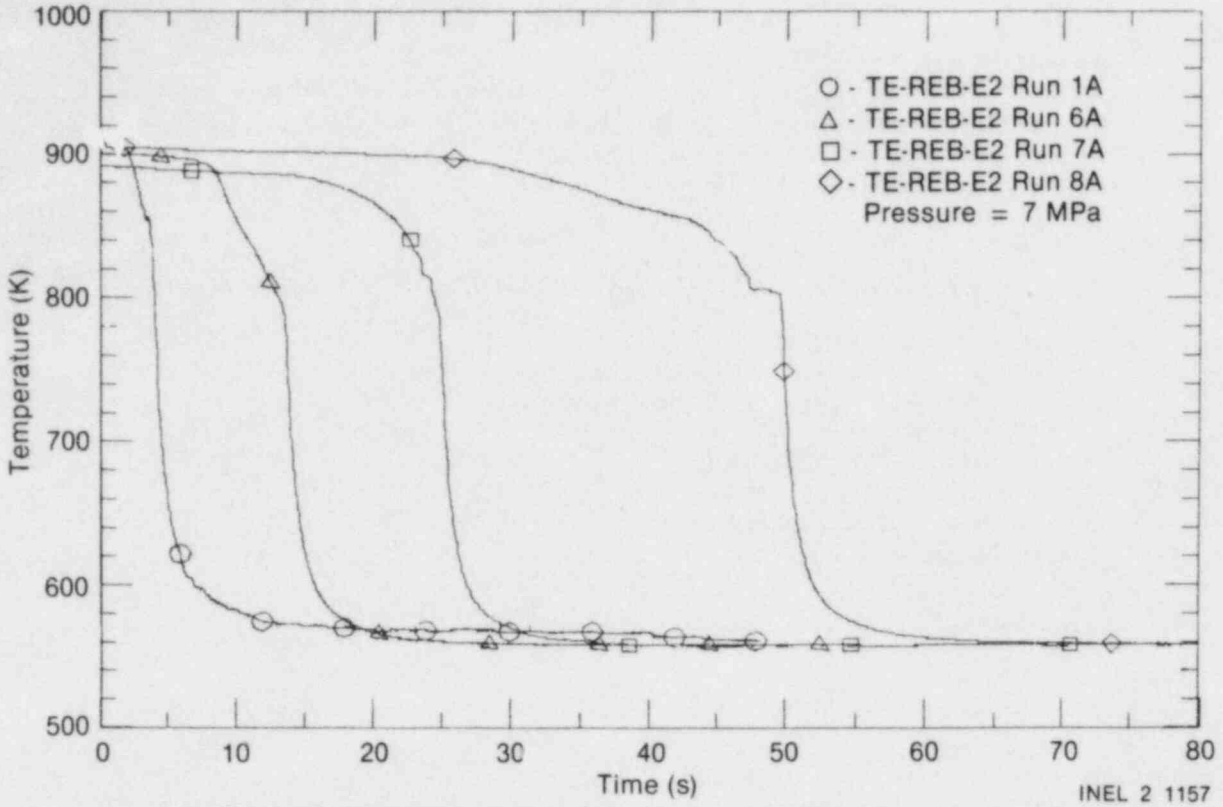

Figure 43. REBEKA heater rod quench behavior at Thermocouple TE-REB-E2 as a function of mass flux for Runs 1A, 6A, 7A, and 8A.

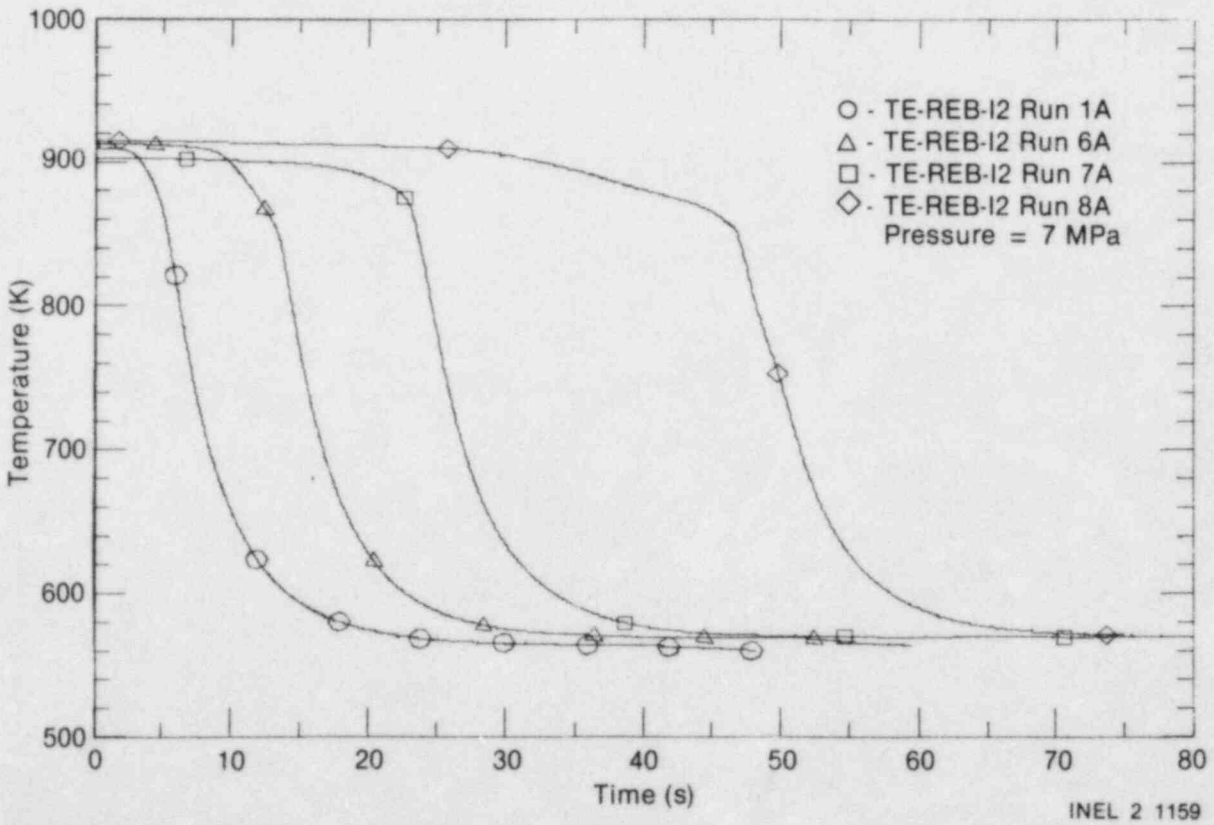

Figure 44. REBEKA heater rod quench behavior at Thermocouple TE-REB-I2 as a function of mass flux for Runs 1A, 6A, 7A, and 8A.

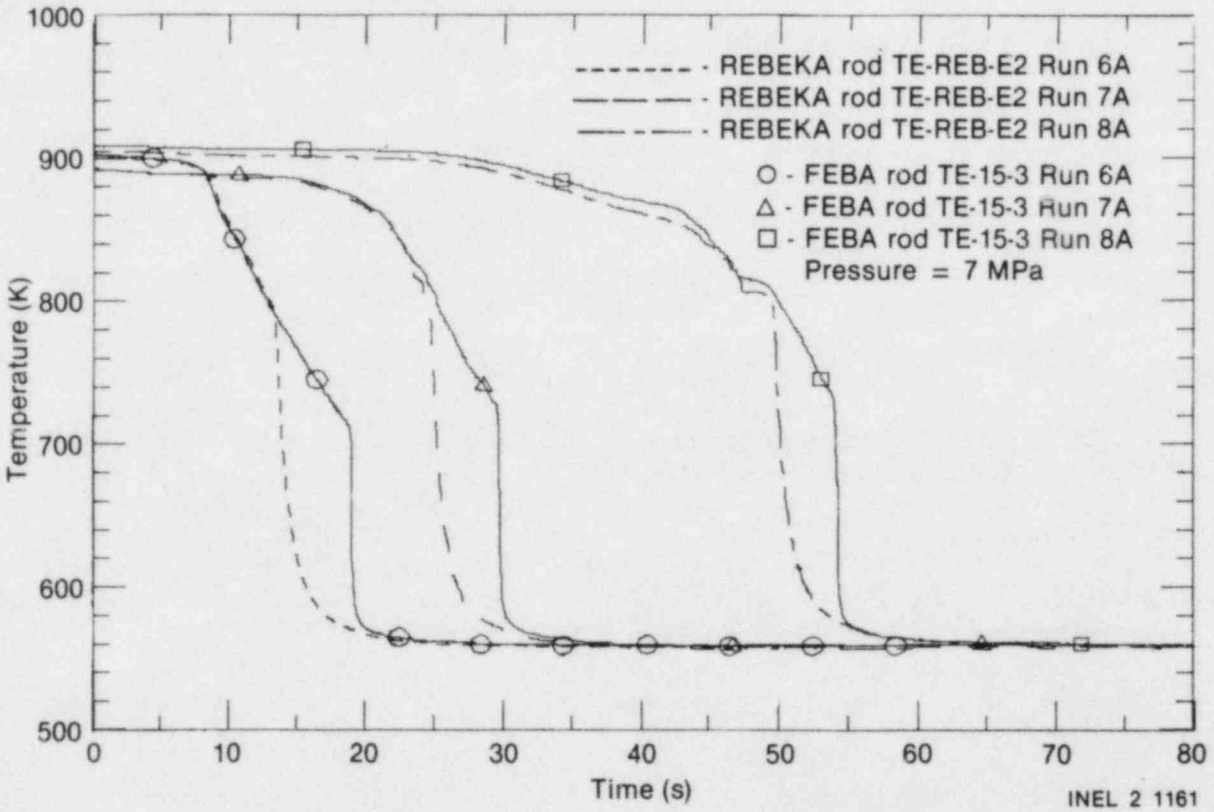

Figure 45. REBEKA and FEBA heater rod quench behaviors in the same bundle as a function of mass flux for Runs 6A, 7A, and 8A.

6. CONCLUSIONS

The separate effects experiment program conducted in the LTSF with REBEKA (cartridge-type) and FEBA (solid-type) heater rods was performed satisfactorily; however, the quality of the data was compromised due to the failure of the primary junctions of the cladding-embedded thermocouples in the REBEKA rod. Nevertheless, valuable data were obtained from the secondary junctions formed in the embedded thermocouple wires, such that the objectives of the experiment program could be met. Based on the results of the experiment, the following conclusions can be stated:

1. Cladding external thermocouples have a negligible effect on the cooldown rate and quench behavior of a REBEKA heater rod over the range of LOCA-type, high-pressure thermal-hydraulic reflood conditions examined. Since the REBEKA rod has been shown to satisfactorily simulate the thermal response of a nuclear fuel rod, these results are considered applicable to LOFT nuclear fuel rods.

2. For rapid, high-pressure cooling transients, cladding external thermocouples are selectively cooled during the quenching process and do not accurately measure cladding temperature during this part of the transient. Consequently, the value of LOFT external thermocouple data in validating computer code models during quenching is somewhat limited.

3. The prototype LOFT cladding-embedded thermocouple design used in the REBEKA rod is inadequate for use in LOFT fuel rods. The thermocouple wires may fracture at the point where the wire is reduced down to its smallest diameter prior to being embedded in the cladding. The laser welding technique used to weld the thermocouples into the slot in the cladding insert needs to be improved to prevent burning holes through the thermocouple sheath. Laser welding on both sides of the slot caused tension forces that created cracks in the laser welds and the sheath of the prototype thermocouples. See Appendix A for information on further development efforts on these thermocouples.

4. The quench behavior of solid-type (FEBA) electrical heater rods under large-break LOCA thermal-hydraulic conditions is significantly different than that of the REBEKA cartridge-type heater rod and a nuclear fuel rod. Due to the higher thermal diffusivity of a solid-type heater rod and lack of a pellet-cladding gap, the rod undergoes a lengthy period of precursory cooling before quenching; whereas, a cartridge-type heater rod and a nuclear fuel rod quench very rapidly from high temperatures when subjected to rapid flooding conditions.

5. The REBEKA and FEBA rod data provide important information from which to assess the capability of best estimate computer codes to predict cladding quench behavior.

7. REFERENCES

1. D. L. Reeder, *LOFT System and Test Description (5.5-ft Nuclear Core 1 LOCEs)*, NUREG/CR-0247, TREE-1208, July 1978.

2. M. McCormick-Barger, *Experiment Data Report for LOFT Power Ascension Test L2-2*, NUREG/CR-0492, TREE-1322, February 1979.

3. P. G. Prassinos, B. M. Galusha, D. B. Engelman, *Experiment Data Report for LOFT Power Ascension Experiment L2-3*, NUREG/CR-0792, TREE-1326, July 1979.

4. R. C. Gottula and J. A. Good, *The Effect of Cladding Surface Thermocouples on the Quench Behavior of an Electrical Heater Rod*, L0-00-80-115, March 5, 1980.

5. E. L. Tolman, W. E. Driskell, M. L. Carboneau, *Comparison of Nuclear and Electric Heater Rod Responses for Large Break PWR LOCA Conditions*, EGG-LOFT-5529, October 1981.

6. N. S. Aksan, *Evaluation of Analytical Capability to Predict Cladding Quench*, EGG-LOFT-5555, August 1982.

7. C. S. Olsen, *Zircaloy Cladding Collapse Under Off-Normal Temperature and Pressure Conditions*, TREE-NUREG-1239, April 1978, p. 27.

8. J. P. Adams and V. T. Berta, *Response of LOFT SPNDs to Reactor Coolant Density Variations During LOCA Simulations*, Nuclear Technology, August 1982.

9. J. C. Lin, *Posttest Analysis of LOFT Loss-of-Coolant Experiment L2-3*, EGG-LOFT-5075, March 1980.

10. D. M. Snider, *INVERT 1.0—A Program for Solving the Nonlinear Inverse Heat Conduction Problem for One-Dimensional Solids*, EGG-2068, February 1981.

11. R. W. Garner, *PBF Thermocouple Effects Tests, Test Series TC-4, Quick Look Report*, EGG-TFBP-5465, August 1981.

APPENDIX A
PROTOTYPE CLADDING-EMBEDDED THERMOCOUPLE DEVELOPMENT AND DESIGN

APPENDIX A
PROTOTYPE CLADDING-EMBEDDED THERMOCOUPLE DEVELOPMENT AND DESIGN

In order to eliminate the uncertainty in cladding external thermocouple measurements of cladding temperature on fuel rods in the Loss-of-Fluid Test (LOFT) reactor core,[A-1] a development effort was undertaken at the Idaho National Engineering Laboratory (INEL) to make a small-diameter thermocouple that could be embedded on the inner side of the fuel rod cladding. The development effort consisted of three phases, or generations. The prototype, or first-generation, thermocouples were installed in a REBEKA heater rod[a] for quench experiments conducted in the LOFT Test Support Facility (LTSF) at the INEL. A description of the development effort, various problems encountered, and the basic differences between the different phases of development are discussed in this appendix.

It was desired to fabricate a very small-diameter thermocouple that could be embedded on the inner surface of nuclear fuel rod cladding. In order to minimize the perturbation on heat flux and temperature distribution within the fuel rod near the thermocouple junction, the thermocouple was to be embedded in the cladding for at least three pellet lengths (~40 mm) before exiting the cladding, after which the thermocouple lead was to follow the groove in the pellets and exit at the top of the fuel rod.

In the past, small-diameter thermocouples were made by using the smallest insulators available, along with thin-walled sheath material. The prototype (or first generation) thermocouples used a 1.6-mm-diameter Zircaloy sheath with an initial wall thickness of 0.127 to 0.14 mm. The thermocouple wire was reduced to a diameter of 0.762 mm using a series of draw steps with intermediate anneals at 923 K. The junction end of the thermocouple was further drawn to a diameter of 0.457 mm over a length of 44 to 57 mm and then flattened into a rectangular shape with a thickness of 0.254 mm and a width of 0.635 mm.

Two major problems were encountered in fabricating the prototype thermocouples. The first was not knowing how to simultaneously anneal the thermocouple sheath and the thermoelements. As a result, the thermoelements (Chromel and Alumel) were necked down where the thermocouple was reduced in diameter from 0.762 to 0.457 mm. This resulted in the fracture and failure of many of the thermoelements. The failure rate exceeded 50% of those fabricated. The sheath diameter of 0.457 mm was about the minimum obtainable, and there may have been some necking down of the thermoelements of those thermocouples successfully drawn to 0.457 mm diameter. Since the thermoelements were very small (0.064 to 0.076 mm diameter), it was virtually impossible to detect the amount of necking down from resistance measurements or x-ray. Therefore, for the prototype thermocouples used in the REBEKA rod, the thermoelements could easily have been on the verge of breaking under minimal stresses.

The second problem had to do with cracking of the sheath wall as a result of the small sheath wall thickness in the flattened area. The final sheath wall thickness of the prototype thermocouples was about 0.05 mm. This wall thickness cannot provide much strength, when the grain size of the metal is an appreciable fraction of the wall thickness. Grain boundaries provide built-in fracture lines where cracking can readily occur under stress, such as during the flattening process. Cracks in the sheaths of the prototype instruments were not uncommon. Several of the prototype instruments did not pass a helium leak test due to small sheath cracks. Another problem caused by the thin walled sheath was the possibility of burn-through during the laser welding operation of installing the thermocouple into the cladding insert.

The second generation of thermocouples was similar to the first generation of thermocouples in that the same size sheath material was used and the swaging and annealing process was the same. However, the second generation of thermocouples were only drawn to 0.508 mm diameter and flattened to 0.305 mm, as compared to 0.457 mm diameter and 0.254 mm, respectively, for the prototype instruments. The problem of necking down

a. The REBEKA rod is a cartridge-type electrical heater rod provided by the Karlsruhe Nuclear Reactor Center in Karlsruhe, Germany.

and breakage of the thermoelements was less severe in the second-generation thermocouples, but not eliminated. Cracks in the thin-walled sheath were still a problem.

The second-generation thermocouples were used in the fuel rods for the TC-4 Test Series[A-2] conducted in the Power Burst Facility and exhibited a higher reliability than the prototype instruments used in the REBEKA rod. Second-generation thermocouples were also installed in the LOFT F1 fuel bundle.

The third generation of thermocouples used a thicker wall sheath material in an attempt to eliminate the sheath cracking problem. The initial sheath diameter was 1.473 to 1.524 mm and the initial wall thickness was 0.203 mm. This led to a heavier sheath wall thickness after the swaging and flattening process of 0.076 to 0.089 mm and reduced the sheath cracking problem, but did not totally eliminate it. Also, the heavier wall sheath should make burn-through less likely during the laser welding process of installing the thermocouple into the cladding insert.

A different annealing process was used for the third-generation thermocouples. The thermocouples were annealed at 1396 K for 30 min after every third draw pass. This simultaneously annealed the sheath and the thermoelements such that necking down and breaking of the thermoelements was virtually eliminated. The third-generation thermocouples were made as spares for the LOFT F1 fuel bundle and for future LOFT fuel rods.

In summary, the prototype cladding embedded thermocouples were unreliable and not adequate for use in LOFT fuel rods. However, further development of the thermocouple has led to a potentially more reliable design that has undergone testing in the Power Burst Facility and has been installed in LOFT fuel rods for the F1 fuel bundle.

References

A-1. D. L. Reeder, *LOFT System and Test Description (5.5-ft Nuclear Core 1 LOCEs)*, NUREG/CR-0247, TREE-1208, July 1978.

A-2. R. W. Garner, *PBF Thermocouple Effects Tests, Test Series TC-4, Quick Look Report*, EGG-TFBP-5465, August 1981.

APPENDIX B
REBEKA ROD POST-MORTEM RESULTS INCLUDING CLADDING-EMBEDDED THERMOCOUPLE BEHAVIOR

APPENDIX B
REBEKA ROD POST-MORTEM RESULTS INCLUDING CLADDING-EMBEDDED THERMOCOUPLE BEHAVIOR

Due to the failure of the cladding embedded thermocouples (TE-REB-E1 and -E2) and inadvertent collapse of the cladding of the REBEKA rod[a] during the quench experiment program,[b] a post-mortem was conducted on the REBEKA rod. The objectives of the post-mortem were (a) to investigate the failure mechanism of the primary cladding embedded thermocouple junctions which could provide useful information for future embedded thermocouple designs and installation procedures, (b) to investigate the reason for the formation of the secondary junctions in the embedded thermocouple wires, and (c) to measure the internal pressure in the REBEKA rod to determine why the cladding collapsed.

The first step of the post-mortem was to measure the internal pressure of the REBEKA rod prior to cutting the rod. Due to scheduling problems, the pressure test was not conducted until approximately 3 months after completion of the quench experiments (November 3, 1981). Therefore, if the rod was leaking, the pressure measured would not necessarily reflect the internal pressure of the rod during or immediately after the experiments; however, it would indicate if the rod had leaked or not. A specially designed gas sampling system was used to perform this test. The rod was punctured with a small-diameter drill, and the gas was allowed to escape into the sampling system. The volume of gas in the rod was measured to be 56.4 std cc ± 3% and the void volume in the rod was measured to be 29.6 cc ± 5%. The final pressure in the rod was 193 kPa, as compared to an initial pressure of 2.41 MPa, indicating that the rod did have a significant leak. It is hypothesized that the REBEKA rod leaked enough helium prior to and during the experiment program to allow the cladding to collapse. A probable cause for the leakage was discovered later in the post-mortem analysis.

a. The REBEKA rod is a cartridge-type electrical heater rod provided by the Karlsruhe Nuclear Reactor Center in Karlsruhe, Germany.

b. The quench experiment program was conducted at the Loss-of-Fluid Test (LOFT) Test Support Facility at the Idaho National Engineering Laboratory.

The next step in the post-mortem analysis was to (a) investigate the condition of the embedded thermocouples and probable causes of failure and (b) examine the gap between the aluminum oxide, Al_2O_3, pellets and the sheath and the locations of the embedded thermocouple wires in the slots in the Al_2O_3 pellets at the axial level of the secondary junctions in these wires. In order to accomplish this, the REBEKA rod was sectioned transversely at the five locations shown in Figure B-1. Sample 1 in Figure B-1 was used to examine the condition of the embedded region of the thermocouples in the cladding inserts, particularly where the thermocouple comes out of the groove which could be a likely location of failure. Sample 2 was to be used to examine the pellet-cladding gap at the location of the secondary junction in Thermocouple TE-REB-E2 and the condition of the thermocouple wires where they reduce in diameter from 0.762 to 0.457 mm. Unfortunately this sample disintegrated in the cutting saw due to vibration while Cut 3 was being made. Therefore, any information from Sample 2 was lost.

Sample 3 was cut to observe the pellet-cladding gap and condition of the thermocouple wires at the axial level of the secondary junction in Thermocouple TE-REB-E1. This sample remained intact during the cutting operation.

To observe the embedded thermocouples in the cladding inserts, Sample 1 was cut longitudinally in two places to allow the cladding to fall away from the Al_2O_3 pellets. Direct visual observations indicated both Thermocouples TE-REB-E1 and TE-REB-E2 were still intact in the slots in the inserts and neither thermocouple was fractured or damaged where they came out of the slots in the inserts. However, further observations with the scanning electron microscope (SEM) revealed significant problems with both thermocouples. Numerous cracks in the thermocouple sheath were apparent. Figures B-2 and B-3 show cracks in the sheath of TE-REB-E2 at the junction end at 50X and 130X magnification, respectively. Cracks are also shown in the cross section in Figure B-4. These cracks may or may not have been in the sheath prior to laser welding the thermocouples in the insert. However, cracks in the sheath were prevalent in the areas of

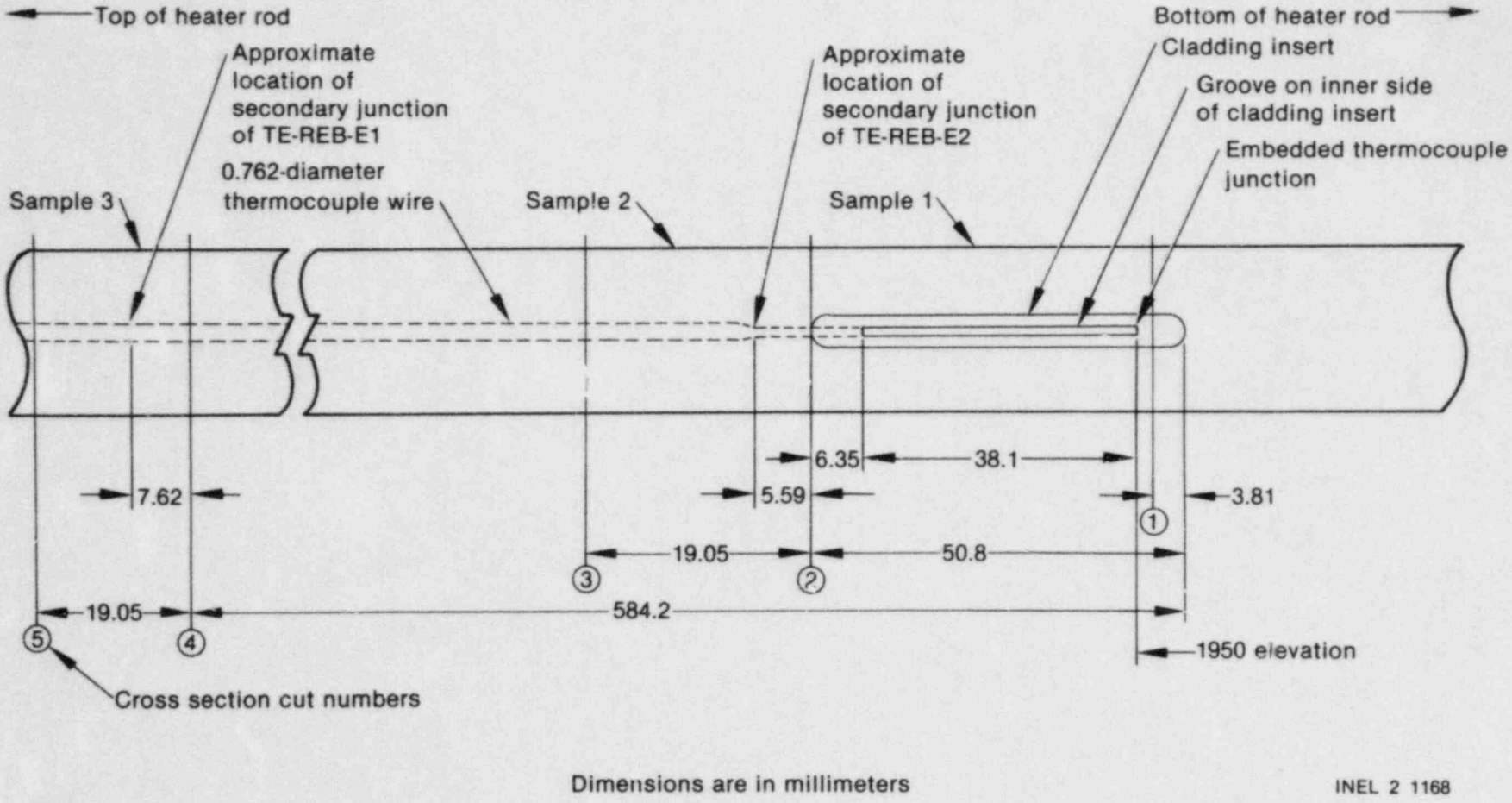

Figure B-1. Transverse cross section locations for post-mortem analysis of REBEKA heater rod.

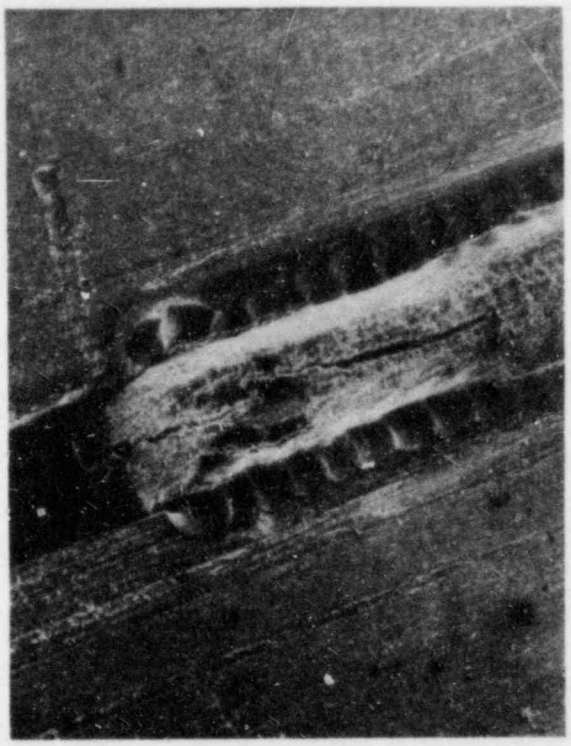

Figure B-2. Cracks in sheath of Thermocouple TE-REB-E2 at embedded junction (50X).

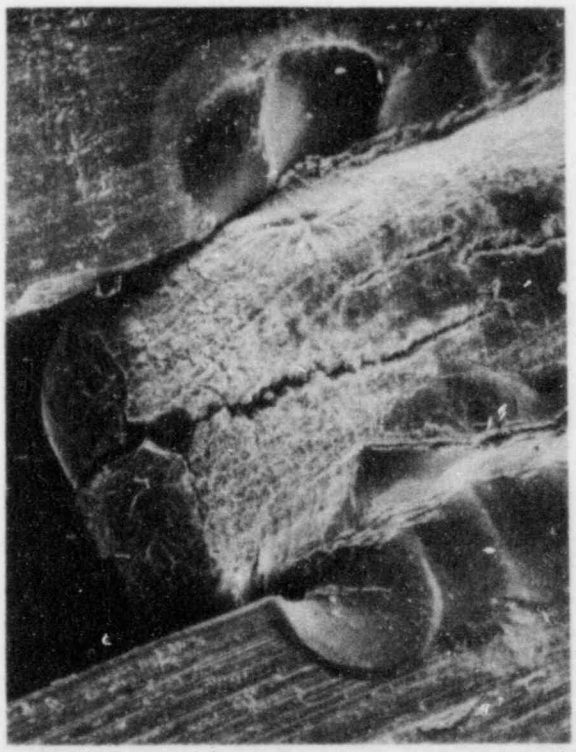

Figure B-3. Cracks in sheath of Thermocouple TE-REB-E2 at embedded junction (130X).

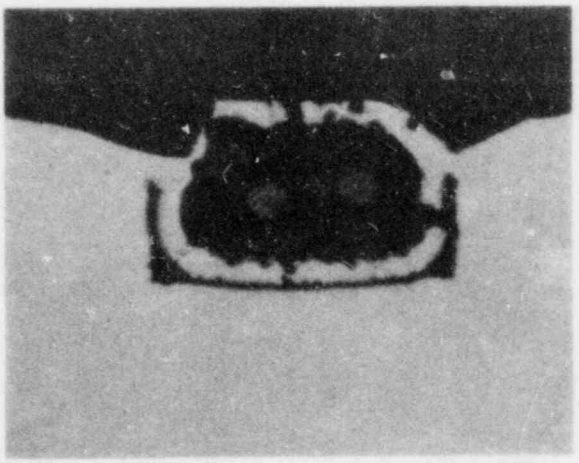

Figure B-4. Cracks in sheath of Thermocouple TE-REB-E2 at embedded junction (100X).

the laser welds, as shown in Figure B-5 along TE-REB-E1 and Figure B-6 along TE-REB-E2.

Cracks were also prevalent along the laser welds where the thermocouples were welded into the slot. This is depicted in Figure B-7 for TE-REB-E1. This may have been due to the thermocouple fitting

Figure B-5. Cracks in sheath of Thermocouple TE-REB-E1 near a laser weld (200X).

Figure B-6. Cracks in sheath of Thermocouple TE-REB-E2 near a laser weld (100X).

Figure B-7. Crack in laser weld along Thermocouple TE-REB-E1 in embedded region (100X).

loosely in the slot in the insert such that the first laser weld on one side of the thermocouple pulled the thermocouple to that side. The laser weld on the opposite would then pull the thermocouple in the opposite direction, putting a stress on the welds and the sheath.

The thermocouple sheath was completely burned through at numerous locations along the laser welds. Figures B-8, B-9, and B-10 show a large burn-through at the junction end of TE-REB-E1 at 50X, 200X, and 1000X magnification, respectively. The thermoelement and insulation inside the thermocouple can be seen in Figure B-10. Figure B-11 further illustrates this burn-through. Figure B-12 shows another hole in the sheath of TE-REB-E2 caused by burn-through at a laser weld.

Other locations along the embedded regions of TE-REB-E1 and TE-REB-E2 showed an apparent blowout of the sheath. This is shown in Figures B-13, B-14, and B-15 at 50X, 200X, and 100X magnification, respectively, for TE-REB-E1 and Figures B-16 and B-17 at 50X and 200X magnification, respectively, at another location for TE-REB-E1. No apparent reason for a blowout was obvious. This phenomena could also have been

Figure B-8. Sheath burn-through at embedded junction of Thermocouple TE-REB-E1 (50X).

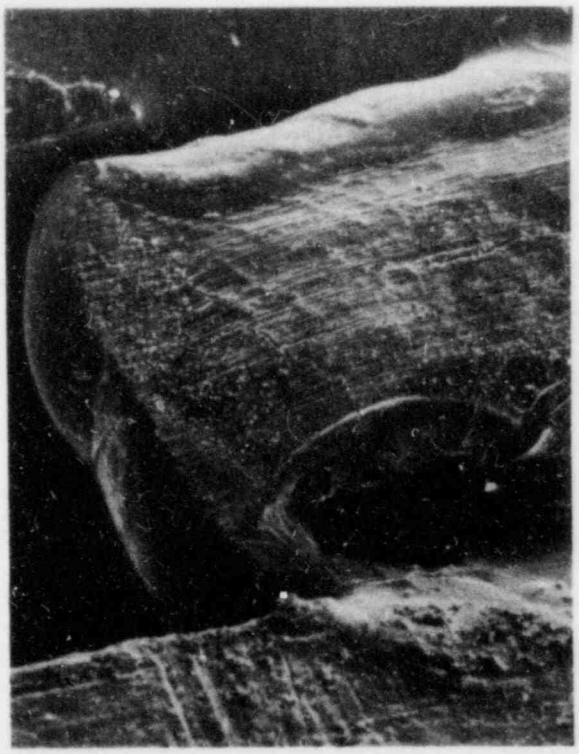

Figure B-9. Sheath burn-through at embedded junction of Thermocouple TE-REB-E1 (200X).

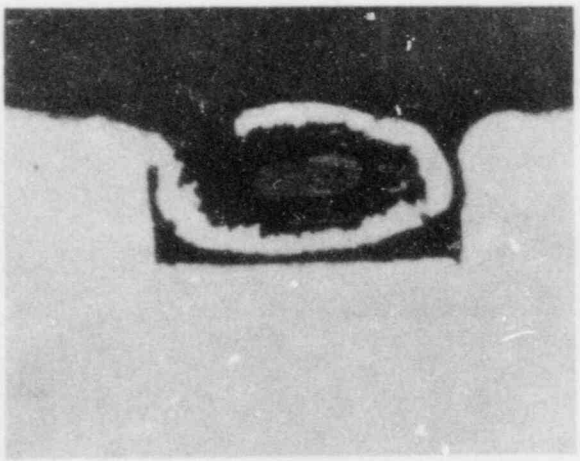

Figure B-11. Sheath burn-through at embedded junction of Thermocouple TE-REB-E1 (100X).

Figure B-10. Sheath burn-through at embedded junction of Thermocouple TE-REB-E1 (1000X).

Figure B-12. Sheath burn-through at a laser weld along Thermocouple TE-REB-E2 (200X).

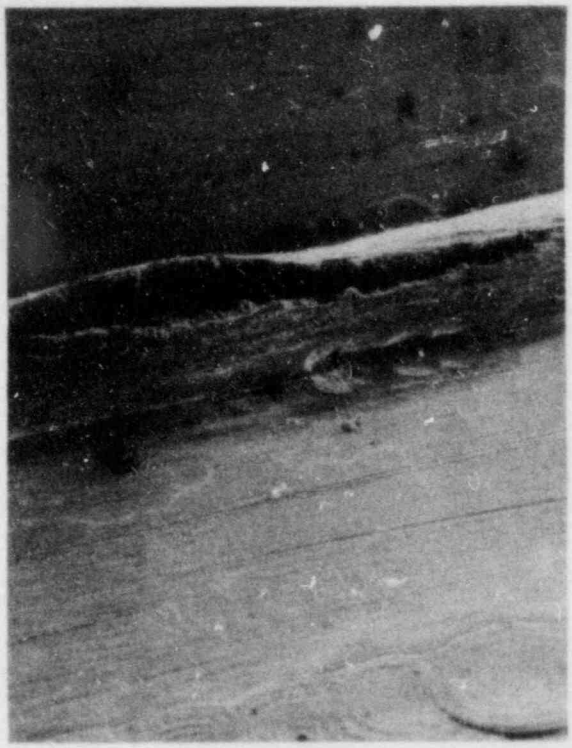

Figure B-13. Apparent sheath blowout along Thermocouple TE-REB-E1 in the embedded region (50X).

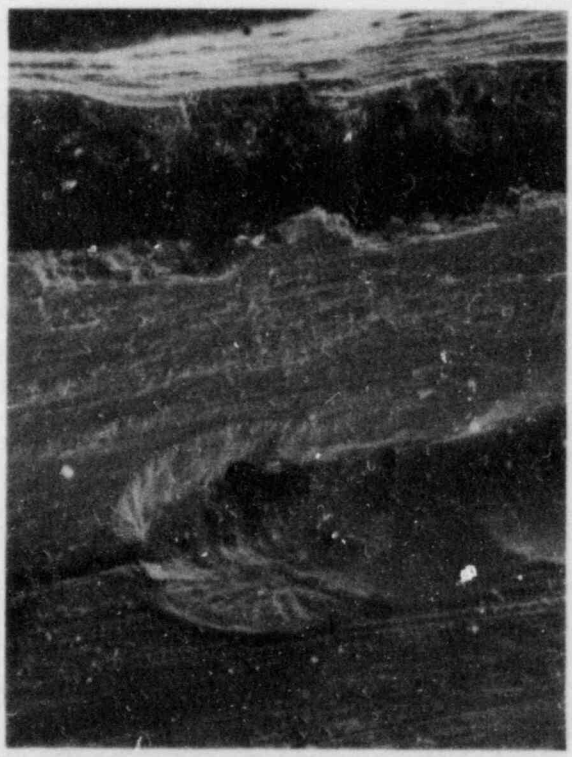

Figure B-14. Apparent sheath blowout along Thermocouple TE-REB-E1 in the embedded region (200X).

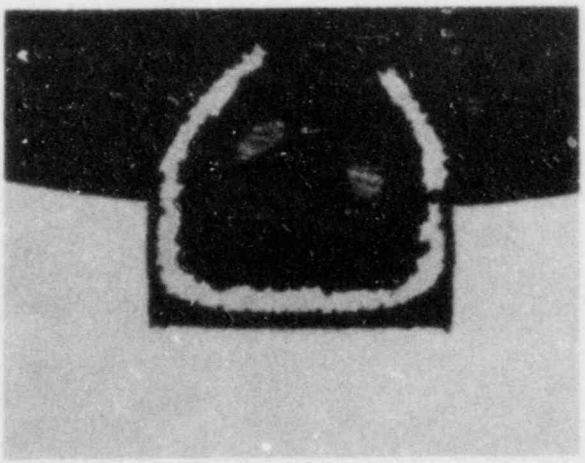

Figure B-15. Apparent sheath blowout along Thermocouple TE-REB-E1 in the embedded region (100X).

Figure B-16. Apparent sheath blowout along Thermocouple TE-REB-E1 in the embedded region (50X).

Figure B-17. Apparent sheath blowout along Thermocouple TE-REB-E1 in the embedded region (200X).

caused by thermal stresses. In addition, the thermocouple insulator appeared to have increased in volume, forcing the thermocouple sheath out away from the slot,as shown in Figures B-15 and B-18, and could have caused the blowout.

Figure B-19 shows TE-REB-E1 just beyond where the thermocouple comes out of the slot in the insert. The insert laser weld can also be seen in this figure. TE-REB-E1 must have been laying against the cladding when the insert weld was done, as it can be seen that the thermocouple sheath was burned through at that location.

The necking down of the thermoelements, discussed in Appendix A, near where the thermocouple wire was reduced from 0.762 to 0.457 mm diameter could be observed with the SEM. Figures B-20 and B-21 show the degradation of the thermoelements at 80X and 400X magnification, respectively. Figures B-22 and B-23 show the fractured end of TE-REB-E2 at 500X magnification. This is typical of a fracture one would observe on a thermoelement that had previously been necked down. Figure B-24 shows the fractured end of TE-REB-E1 at 500X magnification. It is hypothesized that the thermoelements were necked down during their initial fabrication process and then fractured prior to the beginning of the experiment program. This would be consistent with the erratic loop resistance measurements taken on the thermocouples prior to the experiments as discussed in Section 4 of this report.

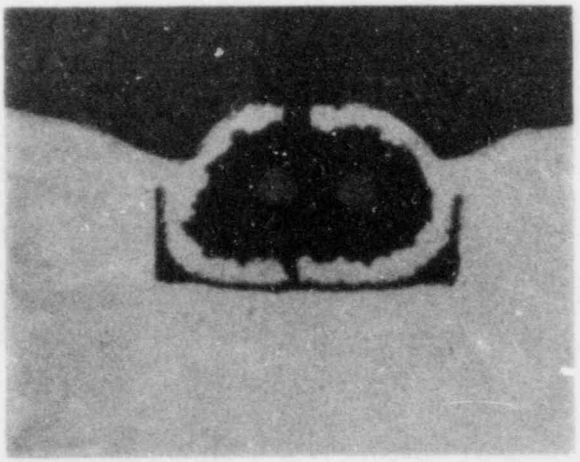

Figure B-18. Expansion of Thermocouple TE-REB-E2 in the embedded region (100X).

Figure B-19. Burn-through of Thermocouple TE-REB-E1 sheath at cladding insert laser weld (50X).

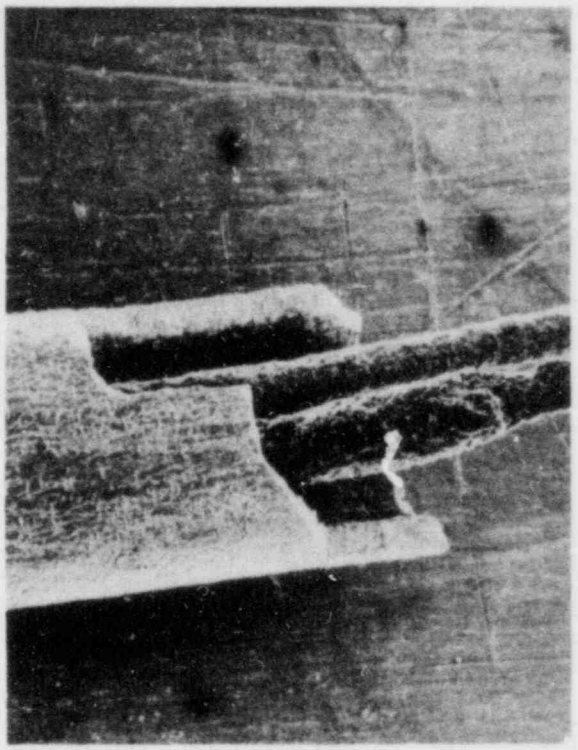

Figure B-20. Neckdown of thermoelements in Thermocouple TE-REB-E2 (80X).

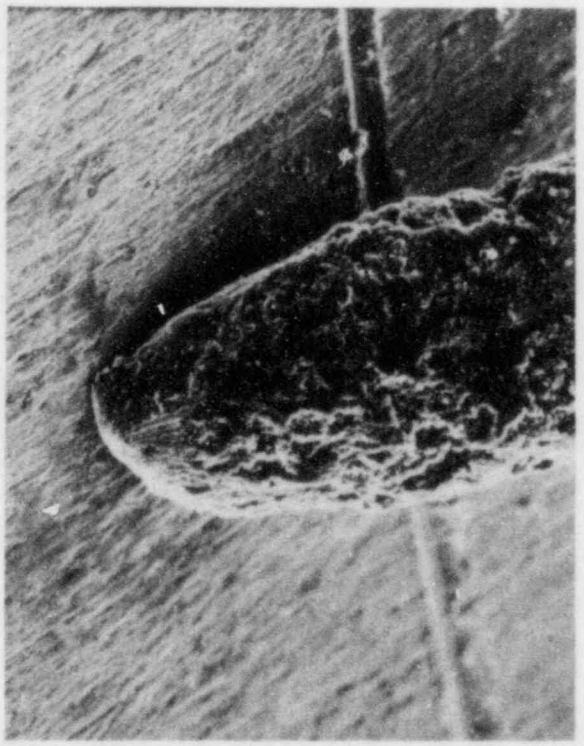

Figure B-22. Fractured end of Thermocouple TE-REB-E2 thermoelement (500X).

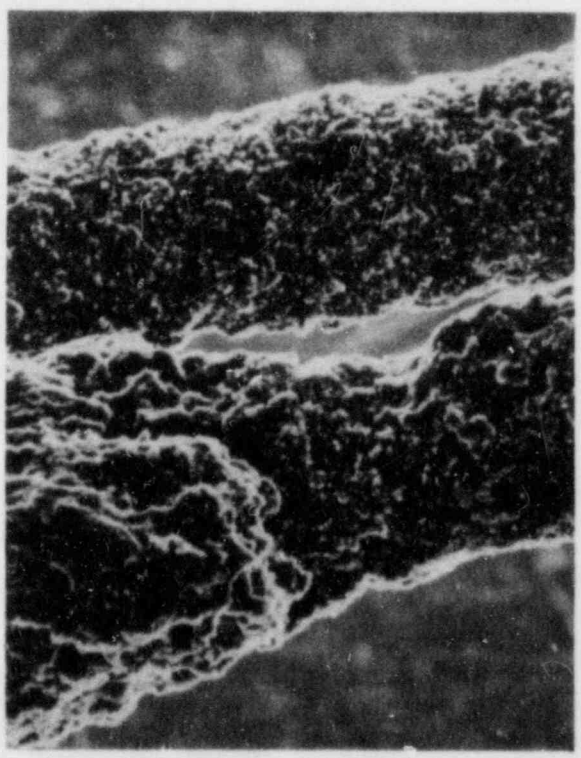

Figure B-21. Neckdown of thermoelements in Thermocouple TE-REB-E2 (400X).

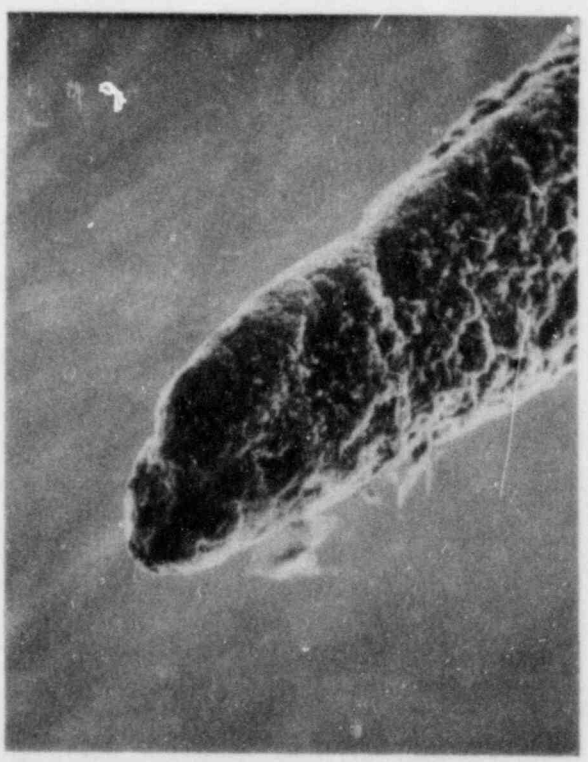

Figure B-23. Fractured end of Thermocouple TE-REB-E2 thermoelement (500X).

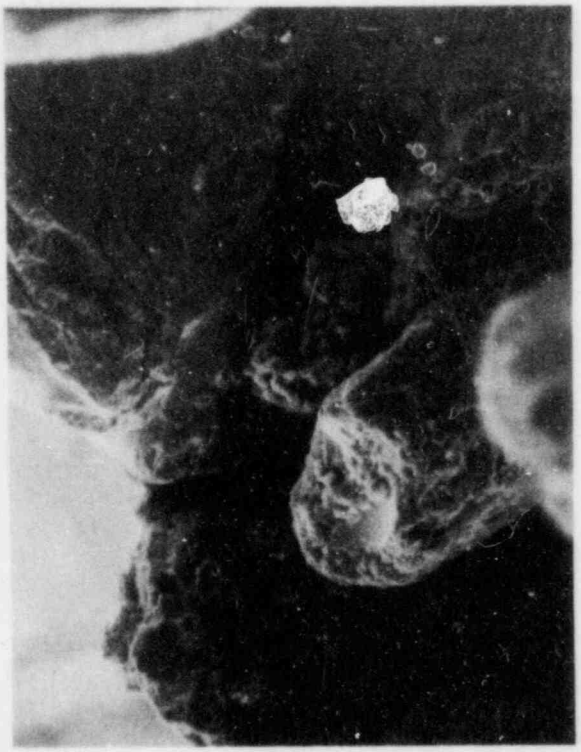

Figure B-24. Fractured end of Thermocouple TE-REB-E1 thermoelement (500X).

Figures B-25 and B-26 show a cross section at the embedded junctions of TE-REB-E1 and TE-REB-E2, respectively. It can be seen that both junctions were intact and that the thermocouple failure did not occur at the embedded junctions.

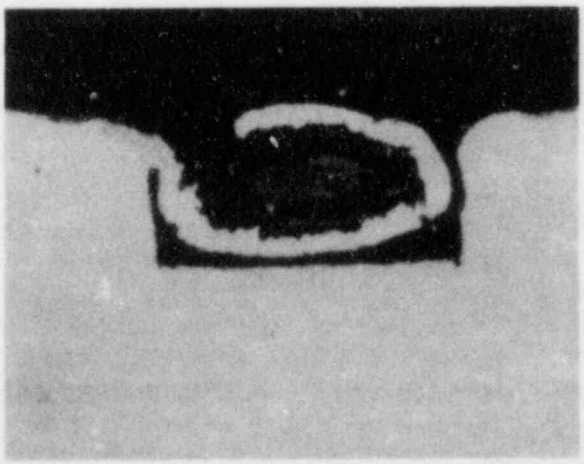

Figure B-25. Embedded junction of Thermocouple TE-REB-E1 (100X).

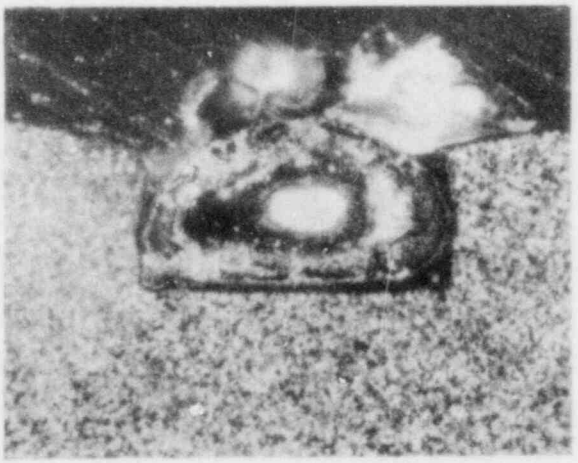

Figure B-26. Embedded junction of Thermocouple TE-REB-E2 (100X).

Sample 2 was destroyed, so no information was obtained concerning the secondary junction of TE-REB-E2. However, some information was obtained from Sample 3. Figure B-27 shows a cross section of TE-REB-E2 in Sample 3. The thermoelements and insulator appeared to be in good condition at that location. Figure B-28 shows a cross section of TE-REB-E1 in Sample 3. It can be seen that the thermoelements were not in contact which could cause a short, but the insulation in that area had turned black. A chemical analysis performed on TE-REB-E1 at this location determined the content of the black material surrounding the Alumel thermoelement was composed of 67% nickel, 25% silicon, and 8% aluminum by weight. The black material surrounding the Chromel thermoelement was composed of 67% nickel, 22% silicon, 9% chromium, and 2% aluminum by weight. The secondary junctions formed in TE-REB-E1 and TE-REB-E2 were most likely a short caused by a conductive path through the black material.

The mechanism or chemical reaction to form the black material around the thermoelements has not been determined. It was previously discovered that acetone, used to degrease Zircaloy cladding, may leave contaminants which, upon heating during annealing, will produce blackening of Al_2O_3 insulation. Tests to verify this result reproduced the phenomena in one case, but did not in another. The purity of the acetone could vary from bottle to bottle, and the degree to which acetone is cleaned off of the Zircaloy cladding could be variable. So whether or not blackening of the Al_2O_3 insulation takes place could be a function of these parameters. However, this could explain the blackening of the

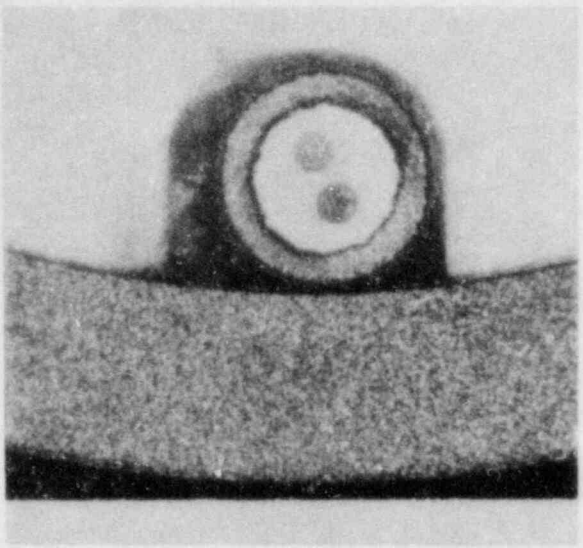

Figure B-27. Cross section of Thermocouple TE-REB-E2 at the 2545-mm elevation of the REBEKA heater rod.

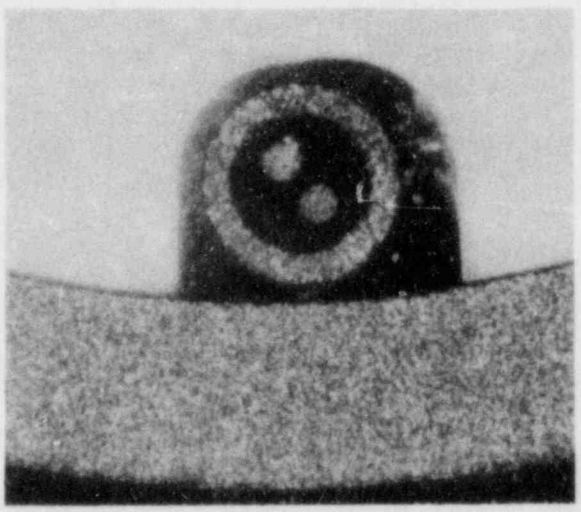

Figure B-28. Cross section of Thermocouple TE-REB-E1 at the 2534-mm elevation on the REBEKA heater rod.

Al_2O_3 insulation in Sample 3 of TE-REB-E1 shown in Figure B-28. In any case, this phenomenon is undesirable for thermocouples that may be installed in LOFT fuel rods.[B-1] It would be valuable to conduct a post-mortem on the fuel rods used in the TC-4 Test Series[B-2] conducted in the Power Burst Facility to determine if a similar phenomenon was experienced in the cladding embedded thermocouples used in those tests.

In summary, the following conclusions can be stated based on the results of the REBEKA rod post-mortem examination:

1. The REBEKA rod depressurized, most likely prior to the initiation of the nine-rod bundle quench experiment runs, allowing the cladding to collapse during the runs. Holes burned through the embedded thermocouple sheath during installation in the cladding insert, as well as cracks in the thermocouple sheath, caused the most likely leak path of the helium through the thermocouple and out of the rod.

2. Both embedded thermocouples failed prior to the experiment. The thermoelements appeared to have necked down and fractured near where the thermocouple was reduced from 0.762 to 0.457 mm diameter. Both embedded junctions were intact and the thermocouples were intact in the cladding insert at completion of the experiments.

3. Secondary junctions were formed in both embedded thermocouple wires. A material was formed around the thermoelements with a sufficiently high electrical conductivity to cause a short between the thermoelements. The mechanism is not fully understood at this time.

References

B-1. D. L. Reeder, *LOFT System and Test Description (5.5-ft Nuclear Core 1 LOCEs)*, NUREG/CR-0247, TREE-1208, July 1978.

B-2. R. W. Garner, *PBF Thermocouple Effects, Test Series TC-4, Quick Look Report*, EGG-TFBP-5465, August 1981.

APPENDIX C
INVERT COMPUTER CODE MODEL

APPENDIX C
INVERT COMPUTER CODE MODEL

Due to the early failure of the cladding embedded thermocouples in the REBEKA rod[a] during the quench experiment program,[b] the actual temperature of the REBEKA rod cladding was not measured. In addition, a direct comparison of the cladding-embedded and external thermocouple measurements during the experiment could not be made to quantify the ability of the external thermocouples to measure cladding temperature. Therefore, inverse heat conduction calculations were made to predict the cladding surface temperature of the REBEKA rod for each experiment run. This made it possible to evaluate the ability of the cladding external thermocouple to measure the actual cladding temperature during rapid cooling transients. Also, the calculated cladding surface temperatures were used to compare the quench behavior of the REBEKA rod with and without cladding external thermocouples, as reported in Section 5 of this report.

The INVERT computer code[C-1] was used to perform the inverse heat conduction calculations. INVERT solves the nonlinear inverse heat conduction problem for a one-dimensional solid. The inverse solution is used to determine an unknown surface heat flux and temperature distribution in a solid using the measured temperature history at one interior location.

A 27-node, one-dimensional model of the REBEKA rod was constructed. A diagram is shown in Figure C-1. The model included the Zircaloy cladding, the aluminum oxide (Al_2O_3) pellets, the Inconel sheath around the heater element, boron nitride insulation, the Inconel heater element, and the magnesium oxide core. Also, a helium gas gap was modeled between the cladding and the Al_2O_3 pellets and between the Al_2O_3 pellets and the Inconel heater element sheath. The material properties used in the model were published by the Karlsruhe Nuclear Reactor Center.[C-2] The units

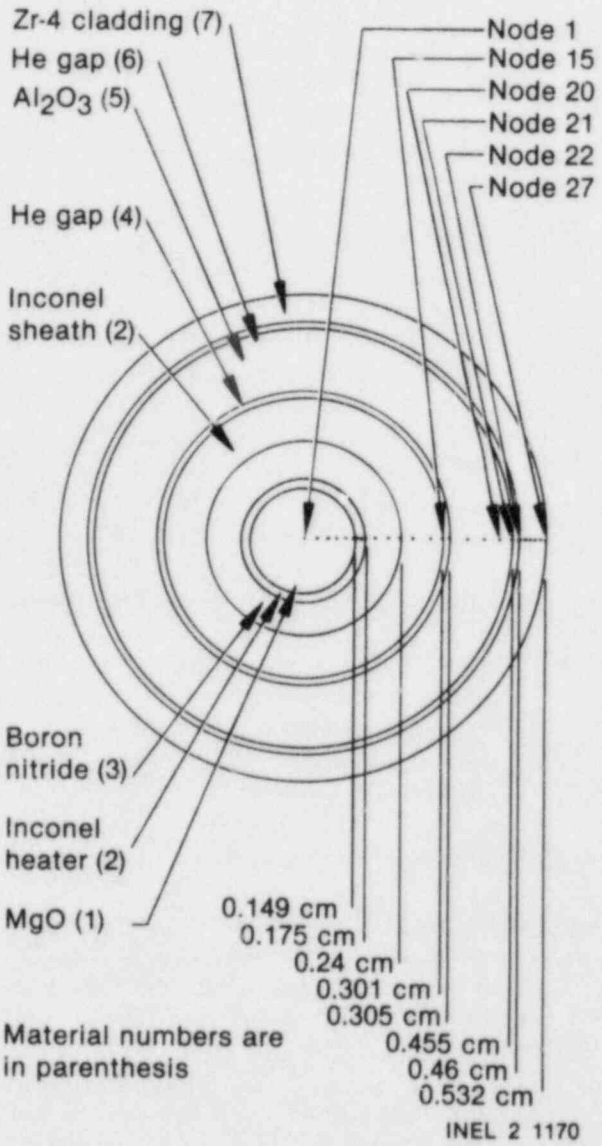

Figure C-1. INVERT computer code model of REBEKA heater rod.

used in the program were s, cm, K, and calories. The inner helium gap width was calculated to be 0.04 mm at 900 K, considering the thermal expansion of the Inconel sheath and the Al_2O_3 pellets. This value was used in the model. The outer gap width and outer diameter of the cladding used in the model were determined from the diameter measurements taken on the rod throughout the quench experiment program, as listed in Appendix E.

a. The REBEKA rod is a cartridge-type electrical heater rod provided by the Karlsruhe Nuclear Reactor Center in Karlsruhe, Germany.

b. The quench experiment program was conducted at the Loss-of-Fluid Test (LOFT) Test Support Facility at the Idaho National Engineering Laboratory.

Parameter studies were conducted to determine:

1. Influence of heater rod power on the calculation
2. The optimum number of advance time steps to use in the program
3. The optimum time step to use in the program
4. Whether to use cladding internal Thermocouple TE-REB-I2 or the secondary junctions of cladding embedded Thermocouple TE-REB-E2 (or TE-REB-E1) as the input temperature measurement
5. If TE-REB-E2 or TE-REB-E1 was used as the input temperature measurement, at what radial position (or node) should the thermocouple junction be located
6. How the Al_2O_3 pellet should be modeled in the vicinity of the embedded thermocouple wire since the slot in the pellets does not allow a truly one-dimensional problem and the gap conductance between the thermocouple wire and the Al_2O_3 pellet was unknown.

Calculations were made both with and without the measured rod power. Due to the extremely low power level on the REBEKA rod, the rod power had an insignificant effect on the calculated temperature history and quench behavior of the rod. However, the measured rod power was included in all of the INVERT calculations.

The optimum number of advance time steps and the optimum time step to use depended on whether TE-REB-I2 or one of the embedded thermocouple wires was to be used as the input temperature history. This is due to the difference in the radial distance of each of these thermocouples from the cladding surface. The optimum number of advance time steps for either case was determined to be six. The optimum time step was larger when using TE-REB-I2 due to its large radial distance from the cladding surface. The optimum time step when using TE-REB-E1 or TE-REB-E2 as the input temperature was 0.1 s.

Calculations were made using TE-REB-I2 and TE-REB-E2 as the input temperature. Less accurate predictions of the cladding temperature were obtained using TE-REB-I2 due to its large radial distance and decoupling from the cladding. Figure C-2 shows a typical comparison of the predicted cladding surface temperature using TE-REB-I2 and TE-REB-E2 as the input temperature for quench Experiment Run 1, see Table 5 in the body of this report.

The actual location of the embedded thermocouple wires in the slots in the Al_2O_3 pellets at the secondary junctions was not precisely known. Therefore, the assumed location of the junction for input to the INVERT program had some bearing on the predicted cladding surface temperature. Figures B-27 and B-28 give some insight as to the configuration of the embedded thermocouple wires in the slot in the Al_2O_3 pellets. Calculations were made assuming the thermocouple junction was at various radial positions in the model. Figure C-3 shows a comparison of the predicted cladding temperatures assuming the thermocouple junction was at Node 22 on Figure C-1 (the inner surface of the cladding), Node 21 (the outer surface of the Al_2O_3 pellet), and at Node 20 (representing some thermal resistance in addition to the gap between the thermocouple junction and the cladding). It was determined that the most realistic location to assume the thermocouple junction to be was at Node 21 (equivalent to the outer surface of the Al_2O_3 pellets). Thus, the influence of the gap between the cladding and pellets was included in the calculations.

Finally, the slot in the Al_2O_3 pellets and the thermocouple wire geometry could not be modeled explicitly with a one-dimensional code if the gap conductance between the thermocouple and the Al_2O_3 pellet was not known. This region was modeled by assuming the Al_2O_3 pellet was annular and symmetrical without the slot, and then the thermal conductivity of the Al_2O_3 material was adjusted. The thermal conductivity was adjusted until the INVERT calculated temperature at the location of Thermocouple TE-REB-I2 (Node 15) was equivalent to the temperature measured by TE-REB-I2 for each experiment run. This allowed the proper amount of heat transfer through this region to the cladding, such that a realistic cladding temperature could be predicted.

The final calculations were made using output from either Thermocouple TE-REB-E2 or TE-REB-E1 as the input temperature and assuming the secondary thermocouple junction was at

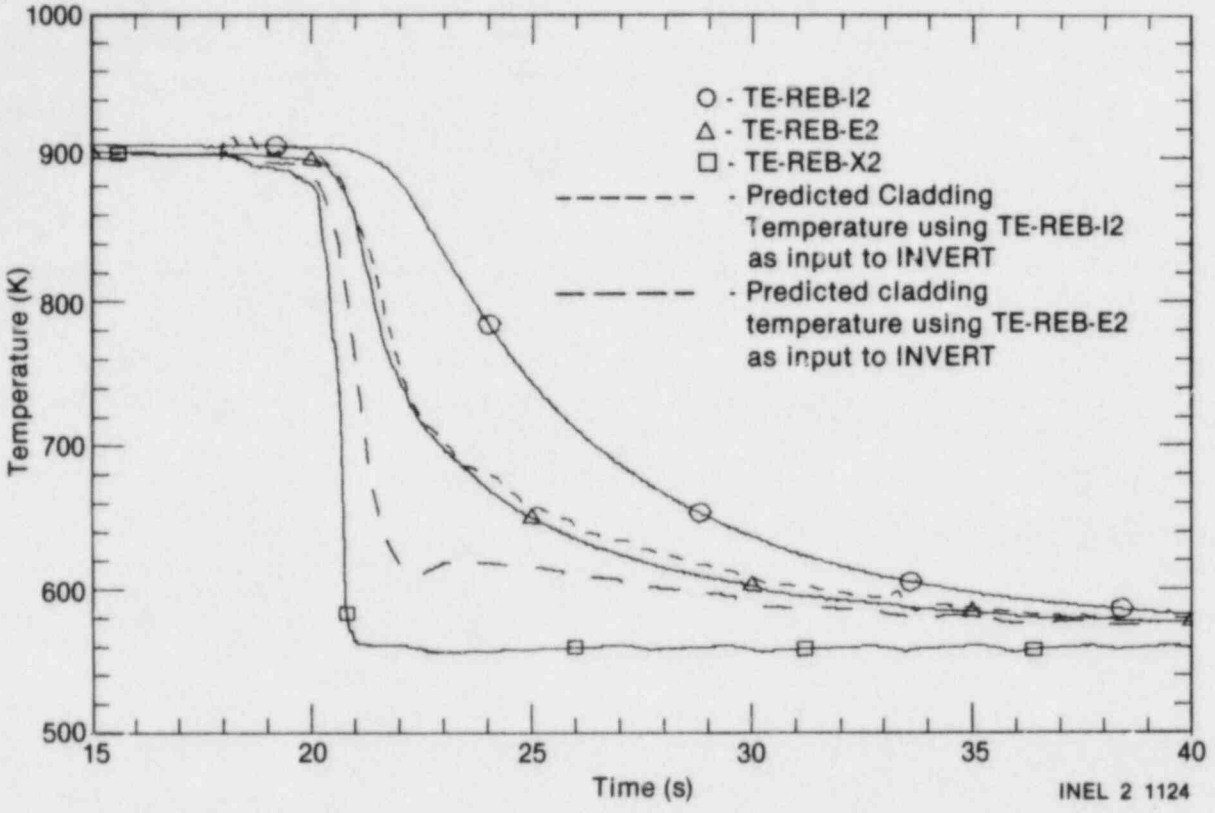

Figure C-2. Predicted cladding surface temperatures for Run 1 as a function of INVERT code input temperature response.

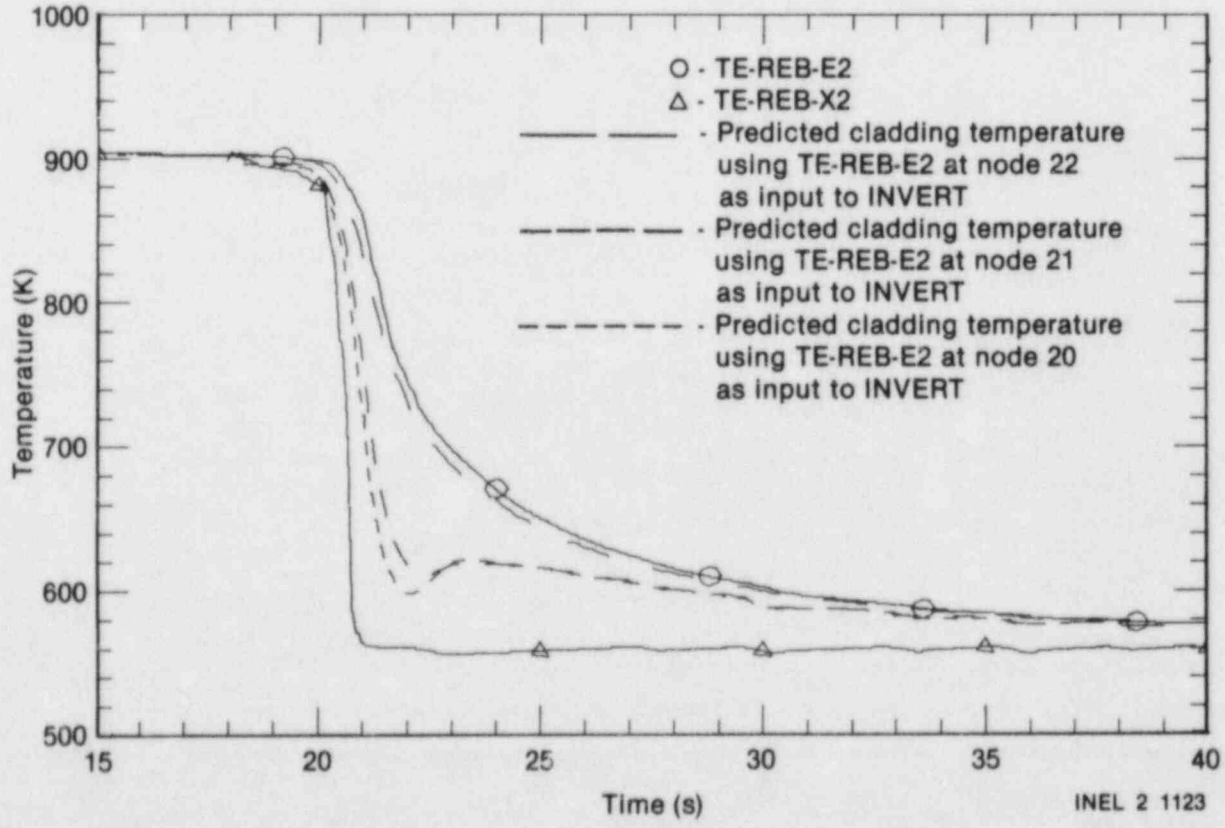

Figure C-3. Predicted cladding surface temperatures for Run 1 as a function of radial location of INVERT code input temperature response.

Node 21 (the outer surface of the Al_2O_3 pellet) and by adjusting the thermal conductivity of the Al_2O_3 material as previously described. Figure C-4 shows the INVERT calculated values for Experiment Run 1. The predicted cladding outer surface temperature is shown along with a comparison of the INVERT predicted temperature at the location of TE-REB-I2 (Node 15) and the measured value from TE-REB-I2. The INVERT calculated surface heat flux and heat transfer coefficient (based on $T_{WALL} - T_{SAT}$) are plotted in Figures C-5 and C-6, respectively. These values and the overall calculation are shown to be realistic, and they result in a prediction of cladding surface temperature much closer to the actual cladding temperature than that measured by TE-REB-E1 or TE-REB-E2. The predicted cladding surface temperature is estimated to be within ± 25 K of the actual cladding temperature.

The calculations for the other experiment runs were similar. Listings of the INVERT input are shown for Experiment Runs 1, 2, 3, 1A, 2A, 3A, 3AR, and 4A in Tables C-1 through C-8. INVERT calculations were not conducted for the low-flow experiment runs.

References

C-1. D. M. Snider, *INVERT 1.0—A Program for Solving the Nonlinear Inverse Heat Conduction Problem for One-Dimensional Solids*, EGG-2068, February 1981.

C-2. K. Wagner and T. Vollmer, *Zusammenstellung von Stoffwerten fur Warmeleitrechnungen an LWR-Brennstaben und deren Simulatoren*, KfK-Ext. 15/77-2, August 1977.

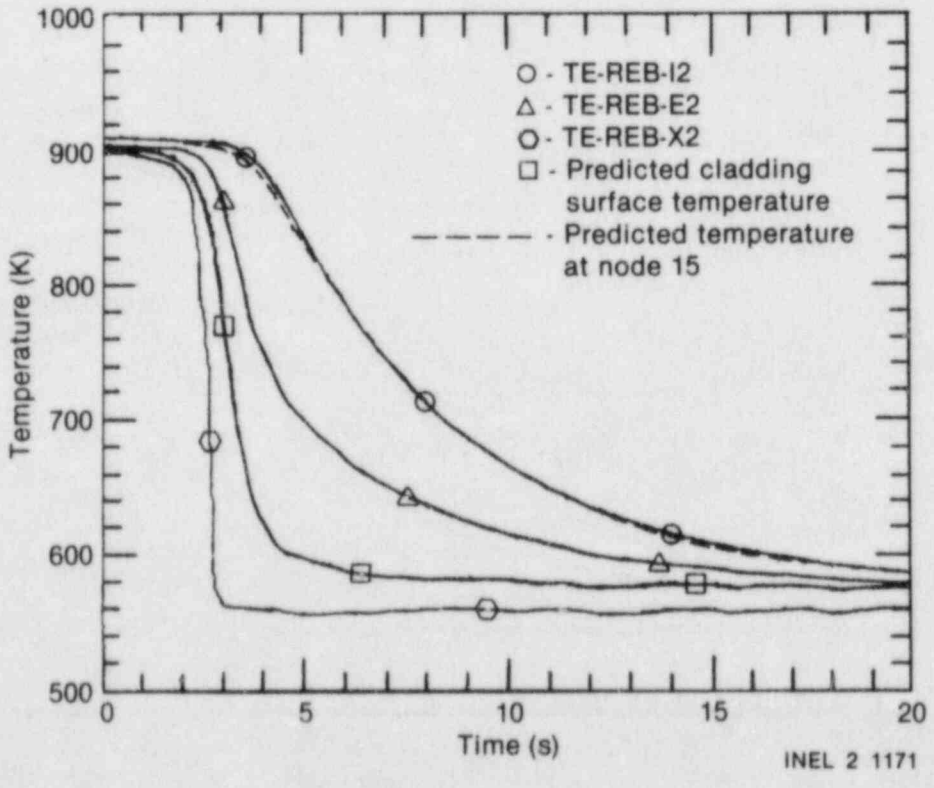

Figure C-4. Predicted cladding surface temperatures for Run 1 and predicted and measured temperatures at the location of Thermocouple TE-REB-I2 (Node 15).

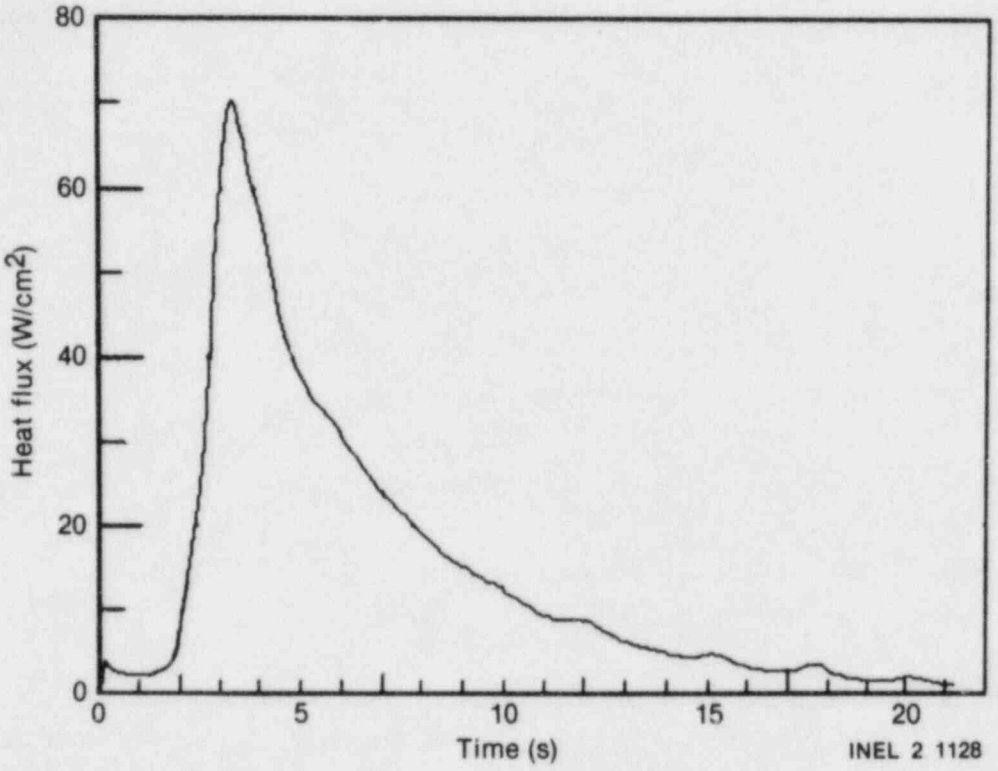

Figure C-5. Calculated surface heat flux versus time for Run 1.

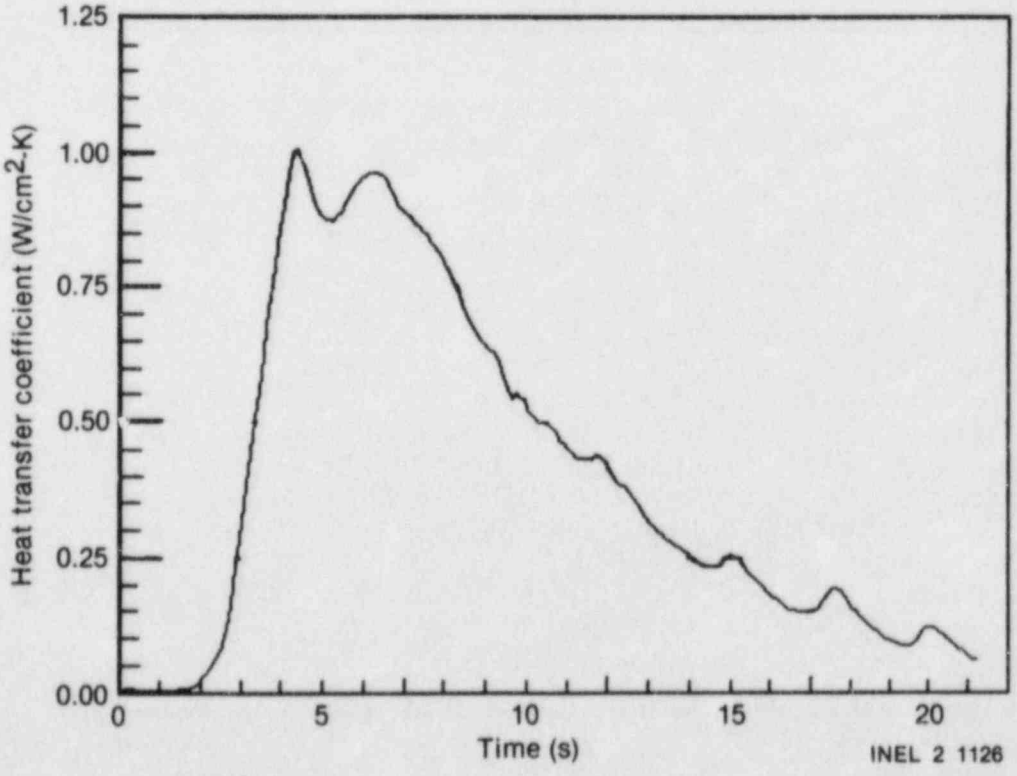

Figure C-6. Calculated surface heat transfer coefficient versus time for Run 1.

Table C-1. Invert code input for Experiment Run 1

```
100  =  ATTACH,TC1,ID=ROG,TYPE=CWAF
110  =  PROP
120  =  K,1 MAGNESIUM OXIDE
130  =  373.,.07
140  =  548.18,.07780, 573.18,.07773, 598.18,.07727, 623.18,.07682
150  =  648.18,.07591,673.18,.07546, 698.18,.07455, 723.18,.07364
160  =  748.18,.07273,773.18,.07182,950.,.071
170  =  CP,1  MAGNESIUM OXIDE
180  =  373.,3.349
190  =  548.18,3.7033,573.18,3.7452,598.18,3.7732,623.18,3.8012
200  =  648.18,3.8225, 673.18,3.8505, 698.18,3.8644, 723.18,3.8756
210  =  748.18,3.9133,773.18,3.9342,950.,3.95
220  =  K,2 INCONEL
230  =  373.,.19
240  =  548.18,.2200, 573.18,.2270, 598.18,.2296, 623.18,.2339
250  =  648.18,.2400, 673.18,.2455, 698.18,.2496, 723.18,.2539
260  =  748.18,.2600,773.18,.2635,950.,.304
270  =  CP,2  INCONEL
280  =  373.,3.903
290  =  548.18,4.2373, 573.18,4.2744, 598.18,4.3182, 623.18,4.3545
300  =  648.18,4.3916, 673.18,4.4278, 698.18,4.4716, 723.18,4.5087
310  =  748.18,4.5450,773.18,4.5745,950.,4.6
320  =  K,3  BORON NITRIDE
330  =  .186
340  =  CP,3  BORON NITRIDE
350  =  373.,1.862
360  =  548.18,2.5529, 573.18,2.6190, 598.18,2.6768, 623.18,2.7595
370  =  648.18,2.8256, 673.18,2.8834, 698.18,2.9246, 723.18,2.9742
380  =  748.18,3.0321,773.18,3.0569,950.,3.08
390  =  K,4  INNER HELIUM GAP
400  =  300.,.00152,500.,.00214,600.,.00242,700.,.00268
410  =  800.,.00293,900.,.00314,1000.,.0034,1200.,.00384
420  =  CP,4  INNER HELIUM GAP
430  =  .00052
440  =  K,5  ALUMINUM OXIDE
460  =  373.,.07,973.,.04
490  =  CP,5  ALUMINUM OXIDE
500  =  373.,3.55
510  =  548.18,4.1142, 573.18,4.1556, 598.18,4.2050, 623.18,4.2465
520  =  648.18,4.2959, 673.18,4.3456, 698.18,4.3703, 723.18,4.3950
530  =  748.18,4.4281,773.18,4.4695,873.,4.563,1073.,4.704
540  =  K,6  OUTER HELIUM GAP
550  =  300.,.00152
560  =  500.,.00214,600.,.00242,700.,.00268,800.,.00293,900.,.00314
570  =  1000.,.0034,1200.,.00384
580  =  CP,6  OUTER HELIUM GAP
590  =  .00052
600  =  K,7  ZIRCALOY CLADDING
610  =  373.,.137
620  =  0. .13845,548.18,.1635, 573.18,.1652, 598.18,.1687
630  =  623.18,.1713
```

Table C-1. (continued)

```
640  =  648.18,.1739, 673.18,.1757, 698.18,.1797, 723.18,.1826
650  =  748.18,.1852,773.18,.1896,973.,.214
660  =  CP,7  ZIRCALOY CLADDING
670  =  373.,1.965
680  =  548.18,2.0366, 573.18,2.0503, 598.18,2.0791, 623.18,2.1073
690  =  648.18,2.1217, 673.18,2.1361, 698.18,2.1505, 723.18,2.1643
700  =  748.18,2.1787,773.18,2.1931,843.,2.216,1083.,2.351
710  =  END
720  =  MODEL
730  =  CARD1,27,0.0,2
740  =  CARD2,.149,6,.175,9,.240,12,.301,15,.305,16,.455,21
750  =  CONT,.460,22,.532,27
760  =  CARD3,1,6,2,9,3,12,2,15,4,16,5,21,6,22,7,27
770  =  CARD4,0.0,6,0.1148,9,0.0,27
780  =  CARD5,910.,9,909.,12,908.,16,907.,18,906.,20
790  =  CONT,905.,22,904.,24,903.,26,902.,27
800  =  END
810  =  TIME,17.92,40.,.1,6
820  =  CONTROL,PRINTFREQ = 10,NODE1 = 15,NODE2 = 22
830  =  BCINITIAL,.0014,559.
840  =  PRESSURE,16
850  =  DATA,20,0,17,21,0,0,0,0,TCRUN1AA
```

Table C-2. Invert code input for Experiment Run 2

```
100  =  ATTACH,TC1,ID = ROG,TYPE = CWAF
110  =  PROP
120  =  K,1  MAGNESIUM OXIDE
130  =  373.,.07
140  =  548.18,.07780, 573.18,.07773, 598.18,.07727, 623.18,.07682
150  =  648.18,.07591,673.18,.07546, 698.18,.07455, 723.18,.07364
160  =  748.18,.07273,773.18,.07182,950.,.071
170  =  CP,1  MAGNESIUM OXIDE
180  =  373.,3.349
190  =  548.18,3.7033,573.18,3.7452,598.18,3.7732,623.18,3.8012
200  =  648.18,3.8225, 673.18,3.8505, 698.18,3.8644, 723.18,3.8756
210  =  748.18,3.9133,773.18,3.9342,950.,3.95
220  =  K,2 INCONEL
230  =  373.,.19
240  =  548.18,.2200, 573.18,.2270, 598.18,.2296, 623.18,.2339
250  =  648.18,.2400, 673.18,.2455, 698.18,.2496, 723.18,.2539
260  =  748.18,.2600,773.18,.2635,950.,.304
270  =  CP,2  INCONEL
280  =  373.,3.903
290  =  548.18,4.2373, 573.18,4.2744, 598.18,4.3182, 623.18,4.3545
300  =  648.18,4.3916, 673.18,4.4278, 698.18,4.4716, 723.18,4.5087
310  =  748.18,4.5450,773.18,4.5745,950.,4.6
320  =  K,3  BORON NITRIDE
330  =  .186
```

Table C-2. (continued)

```
340  =  CP,3  BORON NITRIDE
350  =  373.,1.862
360  =  548.18,2.5529, 573.18,2.6190, 598.18,2.6768, 623.18,2.7595
370  =  648.18,2.8256, 673.18,2.8834, 698.18,2.9246, 723.18,2.9742
380  =  748.18,3.0321,773.18,3.0569,950.,3.08
390  =  K,4  INNER HELIUM GAP
400  =  300.,.00152,500.,.00214,600.,.00242,700.,.00268
410  =  800.,.00293,900.,.00314,1000.,.0034,1200.,.00384
420  =  CP,4  INNER HELIUM GAP
430  =  .00052
440  =  K,5  ALUMINUM OXIDE
450  =  373.,.07,973.,.004
460  =  CP,5  ALUMINUM OXIDE
470  =  373.,3.55
480  =  548.18,4.1142, 573.18,4.1556, 598.18,4.2050, 623.18,4.2465
490  =  648.18,4.2959, 673.18,4.3456, 698.18,4.3703, 723.18,4.3950
500  =  748.18,4.4281,773.18,4.4695,873.,4.563,1073.,4.704
510  =  K,6  OUTER HELIUM GAP
520  =  300.,.00152
530  =  500.,.00214,600.,.00242,700.,.00268,800.,.00293,900.,.00314
540  =  1000.,.0034,1200.,.00384
550  =  CP,6  OUTER HELIUM GAP
560  =  .00052
570  =  K,7  ZIRCALOY CLADDING
580  =  373.,.137
590  =  0. .13845,548.18,.1635, 573.18,.1652, 598.18,.1687
600  =  623.18,.1713
610  =  648.18,.1739, 673.18,.1757, 698.18,.1797, 723.18,.1826
620  =  748.18,.1852,773.18,.1896,973.,.214
630  =  CP,7  ZIRCALOY CLADDING
640  =  373.,1.965
650  =  548.18,2.0366, 573.18,2.0503, 598.18,2.0791, 623.18,2.1073
660  =  648.18,2.1217, 673.18,2.1361, 698.18,2.1505, 723.18,2.1643
670  =  748.18,2.1787,773.18,2.1931,843.,2.216,1083.,2.351
680  =  END
690  =  MODEL
700  =  CARD1,27,0.0,2
710  =  CARD2,.149,6,.175,9,.240,12,.301,15,.305,16,.459,21
720  =  CONT,.460,22,.532,27
730  =  CARD3,1,6,2,9,3,12,2,15,4,16,5,21,6,22,7,27
740  =  CARD4,0.0,6,0.1148,9,0.0,27
750  =  CARD5,910.,9,909.,12,908.,16,907.,18,906.,20
760  =  CONT,905.,22,904.,24,903.,26,902.,27
770  =  END
780  =  TIME,25.4,45.,.1,6
790  =  CONTROL,PRINTFREQ = 10,NODE1 = 15,NODE2 = 22
800  =  BCINITIAL,.0014,559.
810  =  PRESSURE,16
820  =  DATA,17,0,0,21,0,0,0,0,BFQT42RUN2
```

Table C-3. Invert code input for Experiment Run 3

```
100  =  ATTACH,TC1,ID=ROG,TYPE=CWAF
110  =  PROP
120  =  K,1  MAGNESIUM OXIDE
130  =  373.,.07
140  =  548.18,.07780, 573.18,.07773, 598.18,.07727, 623.18,.07682
150  =  648.18,.07591,673.18,.07546, 698.18,.07455, 723.18,.07364
160  =  748.18,.07273,773.18,.07182,950.,.071
170  =  CP,1  MAGNESIUM OXIDE
180  =  373.,3.349
190  =  548.18,3.7033,573.18,3.7452,598.18,3.7732,623.18,3.8012
200  =  648.18,3.8225, 673.18,3.8505, 698.18,3.8644, 723.18,3.8756
210  =  748.18,3.9133,773.18,3.9342,950.,3.95
220  =  K,2 INCONEL
230  =  373.,.19
240  =  548.18,.2200, 573.18,.2270, 598.18,.2296, 623.18,.2339
250  =  648.18.,2400, 673.18,.2455, 698.18,.2496, 723.18,.2539
260  =  748.18,.2600,773.18,.2635,950.,.304
270  =  CP,2  INCONEL
280  =  373.,3.903
290  =  548.18,4.2373, 573.18,4.2744, 598.18,4.3182, 623.18,4.3545
300  =  648.18,4.3916, 673.18,4.4278, 698.18,4.4716, 723.18,4.5087
310  =  748.18,4.5450,773.18,4.5745,950.,4.6
320  =  K,3  BORON NITRIDE
330  =  .186
340  =  CP,3  BORON NITRIDE
350  =  373.,1.862
360  =  548.18,2.5529, 573.18,2.6190, 598.18,2.6768, 623.18,2.7595
370  =  648.18,2.8256, 673.18,2.8834, 698.18,2.9246, 723.18,2.9742
380  =  748.18,3.0321,773.18,3.0569,950.,3.08
390  =  K,4  INNER HELIUM GAP
400  =  300.,.00152,500.,.00214,600.,.00242,700.,.00268
410  =  800.,.00293,900.,.00314,1000.,.0034,1200.,.00384
420  =  CP,4  INNER HELIUM GAP
430  =  .00052
440  =  K,5  ALUMINUM OXIDE
450  =  373.,.07,973.,.004
560  =  CP,5  ALUMINUM OXIDE
470  =  373.,3.55
480  =  548.18,4.1142, 573.18,4.1556, 598.18,4.2050, 623.18,4.2465
490  =  648.18,4.2959, 673.18,4.3456, 698.18,4.3703, 723.18,4.3950
500  =  748.18,4.4281,773.18,4.4695,873.,4.563,1073.,4.704
510  =  K,6  OUTER HELIUM GAP
520  =  300.,.00152
530  =  500.,.00214,600.,.00242,700.,.00268,800.,.00293,900.,.00314
540  =  1000.,.0034,1200.,.00384
550  =  CP,6  OUTER HELIUM GAP
560  =  .00052
570  =  K,7  ZIRCALOY CLADDING
580  =  373.,.137
590  =  0. .13845,548.18,.1635, 573.18,.1652, 598.18,.1687
600  =  623.18,.1713
```

Table C-3. (continued)

```
610   =   648.18,.1739, 673.18,.1757, 698.18,.1797, 723.18,.1826
620   =   748,.1852,773.18,.1896,973.,.214
630   =   CP,7  ZIRCALOY CLADDING
640   =   373.,1.965
650   =   548.18,2.0366, 573.18,2.0503, 598.18,2.0791, 623.18,2.1073
660   =   648.18,2.1217, 673.18,2.1361, 698.18,2.1505, 723.18,2.1643
670   =   748.18,2.1787,773.18,2.1931,843.,2.216,1083.,2.351
680   =   END
690   =   MODEL
700   =   CARD1,27,0.0,2
710   =   CARD2,.149,6,.175,9,.240,12,.301,15,.305,16,.459,21
720   =   CONT,.460,22,.532,27
730   =   CARD3,1,6,2,9,3,12,2,15,4,16,5,21,6,22,7,27
740   =   CARD4,0.0,6,0.1148,9,0.0,27
750   =   CARD5,910.,9,909.,12,908.,16,907.,18,906.,20
760   =   CONT,905.,22,904.,24,903.,26,902.,27
770   =   END
780   =   TIME,18.88,45.,.1,6
790   =   CONTROL,PRINTFREQ = 10,NODE1 = 15,NODE2 = 22
800   =   BCINITIAL,.0014,559.
810   =   PRESSURE,16
820   =   DATA,17,0,0,21,0,0,0,0,BFQT42RUN3
```

Table C-4. Invert code input for Experiment Run 1A

```
100   =   ATTACH,TC1,ID = ROG,TYPE = CWAF
110   =   PROP
120   =   K,1  MAGNESIUM OXIDE
130   =   373.,.07
140   =   548.18,.07780, 573.18,.07773, 598.18,.07727, 623.18,.07682
150   =   648.18,.07591,673.18,.07546, 698.18,.07455, 723.18,.07364
160   =   748.18,.07273,773.18,.07182,950.,.071
170   =   CP,1  MAGNESIUM OXIDE
180   =   373.,3.349
190   =   548.18,3.7033,573.18,2.7452,598.18,3.7732,623.18,3.8012
200   =   648.18,3.8225, 673.18,3.8505, 698.18,3.8644, 723.18,3.8756
210   =   748.18,3.9133,773.18,3.9342,950.,3.95
220   =   K,2 INCONEL
230   =   373.,.19
240   =   548.18,.2200, 573.18,.2270, 598.18,.2296, 623.18,.2339
250   =   648.18,.2400, 673.18,.2455, 698.18,.2496, 723.18,.2539
260   =   748.18,.2600,773.18,.2635,950.,.304
270   =   CP,2  INCONEL
280   =   373.,3.903
290   =   548.18,4.2373, 573.18,4.2744, 598.18,4.3182, 623.18,4.3545
300   =   648.18,4.3916, 673.18,4.4278, 698.18,4.4716, 723.18,4.5087
310   =   748.18,4.5450,773.18,4.5745,950.,4.6
320   =   K,3  BORON NITRIDE
330   =   .186
```

Table C-4. (continued)

```
340  =  CP,3  BORON NITRIDE
350  =  373.,1.862
360  =  548.18,2.5529, 573.18,2.6190, 598.18,2.6768, 623.18,2.7595
370  =  648.18,2.8256, 673.18,2.8834, 698.18,2.9246, 723.18,2.9742
380  =  748.18,3.0321,773.18,3.0569,950.,3.08
390  =  K,4  INNER HELIUM GAP
400  =  300.,.00152,500.,.00214,600.,.00242,700.,.00268
410  =  800.,.00293,900.,.00314,1000.,.0034,1200.,.00384
420  =  CP,4  INNER HELIUM GAP
430  =  .00052
440  =  K,5  ALUMINUM OXIDE
450  =  373.,.07,973.,.004
460  =  CP,5  ALUMINUM OXIDE
470  =  373.,3.55
480  =  548.18,4.1142, 573.18,4.1556, 598.18,4.2050, 623.18,4.2465
490  =  648.18,4.2959, 673.18,4.3456, 698.18,4.3703, 723.18,4.3950
500  =  748.18,4.4281,773.18,4.4695,873.,4.563,1073.,4.704
510  =  K,6  OUTER HELIUM GAP
520  =  300.,.00152
530  =  500.,.00214,600.,.00242,700.,.00268,800.,.00293,900.,.00314
540  =  1000.,.0034,1200.,.00384
550  =  CP,6  OUTER HELIUM GAP
560  =  .00052
570  =  K,7  ZIRCALOY CLADDING
580  =  373.,.137
590  =  0. .13845,548.18,.1635, 573.18,.1652, 598.18,.1687
600  =  623.18,.1713
610  =  648.18,.1739, 673.18,.1757, 698.18,.1797, 723.18,.1826
620  =  748.18,.1852,773.18,.1896,973.,.214
630  =  CP,7  ZIRCALOY CLADDING
640  =  373.,1.965
650  =  548.18,2.0366, 573.18,2.0503, 598.18,2.0791, 623.18,2.1073
660  =  648.18,2.1217, 673.18,2.1361, 698.18,2.1505, 723.18,2.1643
670  =  748.18,2.1787,773.18,2.1931,843.,2.216,1083.,2.351
680  =  END
690  =  MODEL
700  =  CARD1,27,0.0,2
710  =  CARD2,.149,6,.175,9,.240,12,.301,15,.305,16,.459,21
720  =  CONT,.460,22,.532,27
730  =  CARD3,1,6,2,9,3,12,2,15,4,16,5,21,6,22,7,27
740  =  CARD4,0.0,6,0.1148,9,0.0,27
750  =  CARD5,910.,9,909.,12,908.,16,907.,18,906.,20
760  =  CONT,905.,22,904.,24,903.,26,902.,27
770  =  END
780  =  TIME,18.16,40. .1,6
790  =  CONTROL,PRINTFREQ = 10,NODE1 = 15,NODE2 = 22
800  =  BCINITIAL,.0014,559.
810  =  PRESSURE,14
820  =  DATA,15,0,0,21,0,0,0,0,BFQT43RUN1
```

Table C-5. Invert code input for Experiment Run 2A

```
100 =   ATTACH,TC1,ID=ROG,TYPE=CWAF
110 =   PROP
120 =   K,1  MAGNESIUM OXIDE
130 =   373.,.07
140 =   548.18,.07780, 573.18,.07773, 598.18,.07727, 623.18,.07682
150 =   648.18,.07591,673.18,.07546, 698.18,.07455, 723.18,.07364
160 =   748.18,.07273,773.18,.07182,950.,.071
170 =   CP,1  MAGNESIUM OXIDE
180 =   373.,3.349
190 =   548.18,3.7033,573.18,3.7452,598.18,3.7732,623.18,3.8012
200 =   648.18,3.8225, 673.18,3.8505, 698.18,3.8644, 723.18,3.8756
210 =   748.18,3.9133,773.18,3.9342,950.,3.95
220 =   K,2 INCONEL
230 =   373.,.19
240 =   548.18,.2200, 573.18,.2270, 598.18,.2296, 623.18,.2339
250 =   648.18,.2400, 673.18,.2455, 698.18,.2496, 723.18,.2539
260 =   748.18,.2600,773.18,.2635,950.,.304
270 =   CP,2  INCONEL
280 =   373.,3.903
290 =   548.18,4.2373, 573.18,4.2744, 598.18,4.3182, 623.18,4.3545
300 =   648.18,4.3916, 673.18,4.4278, 698.18,4.4716, 723.18,4.5087
310 =   748.18,4.5450,773.18,4.5745,950.,4.6
320 =   K,3  BORON NITRIDE
330 =   .186
340 =   CP,3  BORON NITRIDE
350 =   373.,1.862
360 =   548.18,2.5529, 573.18,2.6190, 598.18,2.6768, 623.18,2.7595
370 =   648.18,2.8256, 673.18,2.8834, 698.18,2.9246, 723.18,2.9742
380 =   748.18 3.0321,773.18,3.0569,950.,3.08
390 =   K,4  INNER HELIUM GAP
400 =   300.,.00152,500.,.00214,600.,.00242,700.,.00268
410 =   800.,.00293,900.,.00314,1000.,.0034,1200.,.00384
420 =   CP,4  INNER HELIUM GAP
430 =   .00052
440 =   K,5  ALUMINUM OXIDE
450 =   373.,.07,973.,.004
460 =   CP,5  ALUMINUM OXIDE
470 =   373.,3.55
480 =   548.18,4.1142, 573.18,4.1556, 598.18,4.2050, 623.18,4.2465
490 =   648.18,4.2959, 673.18,4.3456, 698.18,4.3703, 723.18,4.3950
500 =   748.18,4.4281,773.18,4.4695,873.,4.563,1073.,4.704
510 =   K,6  OUTER HELIUM GAP
520 =   300.,.00152
530 =   500.,.00214,600.,.00242,700.,.00268,800.,.00293,900.,.00314
540 =   1000.,.0034,1200.,.00384
550 =   CP,6  OUTER HELIUM GAP
560 =   .00052
570 =   K,7  ZIRCALOY CLADDING
580 =   373.,.137
590 =   0. .13845,548.18,.1635, 573.18,.1652, 598.18,.1687
600 =   623.18,1713
```

Table C-5. (continued)

```
610  =  648.18,.1739, 673.18,.1757, 698.18,.1797, 723.18,.1826
620  =  748.18,.1852,773.18,.1896,973.,.214
630  =  CP,7  ZIRCALOY CLADDING
640  =  373.,1.965
650  =  548.18,2.0366, 573.18,2.0503, 598.18,2.0791, 623.18,2.1073
660  =  648.18,2.1217, 673.18,2.1361, 698.18,2.1505, 723.18,2.1643
670  =  748.18,2.1787,773.18,2.1931,843.,2.216,1083.,2.351
680  =  END
690  =  MODEL
700  =  CARD1,27,0.0,2
710  =  CARD2,.149,6,.175,9,.240,12,.301,15,.305,16,.4575,21
720  =  CONT,.460,22,.532,27
730  =  CARD3,1,6,2,9,3,12,2,15,4,16,5,21,6,22,7,27
740  =  CARD4,0.0,6,0.1148,9,0.0,27
750  =  CARD5,910.,9,909.,12,908.,16,907.,18,906.,20
760  =  CONT,905.,22,904.,24,903.,26,902.,27
770  =  END
780  =  TIME,20.08,45.,.1,6
790  =  CONTROL,PRINTFREQ = 10,NODE1 = 15,NODE2 = 22
800  =  BCINITIAL,.0014,559
810  =  PRESSURE,13
820  =  DATA,15,0,0,21,0,0,0,0,BFQT43RUN2
```

Table C-6. Invert code input for Experiment Run 3A

```
100  =  ATTACH,TC1,ID = ROG,TYPE = CWAF
110  =  PROP
120  =  K,1  MAGNESIUM OXIDE
130  =  373.,.07
140  =  548.18,.07780, 573.18,.07773, 598.18,.07727, 623.18,.07682
150  =  648.18,.07591,673.18,.07546, 698.18,.07455, 723.18,.07364
160  =  748.18,.07273,773.18,.07182,950.,.071
170  =  CP,1  MAGNESIUM OXIDE
180  =  373.,3.349
190  =  548.18,3.7033,573.18,3.7452,598.18,3.7732,623.18,3.8012
200  =  648.18,3.8225, 673.18,3.8505, 698.18,3.8644, 723.18,3.8756
210  =  748.18,3.9133,773.18,3.9342,950.,3.95
220  =  K,2 INCONEL
230  =  373.,.19
240  =  548.18,.2200, 573.18,.2270, 598.18,.2296, 623.18,.2339
250  =  648.18,.2400, 673.18,.2455, 698.18,.2496, 723.18,.2539
260  =  748.18,.2600,773.18,.2635,950.,.304
270  =  CP,2  INCONEL
280  =  373.,3.903
290  =  548.18,4.2373, 573.18,4.2744, 598.18,4.3182, 623.18,4.3545
300  =  648.18,4.3916, 673.18,4.4278, 698.18,4.4716, 723.18,4.5087
310  =  748.18,4.5450,773.18,4.5745,950.,4.6
320  =  K,3  BORON NITRIDE
330  =  .186
```

Table C-6. (continued)

```
340  =  CP,3  BORON NITRIDE
350  =  373.,1.862
360  =  548.18,2.5529, 573.18,2.6190, 598.18,2.6768, 623.18,2.7595
370  =  648.18,2.8256, 673.18,2.8834, 698.18,2.9246, 723.18,2.9742
380  =  748.18,3.0321,773.18,3.0569,950.,3.08
390  =  K,4  INNER HELIUM GAP
400  =  300.,.00152,500.,.00214,600.,.00242,700.,.00268
410  =  800.,.00293,900.,.00314,1000.,.0034,1200.,.00384
420  =  PC,4  INNER HELIUM GAP
430  =  .00052
440  =  K,5  ALUMINUM OXIDE
450  =  373.,.07,973.,.004
460  =  CP,5  ALUMINUM OXIDE
470  =  373.,3.55
480  =  548.18,4.1142, 573.18,4.1556, 598.18,4.2050, 623.18,4.2465
490  =  648.18,4.2959, 673.18,4.3456, 698.18,4.3703, 723.18,4.3950
500  =  748.18,4.4281,773.18,4.4695,873.,4.563,1073.,4.704
510  =  K,6  OUTER HELIUM GAP
520  =  300.,.00152
530  =  500.,.00214,600.,.00242,700.,.00268,800.,.00293,900.,.00314
540  =  1000.,.0034,1200.,.00384
550  =  CP,6  OUTER HELIUM GAP
560  =  .00052
570  =  K,7  ZIRCALOY CLADDING
580  =  373.,.137
590  =  0. .13845,548.18,.1635, 573.18,.1652, 598.18,.1687
600  =  623.18,.1713
610  =  648.18,.1739, 673.18,.1757, 698.18,.1797, 723.18,.1826
620  =  748.18,.1852,773.18,.1896,973.,.214
630  =  CP,7  ZIRCALOY CLADDING
640  =  373.,1.965
650  =  548.18,2.0366, 573.18,2.0503, 598.18,2.0791, 623.18,2.1073
660  =  648.18,2.1217, 673 18,2.1361, 698.18,2.1505, 723.18, 2.1643
670  =  748.18,2.1787,773.18,2.1931,843.,2.216,1083.,2.351
680  =  END
690  =  MODEL
700  =  CARD1,27,0.0,2
710  =  CARD2,.149,6,.175,9,.240,12,.301,15,.305,16,.4575,21
720  =  CONT,.460,22,.532,27
730  =  CARD3,1,6,2,9,3,12,2,15,4,16,5,21,6,22,7,27
740  =  CARD4,0.0,6,0.1148,9,0.0,27
750  =  CARD5,910.,9,909.,12,908.,16,907.,18,906.,20
760  =  CONT,905.,22,904.,24,903.,26,902.,27
770  =  END
780  =  TIME,22.1,45.,.1,6
790  =  CONTROL,PRINTFREQ = 10,NODE1 = 15,NODE2 = 22
800  =  BCINITIAL,.0014,559
810  =  PRESSURE,13
820  =  DATA,15,0,0,21,0,0,0,0,BFQT43RUN3
```

Table C-7. Invert code input for Experiment Run 3AR

```
100  =  ATTACH,TC1,ID=ROG,TYPE=CWAF
110  =  PROP
120  =  K,1  MAGNESIUM OXIDE
130  =  373.,.07
140  =  548.18,.07780, 573.18,.07773, 598.18,.07727, 623.18,.07682
150  =  648.18,.07591,673.18,.07546, 698.18,.07455, 723.18,.07364
160  =  748.18,.07273,773.18,.07182,950.,.071
170  =  CP,1  MAGNESIUM OXIDE
180  =  373.,3.349
190  =  548.18,3.7033,573.18,3.7452,598.18,3.7732,623.18,3.8012
200  =  648.18,3.8225, 673.18,3.8505, 698.18,3.8644, 723.18,3.8756
210  =  748.18,3.9133,773.18,3.9342,950.,3.95
220  =  K,2 INCONEL
230  =  373.,.19
240  =  548.18,.2200, 573.18,.2270, 598.18,.2296, 623.18,.2339
250  =  648.18,.2400, 673.18,.2455, 698.18,.2496, 723.18,.2539
260  =  748.18,.2600,773.18,.2635,950.,.304
270  =  CP,2  INCONEL
280  =  373.,3.903
290  =  548.18,4.2373, 573.18,4.2744, 598.18,4.3182, 623.18,4.3545
300  =  648.18,4.3916, 673.18,4.4278, 698.18,4.4716, 723.18,4.5087
310  =  748.18,4.5450,773.18,4.5745,950.,4.6
320  =  K,3  BORON NITRIDE
330  =  .186
340  =  CP,3  BORON NITRIDE
350  =  373.,1.862
360  =  548.18,2.5529, 573.18,2.6190, 598.18,2.6768, 623.18,2.7595
370  =  648.18,2.8256, 673.18,2.8834, 698.18,2.9246, 723.18,2.9742
380  =  748.18,3.0321,773.18,3.0569,950.,3.08
390  =  K,4  INNER HELIUM GAP
400  =  300.,.00152,500.,.00214,600.,.00242,700.,.00268
410  =  800.,.00293,900.,.00314,1000.,.0034,1200.,.00384
420  =  CP,4  INNER HELIUM GAP
430  =  .00052
440  =  K,5  ALUMINUM OXIDE
450  =  373.,.07,973.,.004
460  =  CP,5  ALUMINUM OXIDE
470  =  373.,3.55
480  =  548.18,4.1142, 573.18,4.1556, 598.18,4.2050, 623.18,4.2465
490  =  648.18,4.2959, 673.18,4.3456, 698.18,4.3703, 723.18,4.3950
500  =  748.18,4.4281,773.18,4.4595,873.,4.563,1073.,4.704
510  =  K,6  OUTER HELIUM GAP
520  =  300.,.00152
530  =  500.,.00214,600.,.00242,700.,.00268,800.,.00293,900.,.00314
540  =  1000.,.0034,1200.,.00384
550  =  CP,6  OUTER HELIUM GAP
560  =  .00052
570  =  K,7  ZIRCALOY CLADDING
580  =  373.,.137
590  =  0. .13845,548.18,.1635, 573.18,.1652, 598.18,.1687
600  =  623.18,.1713
```

Table C-7. (continued)

```
610  =  648.18,.1739, 673.18,.1757, 698.18,.1797, 723.18,.1826
620  =  748.18,.1852,773.18,.1896,973.,.214
630  =  CP,7  ZIRCALOY CLADDING
640  =  373.,1.965
650  =  548.18,2.0366, 573.18,2.0503, 598.18,2.0791, 623.18,2.1073
660  =  648.18,2.1217, 673.18,2.1361, 698.18,2.1505, 723.18,2.1643
670  =  748.18,2.1787,773.18,2.1931,843.,2.216,1083.,2.351
680  =  END
690  =  MODEL
700  =  CARD1,27,0.0,2
710  =  CARD2,.149,6,.175,9,.240,12,.301,15,.305,16,.4575,21
720  =  CONT,.460,22,.532,27
730  =  CARD3,1,6,2,9,3,12,2,15,4,16,5,21,6,22,7,27
740  =  CARD4,0.0,6,0.1148,9,0.0,27
750  =  CARD5,910.,9,909.,12,908.,16,907.,18,906.,20
760  =  CONT,905.,22,904.,24,903.,26,902.,27
770  =  END
780  =  TIME,20.4,45.,,1,6
790  =  CONTROL,PRINTFREQ = 10,NODE1 = 15,NODE2 = 22
800  =  BCINITIAL,.0014,559.
810  =  PRESSURE,13
820  =  DATA,15,0,0,21,0,0,0,0,BFQT43RUN3R
```

Table C-8. Invert code input for Experiment Run 4A

```
100  =  ATTACH,TC1,ID = ROG,TYPE = CWAF
110  =  PROP
120  =  K,1  MAGNESIUM OXIDE
130  =  373.,.07
140  =  548.18,.07780, 573.18,.07773, 598.18,.07727, 623.18,.07682
150  =  648.18,.07591,673.18,.07546, 698.18,.07455, 723.18,.07364
160  =  748.18,.07273,773.18,.07182,950.,.071
170  =  CP,1  MAGNESIUM OXIDE
180  =  373.,3.349
190  =  548.18,3.7033,573.18,3.7452,598.18,3.7732,623.18,3.8012
200  =  648.18,3.8225, 673.18,3.8505, 698.18,3.8644, 723.18,3.8756
210  =  748.18,3.9133,773.18,3.9342,950.,3.95
220  =  K,2 INCONEL
230  =  373.,.19
240  =  548.18,.2200, 573.18,.2270, 598.18,.2296, 623.18,.2339
250  =  648.18,.2460, 673.18,.2455, 698.18,.2496, 723.18,.2539
260  =  748.18,.2600,773.18,.2635,950.,.304
270  =  CP,2  INCONEL
280  =  373.,3.903
290  =  548.18,4.2373, 573.18,4.2744, 598.18,4.3182, 623.18,4.3545
300  =  648.18,4.3916, 673.18,4.4278, 698.18,4.4716, 723.18,4.5087
310  =  748.18,4.5450,773.18,4.5745,950.,4.6
320  =  K,3  BORON NITRIDE
330  =  .186
```

Table C-8. (continued)

```
340  =  CP,3  BORON NITRIDE
350  =  373.,1.862
360  =  548.18,2.5529, 573.18,2.6190, 598.18,2.6768, 623.18,2.7595
370  =  648.18,2.8256, 673.18,2.8834, 698.18,2.9246, 723.18,2.9742
380  =  748.18,3.0321,773.18,3.0569,950.,3.08
390  =  K,4  INNER HELIUM GAP
400  =  300.,.00152,500.,.00214,600.,.00242,700.,.00268
410  =  800.,.00293,900.,.00314,1000.,.0034,1200.,.00384
420  =  CP,4  INNER HELIUM GAP
430  =  .00052
440  =  K,5  ALUMINUM OXIDE
450  =  373.,.07,973.,.007
460  =  CP,5  ALUMINUM OXIDE
470  =  373.,3.55
480  =  548.18,4.1142, 573.18,4.1556, 598.18,4.2050, 623.18,4.2465
490  =  648.18,4.2959, 673.18,4.3456, 698.18,4.3703, 723.18,4.3950
500  =  748.18,4.4281,773.18,4.4695,873.,4.563,1073.,4.704
510  =  K,6  OUTER HELIUM GAP
520  =  300.,.00152
530  =  500.,.00214,600.,.00242,700.,.00268,800.,.00293,900.,.00314
540  =  1000.,.0034,1200.,.00384
550  =  CP,6  OUTER HELIUM GAP
560  =  .00052
570  =  K,7  ZIRCALOY CLADDING
580  =  373.,.137
590  =  0. .13845,548.18,.1635, 573.18,.1652, 598.18,.1687
600  =  623.18,.1713
610  =  648.18,.1739, 673.18,.1757, 698.18,.1797, 723.18,.1826
620  =  748.18,.1852,773.18,.1896,973.,.214
630  =  CP,7  ZIRCALOY CLADDING
640  =  373.,1.965
650  =  548.18,2.0366, 573.18,2.0503, 598.18,2.0791, 623.18,2.1073
660  =  648.18,2.1217, 673.18,2.1361, 698.18,2.1505, 723.18,2.1643
670  =  748.18,2.1787,773.18,2.1931,843.,2.216,1083.,2.351
680  =  END
690  =  MODEL
700  =  CARD1,27,0.0,2
710  =  CARD2,.149,6,.175,9,.240,12,.301,15,.305,16,.4575,21
720  =  CONT,.460,22,.532,27
730  =  CARD3,1,6,2,9,3,12,2,15,4,16,5,21,6,22,7,27
740  =  CARD4,0.0,6,0.1148,9,0.0,27
750  =  CARD5,910.,9,909.,12,908.,16,907.,18,906.,20
760  =  CONT,905.,22,904.,24,903.,26,902.,27
770  =  END
780  =  TIME,20.29,40.,.1,6
790  =  CONTROL,PRINTFREQ = 10,NODE1 = 15,NODE2 = 22
800  =  BCINITIAL,.0014,559.
810  =  PRESSURE,13
820  =  DATA,15,0,21,0,0,0,0,BFQT43RUN4
```

APPENDIX D
HEATER ROD QUENCH EXPERIMENTS MEASUREMENTS LIST

APPENDIX D
HEATER ROD QUENCH EXPERIMENTS MEASUREMENTS LIST

Table D-1 is a list of the process and experimental measurements taken during the electric heater rod quench experiment program performed in the Loss-of-Fluid Test (LOFT) Test Support Facility at the Idaho National Engineering Laboratory. The heater rods used in these experiments were solid-type (FEBA) and cartridge-type (REBEKA) heater rods provided by the Karlsruhe Nuclear Reactor Center in Karlsruhe, Germany. Table D-1 lists the measurement identification number, the range, and a description of the measurement. All measurements were sampled and recorded at a rate of 50 samples per second. All measurements were converted to engineering units using a polynominal equation of the form:

$$\text{Meas.} = D_0 + D_1V + D_2V^2 + D_3V^3$$

where V is the original transducer output and the D_i coefficients are constants that depend on calibration data. The measurements in engineering units were then recorded on a digital disk and then transferred to a digital tape.

Table D-1. Heater rod quench experiments measurements list

Measurement	Range	Description
FE-FCV-1T	0 - 0.47 L/s	1/2-in. turbine flowmeter
FE-FCV-1T	0 - 3.17 L/s	1-in. turbine flowmeter
FE-FCV-1T	0 - 28.0 L/s	3-in. turbine flowmeter
DE-B	0 - 10.0 V	Single-beam densitometer at 1950-mm elevation of test section (midpoint)
TE-5	0 - 623 K	Fluid temperature in main loop pressure vessel
TE-OR	0 - 623 K	Fluid temperature upstream of orifice
TE-7-1	0 - 1173 K	FEBA Rod 7 temperature at 150-mm elevation
TE-7-2	0 - 1173 K	FEBA Rod 7 temperature at 1000-mm elevation
TE-7-3	0 - 1173 K	FEBA Rod 7 temperature at 1950-mm elevation
TE-7-4	0 - 1173 K	FEBA Rod 7 temperature at 2900-mm elevation
TE-15-1	0 - 1173 K	FEBA Rod 15 temperature at 150-mm elevation
TE-15-2	0 - 1173 K	FEBA Rod 15 temperature at 1000-mm elevation
TE-15-3	0 - 1173 K	FEBA Rod 15 temperature at 1950-mm elevation
TE-15-4	0 - 1173 K	FEBA Rod 15 temperature at 2900-mm elevation
TE-18-1	0 - 1173 K	FEBA Rod 18 temperature at 150-mm elevation
TE-18-2	0 - 1173 K	FEBA Rod 18 temperature at 1000-mm elevation

Table D-1. (continued)

Measurement	Range	Description
TE-18-3	0 - 1173 K	FEBA Rod 18 temperature at 1950-mm elevation
TE-18-4	0 - 1173 K	FEBA Rod 18 temperature at 2900-mm elevation
TE-19-1	0 - 1173 K	FEBA Rod 19 temperature at 150-mm elevation
TE-19-2	0 - 1173 K	FEBA Rod 19 temperature at 1000-mm elevation
TE-19-3	0 - 1173 K	FEBA Rod 19 temperature at 1950-mm elevation
TE-19-4	0 - 1173 K	FEBA Rod 19 temperature at 2900-mm elevation
TE-22-1	0 - 1173 K	FEBA Rod 22 temperature at 150-mm elevation
TE-22-2	0 - 1173 K	FEBA Rod 22 temperature at 1000-mm elevation
TE-22-3	0 - 1173 K	FEBA Rod 22 temperature at 1950-mm elevation
TE-22-4	0 - 1173 K	FEBA Rod 22 temperature at 2900-mm elevation
TE-33-1	0 - 1173 K	FEBA Rod 33 temperature at 500-mm elevation
TE-33-2	0 - 1173 K	FEBA Rod 33 temperature at 1500-mm elevation
TE-33-3	0 - 1173 K	FEBA Rod 33 temperature at 2400-mm elevation
TE-33-4	0 - 1173 K	FEBA Rod 33 temperature at 3400-mm elevation
TE-37-1	0 - 1173 K	FEBA Rod 37 temperature at 500-mm elevation
TE-37-2	0 - 1173 K	FEBA Rod 37 temperature at 1500-mm elevation
TE-37-3	0 - 1173 K	FEBA Rod 37 temperature at 2400-mm elevation
TE-37-4	0 - 1173 K	FEBA Rod 37 temperature at 3400-mm elevation
TE-77-1	0 - 1173 K	FEBA Rod 77 temperature at 500-mm elevation
TE-77-2	0 - 1173 K	FEBA Rod 77 temperature at 1500-mm elevation
TE-77-3	0 - 1173 K	FEBA Rod 77 temperature at 2400-mm elevation
TE-77-4	0 - 1173 K	FEBA Rod 77 temperature at 3400-mm elevation
TE-82-1	0 - 1173 K	FEBA Rod 82 temperature at 500-mm elevation
TE-82-2	0 - 1173 K	FEBA Rod 82 temperature at 1500-mm elevation
TE-82-3	0 - 1173 K	FEBA Rod 82 temperature at 2400-mm elevation

Table D-1. (continued)

Measurement	Range	Description
TE-82-4	0 - 1173 K	FEBA Rod 82 temperature at 3400-mm elevation
TE-REB-X1	0 - 1173 K	REBEKA rod external thermocouple at 150-mm elevation
TE-REB-X2	0 - 1173 K	REBEKA rod external thermocouple at 1950-mm elevation
TE-REB-X3	0 - 1173 K	REBEKA rod external thermocouple at 1000-mm elevation
TE-REB-X4	0 - 1173 K	REBEKA rod external thermocouple at 2900-mm elevation
TE-REB-E1	0 - 1173 K	REBEKA rod embedded thermocouple at 1950-mm elevation and 0 degree azimuthal
TE-REB-E2	0 - 1173 K	REBEKA rod embedded thermocouple at 1950-mm elevation and 135 degree azimuthal
TE-REB-I1	0 - 1173 K	REBEKA rod internal thermocouple at 2900-mm elevation
TE-REB-I2	0 - 1173 K	REBEKA rod internal thermocouple at 1950-mm elevation
TE-REB-I3	0 - 1173 K	REBEKA rod internal thermocouple at 1000-mm elevation
TE-PT-1	0 - 623 K	Pipe temperature on FCV-1T flange
TE-PT-2	0 - 623 K	Pipe temperature on spool downstream of FCV-1T
TE-PT-3	0 - 623 K	Pipe temperature on lower flange of test section
TE-PT-4	0 - 623 K	Pipe temperature near lower flange of test section
TE-FCV-1T	0 - 623 K	Surface temperature of FCV-1T
TE-SUR	0 - 623 K	Fluid temperature in surge tank
TE-BF3	0 - 623 K	Fluid temperature downstream of main coolant pump
TE-FLUX	0 - 623 K	Intrinsic thermocouple junction on test section vessel wall at 1000-mm elevation
TE-VWTC1	0 - 1173 K	Vessel wall temperature at 150-mm elevation
TE-VWTC2	0 - 1173 K	Vessel wall temperature at 500-mm elevation
TE-VWTC3	0 - 1173 K	Vessel wall temperature at 1000-mm elevation
TE-VWTC4	0 - 1173 K	Vessel wall temperature at 1950-mm elevation
TE-VWTC5	0 - 1173 K	Vessel wall temperature at 2900-mm elevation

Table D-1. (continued)

Measurement	Range	Description
TE-VWTC6	0 - 1173 K	Vessel wall temperature at 3400-mm elevation
TE-FCV-1T	0 - 623 K	Fluid temperature upstream of FCV-1T
PE-3	0 - 17.2 MPa	Pressure vessel pressure in main loop
PE-N-1	0 - 17.2 MPa	Nitrogen supply tank pressure
PE-TS-0	0 - 17.2 MPa	Test section outlet pressure at 3900-mm elevation
PE-FCV-1T	0 - 17.2 MPa	Pressure upstream of FCV-1T in main coolant pipe
PDE-TS-1	0 - 200 kPa	Test section pressure drop
PE-SUR	0 - 17.2 MPa	Pressure in surge tank
PDE-23	0 - 327 kPa	Pressure drop across main loop pressure vessel
PE-AIR	0 - 1.034 MPa	System air pressure
RR-AMP	0 - 100 amps	REBEKA rod current
FR-AMP	0 - 500 amps	Current to the eight peripheral FEBA rods
RR-VOLT	0 - 110 V	REBEKA rod voltage
FR-VOLT	0 - 110 V	Voltage across the eight peripheral FEBA rods

APPENDIX E
REBEKA ROD DIAMETER MEASUREMENTS

APPENDIX E
REBEKA ROD DIAMETER MEASUREMENTS

Diameter measurements of the REBEKA rod[a] were taken during the electric heater rod quench experiment program[b] to determine if any cladding collapse occurred. Cladding collapse was not intended to occur due to the initial pressurization of the rod; however, diameter measurements taken after the first series of experiment runs (Runs 1, 2, and 3) indicated that cladding collapse did occur. Diameter measurements were taken (a) prior to the experiments, (b) after the first series of experiments with cladding external thermocouples, and (c) after the experiments without cladding external thermocouples. The values are listed in Tables E-1, E-2, and E-3, respectively. Measurements were taken at various axial positions and azimuthal positions on the rod.

Figure E-1 shows the average diameter of the rod versus axial position for the three different times during the experiment program that diameter measurements were taken. These data show that the cladding collapsed basically through the hottest portion of the rod. Also, diameter measurements listed in Tables E-2 and E-3 show that the cladding buckled, since the diameter measurements were not uniform around the circumference of the rod. Other evidence that the cladding buckled is shown in the body of this report in Figure 22, where Thermocouple TE-REB-E2 indicated a response typical of a closed gap between the aluminum oxide, Al_2O_3, pellets and the cladding.

These diameter measurements were used to determine the average gap width in the rod at the axial elevations of the secondary junctions of embedded Thermocouples TE-REB-E1 and TE-REB-E2 for use in the INVERT model described in Appendix C.

a. The REBEKA rod is a cartridge-type electrical heater rod provided by the Karlsruhe Nuclear Reactor Center in Karlsruhe, Germany.

b. The electric heater rod quench experiment program was performed at the Loss-of-Fluid Test (LOFT) Test Support Facility at the Idaho National Engineering Laboratory.

Table E-1. REBEKA rod diameter measurements prior to quench experiments

Axial Elevation (mm)	Diameter at Two Azimuthal Locations (mm)		Average Diameter (mm)
	0°	90°	
1000	10.673	10.732	10.703
1950	10.744	10.742	10.743
2900	10.755	10.744	10.75

Table E-2. REBEKA rod diameter measurements after Runs 1 through 3 with cladding external thermocouples

Axial Elevation (mm)	Diameter at Four Azimuthal Locations (mm)				Average Diameter (mm)
	0°	45°	90°	135°	
0	10.77	—	10.742	—	10.756
500	10.739	—	10.732	—	10.736
700	10.721	—	10.721	—	10.721
1000	10.65	—	10.622	—	10.636
1300	10.65	—	10.65	—	10.65
1650	10.574	—	10.559	—	10.567
1925	10.625	10.579	10.589	10.579	10.593
1937	10.648	10.577	10.622	10.571	10.605
1950	10.665	10.571	10.599	10.574	10.602
1963	10.678	10.556	10.625	10.561	10.605
1975	10.643	10.597	10.622	10.599	10.615
1988	10.61	10.627	10.587	10.627	10.613
2001	10.622	10.627	10.64	10.632	10.63
2014	10.599	10.645	10.635	10.643	10.631
2250	10.648	—	10.645	—	10.647
2600	10.683	—	10.678	—	10.681
2900	10.719	—	10.732	—	10.726
3200	10.739	—	10.749	—	10.744
3400	10.739	—	10.749	—	10.744
3900	10.739	—	10.739	—	10.739

Table E-3. REBEKA rod diameter measurements after Runs 1A through 8A without cladding external thermocouples

Axial Elevation (mm)	Diameter at Six Azimuthal Locations (mm)						Average Diameter (mm)
	0°	45°	90°	135°	120°	140°	
0	10.77	—	10.759	—	—	—	10.765
500	10.732	—	10.732	—	—	—	10.732
700	10.635	—	10.716	—	—	—	10.676
1000	10.574	—	10.693	—	—	—	10.634
1300	10.556	—	10.579	—	—	—	10.568
1650	10.589	—	10.533	—	—	—	10.561
1925	10.584	10.569	10.566	10.566	—	—	10.571
1937	10.62	10.566	10.582	10.582	—	—	10.588
1950	10.648	10.564	10.579	10.579	10.597	10.655	10.604
1963	10.577	10.559	10.584	10.599	10.582	10.663	10.594
1975	10.559	10.574	10.589	10.566	—	10.632	10.584
1988	10.569	10.63	10.584	10.566	—	10.574	10.585
2001	10.566	10.592	10.584	10.574	—	—	10.579
2014	10.571	10.602	10.61	10.607	—	—	10.598
2250	10.571	10.602	10.607	10.592	—	—	10.593
2600	10.655	10.671	10.617	10.564	—	—	10.627
2900	10.714	10.709	10.714	10.704	—	—	10.71
3200	10.742	10.734	10.747	10.737	—	—	10.74
3400	10.739	10.734	10.747	10.739	—	—	10.74
3900	10.739	10.737	10.734	10.739	—	—	10.737

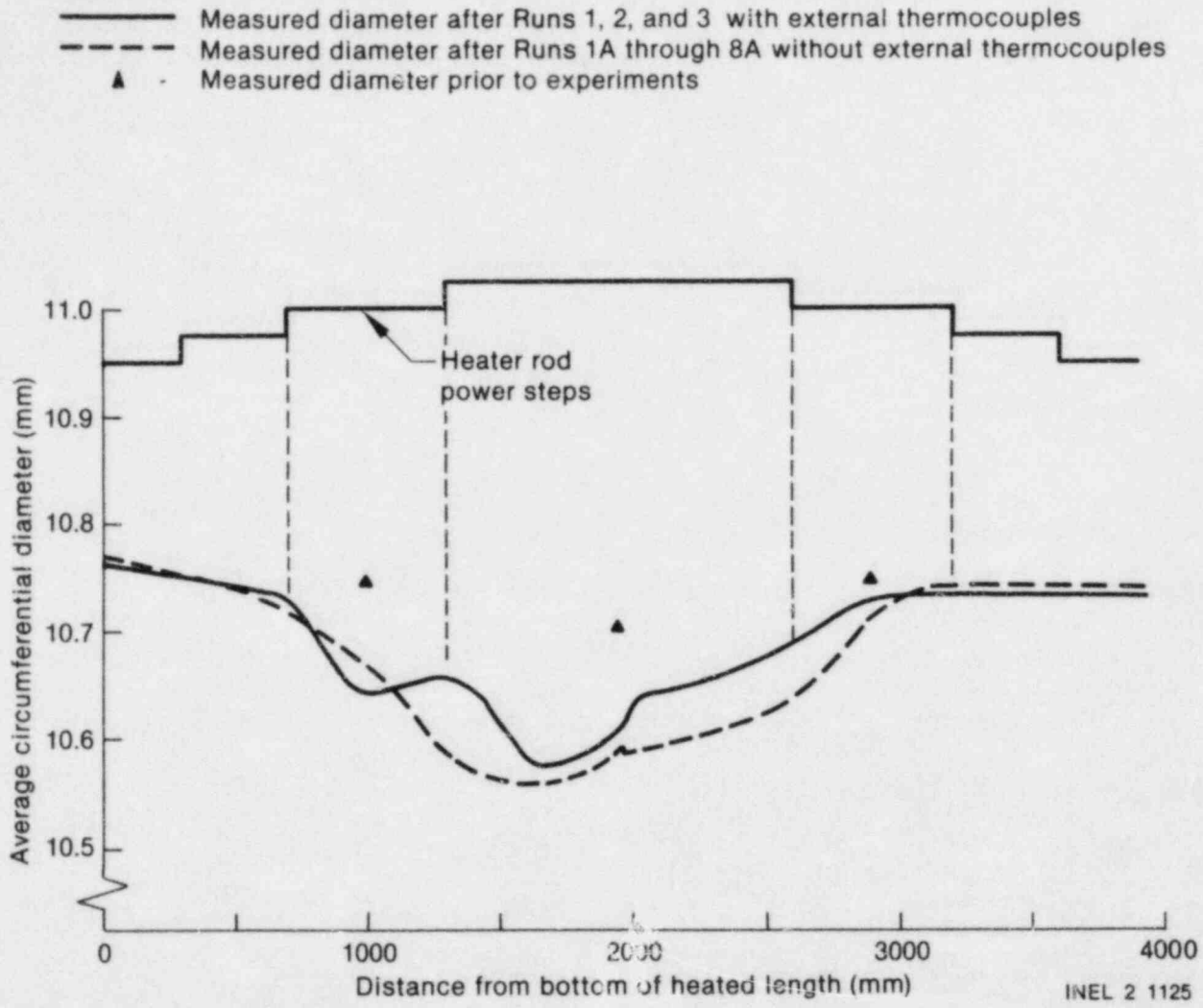

Figure E-1. REBEKA heater rod measured diameter versus elevation.

APPENDIX F
MEASUREMENT UNCERTAINTIES

APPENDIX F
MEASUREMENT UNCERTAINTIES

Measurement uncertainties have been determined for the experimental measurements reported in the body of this report. These include five FEBA rod Type K thermocouples; REBEKA rod internal, embedded, and external thermocouples; test section outlet pressure; and test section flow rate.[a] The measurement uncertainties for the parameters are listed in Table F-1.

The uncertainty in test section outlet pressure includes hysteresis, nonlinearity, repeatability, excitation voltage, and data acquisition system uncertainties. The uncertainties in test section flow rate include nonlinearity, turbine meter bearing drag, electronics error, and noise. The uncertainties in the Type K thermocouple measurements include material impurities, drift, reference junction, polynomial approximation, extension cable, and the data acquisition system. The cladding embedded thermocouples (TE-REB-E1 and TE-REB-E2) have an additional systematic error due to the failure of the primary junctions and uncertainty in the location of the secondary junctions. The magnitude of the error in measuring the cladding temperature is a function of the time in the transient. The estimated systematic error is shown in Figure 26 in the body of this report where the cladding embedded thermocouple reading is compared with the predicted cladding temperature as a function of time in the transient.

The methodology used in determining measurement uncertainties is contained in Reference F-1.

a. The FEBA rod and REBEKA rod are solid-type and cartridge-type electrical heater rods, respectively. These rods were provided by the Karlsruhe Nuclear Reactor Center in Karlsruhe, Germany, for the electric heater rod quench experiment program conducted in the Loss-of-Fluid Test (LOFT) Test Support Facility at the Idaho National Engineering Laboratory.

Reference

F-1. R. W. Golden, *Semiscale Uncertainty Report Methodology*, NUREG/CR-2459, EGG-2142, Vol. 1, September 1982.

Table F-1. Measurement uncertainties

Measurement Identification	Measurement Description	Range	Uncertainty
PE-TS-0	Test section outlet pressure	0-17.2 MPa	±0.093 MPa
FE-FCV-1T	Test section flow rate in 1/2-in. turbine	0-0.47 L/s	±(0.014 L/s + 1.2% of reading)
FE-FCV-1T	Test section flow rate in 1-in. turbine	0-3.17 L/s	±(0.089 L/s + 1.2% of reading)
FE-FCV-1T	Test section flow rate	0-28.0 L/s	±(0.42 L/s + 1.7% of reading)
TE-15-3	FEBA Rod 15 temperature at 1950-mm elevation	0-1173 K	±5.1 K
TE-18-3	FEBA Rod 18 temperature at 1950-mm elevation	0-1173 K	±5.1 K
TE-19-3	FEBA Rod 19 temperature at 1950-mm elevation	0-1173 K	±5.1 K
TE-22-3	FEBA Rod 22 temperature at 1950-mm elevation	0-1173 K	±5.1 K
TE-7-3	FEBA Rod 7 temperature at 1950-mm elevation	0-1173 K	±5.1 K
TE-REB-X2	REBEKA rod external thermocouple at 1950-mm elevation	0-1173 K	±5.1 K
TE-REB-I2	REBEKA rod internal thermocouple at 1950-mm elevation	0-1173 K	±5.1 K
TE-REB-E1	REBEKA rod cladding embedded thermocouple at 1950-mm elevation	0-1173 K	±5.1 K
TE-REB-E2	REBEKA rod cladding embedded thermocouple at 1950-mm elevation	0-1173 K	±5.1 K

EG&G Idaho, Inc.
P.O. Box 1625
Idaho Falls, Idaho 83415